COMPOSITION CONTROL AND ESTIMATION WITH TEMPERATURE MEASUREMENTS FOR MULTICOMPONENT DISTILLATION COLUMNS

Andrea Frau

Università degli Studi di Cagliari
Dottorato di Ricerca in Ingegneria Industriale
XXIII Ciclo

COMPOSITION CONTROL AND ESTIMATION WITH TEMPERATURE MEASUREMENTS FOR MULTICOMPONENT DISTILLATION COLUMNS

Andrea Frau

Supervisors:
Prof. Roberto Baratti
Prof. Jesús Álvarez Calderon

Università degli Studi di Cagliari
Dottorato di Ricerca in Ingegneria Industriale
XXIII Ciclo

Alla mia famiglia,
a chi mi vuole bene
e a chi non beve...

Contents

Abstract

In this Thesis, the problem of controlling and estimating compositions of interest in a multicomponent column with temperature measurements is addressed. This work is motivated by the necessity of (i) regulating some of the effluent compositions around the prescribed values for a given separation, in spite of disturbances entering the column as fluctuations in feed flow rate, composition and temperature, and (ii) estimating such compositions in order to monitor the separation.

These problems cannot be practically solved by composition analyzers, because of their high costs of purchase and maintenance, their reliability issues and the delays in obtaining composition measurements. A possible solution is the employment of temperature measurements, which do not present the abovementioned shortcomings. In a multicomponent distillation column, the compositions in a tray are not uniquely determined by the temperature at the same tray, and therefore temperature sensors cannot provide composition control and estimation without offset. Thus, a methodology that permits the achievement of composition control and estimation objectives within a predetermined tolerance is necessary. The methodology illustrated in this Thesis is applied to a six-component C3-C4 splitter through simulation examples in order to be assessed on the basis of the structural results, according to different control and estimation objectives.

Both control and estimation problems are solved through a unified methodology that consists in the partition of both problems into a structural and an algorithmic part, puts together techniques already employed and new ideas, and permits a systematic design. As regards the control part, the structure is defined as the joint selection of (i) the temperatures to be regulated and (ii) their pairing with the chosen manipulated variables, while the algorithm is the dynamic data processor that processes temperature measurements in order to perform the control task. On the other hand, regarding the estimation part, the structure is defined as the joint selection of (i) a (possibly reduced) estimation model, (ii) the number and locations of temperature measurements, (iii) the states to be innovated through injection of temperature measurements and (iv) the regions in which the temperature can be approximated as the average one, while the algorithm is the dynamic data processor that processes temperature measurements in order to perform the estimation task.

In this Thesis, we propose the temperature gradient with per-component contribution diagram as the mean for the selection of part of the control structure and of the entire estimation structure. Such diagram is the main tool of the used methodology, and consists in plotting temperature gradients at a nominal steady-state together with the contributions due to the components. The diagram is based on the well-known temperature slope criterion, which has extensively been used in control but, as will be shown in this Thesis, provides a simpler and more intuitive criterion for both control and estimation purposes in a multicomponent column, compared to other well-known methods.

As concerns the control algorithm selection, conventional and cascade-type controllers with the assistance of first-order observers are developed on the basis of passivity concepts. Such controllers provide a systematic and easy tuning criteria and an anti-windup protection. Their employment is here extended to a multicomponent case.

Geometric Estimator (GE) (with partial innovation) and Extended Kalman Filter (EKF) (with complete or partial innovation) based algorithms are chosen in order to carry out the estimation task. The GE approach, which provides a systematic tuning criterion, is here extended to a multicomponent case.

Chapter 1

Introduction

This introductory Chapter starts with the illustration of the motivations which lead us to the development of this Thesis. After that, a summary of the Thesis is given, by showing how it is structured in different Chapters. Finally, a list of conference papers and other activities derived from the present work is presented.

1.1 Motivations

Distillation aim is the separation of a mixture into two or more products with specified purities. It is one of the most important activities in a chemical plant, and it is very critical since a high amount of energy is required in order to effectively performing the separation task. The criticity of the operation is shown by the fact that in the USA there are around 40000 distillation columns (Humphrey and Seibert, 1992) which use approximately the 24% of the energy consumed by the manufacturing sector (Lucia, 2007) or in other terms the 7% of the total energy demand of the USA (Gmehling *et al.*, 1994).

From the industrial point of view, distillation objective consists in performing this separation in the presence of disturbances with the maximum quantity of effluent products with the specified requirements and the minimum consumption of energy (energy saving). Product quality under given specifications and energy saving can be achieved with optimal column design made according to nominal operating conditions.

As it can be seen from the title, this Thesis deals with the "Composition control and estimation with temperature measurements for multicomponent distillation columns". Let us see how the title reflects the issues assessed in the present work.

Composition control. Because of the frequent changes in operating conditions,

it follows that the column is usually not able to attain the required separation task without the assistance of a control system. Sometimes product impurities can be larger than requirements, yielding products that must be reprocessed. On the other hand, when products are purer than needed, a certain amount of energy is wasted and the largest possible quantity of effluent products is not obtained. Therefore, the achievement of desired effluent products and the energy saving task must be carried out through an adequate control system. Indeed, weak composition control can imply losses of energy or products which do not satisfy requirements.

Temperature measurements. For a distillation column, the related control task is the regulation of key effluent impurity compositions within admissible ranges. The ideal control would imply the use of composition analyzers, which unfortunately present high costs of purchase and maintenance, reliability problems, and measurement delays. Therefore, they are inadequate for online composition control. However, indirect online composition regulation can be effectively obtained by means of fast and inexpensive temperature measurements, by controlling the temperature at some appropriate column tray.

Composition estimation. The lack of composition analyzers and the associated measurement delays imply the impossibility of online monitoring the compositions of interest. Online composition analysis would be needed in order to monitor column performance and immediately act when the behavior is different from what is expected. The composition estimation task can be performed by composition estimators that can be realized through a simple model driven by temperature measurements.

Multicomponent columns. Control and estimation composition tasks are difficult for multicomponent distillation columns, where compositions in each tray are not uniquely related to the temperature in the same tray, meaning that the use of temperature measurements does not always allow adequate composition control or estimation. A crucial point is the selection of the number and location of the temperature sensors along the column in order to obtain good performance.

The abovementioned issues are the points of departure of the present PhD Thesis, where the global objective is the *development of strategies for composition control and estimation for multicomponent distillation columns, based on temperature measurements.*

1.2 Summary

The system studied in this Thesis is an industrial multicomponent C3-C4 splitter used in order to separate key component impurities according to the given control objectives.

The column is subject to frequent feed changes which make necessary the employment of an adequate control system for maintaining the effluent products impurities at the desired values. The design of a *control system* requires the selection of both a *structure* and an *algorithm*. The structural problem regards the selection of temperature measurements to be used as controlled outputs, because of the unavailability of composition analyzers. Another issue concerns the selection of control inputs and their pairing with temperature outputs. On the other hand, the control algorithm consists in the data processor that performs the control task.

Effluent product compositions need to be monitored in order to be sure that the controlled product impurities lie within the determined specifications. Unfortunately, because of the lack of dedicate composition analyzers, the problem can not be online solved through direct composition measurements. Therefore, the use of temperature measurement is necessary for indirectly inferring composition values. Besides the control case, also the design of an *estimation system* requires the selection of a structure and an algorithm. Here the definition of structure is different since it concerns the reduced model to be used, the number and location of temperature measurements, the composition states to be innovated and the regions where temperature can be approximated as constant. On the other hand, the *estimation algorithm* consists in the data processor that performs the estimation task.

A summary of this Thesis is shown in the following list, where a brief description of each chapter is given.

Chapter 2. An overview of the present Thesis is presented. The control and estimation problems are illustrated together with the most relevant literature. Finally, the contributions of the present Thesis with respect to the existing state of the art are illustrated.

Chapter 3. The multicomponent C3-C4 splitter subject of this Thesis is introduced. The model employed for simulating the column is presented, and the different operating conditions at which the column works are shown. Then, control and estimation problems are introduced, and the *temperature gradient with per-component contribution diagram*, which is used to study column thermodynamics in order to solve such problems, is presented.

Chapter 4. Here, the *control algorithm* task is addressed. The controllers here employed are based on the *nonlinear constructive control theory* and *passivity* concepts, and are the following ones: (i) a conventional controller, (ii) a cascade controller, and (iii) a cascade-type controller based on Control Lyapunov Functions (CLF).

Chapter 5. This Chapter deals with the *control structure* problem. The temperature gradient with per-component contribution diagram is here used for selecting temperature sensor locations, on the basis of a systematic procedure. Other already established criteria are used for selecting manipulated inputs. Then, the

structural analysis is assessed through the illustration of structural results.

Chapter 6. The *estimator structure* design methodology is here presented. By structure we mean: (i) the model reduction (in this case the selection of both the compositions to be modeled and the regions in which temperature is assumed to be constant), (ii) the number and location of temperature measurements, (iii) the compositions to be innovated by temperature measurement injection and (iv) the regions where temperature can be approximated as constant. Such structure is designed on the basis of the temperature gradient with per-component contribution diagram in conjunction with a systematic procedure.

Chapter 7. The estimators chosen as *estimation algorithms* are here introduced. The focus is on the *Geometric Observer (GE)*, which is a nonlinear Luenberger-type observer and is used in its version with partial innovation. On the other hand, the well-known *Extended Kalman Filter (EKF)* with complete and partial innovation is used for comparison purposes.

Chapter 8. Estimation structural results are assessed and listed in this Chapter.

Chapter 9. The connections between control and estimation structural analysis are here shown.

Chapter 10. Conclusions and recommendations for future research are given.

1.3 Presentations

Some of the topics the present Thesis were presented in both national and international conferences.

Chapter 4 and 5 contents will be submitted for publication in journals.

Chapter 6, 7 and 8 contents were presented in the following conference papers:

- Frau. A., R. Baratti and J. Álvarez (2009). Composition estimation of a six-component distillation column with temperature measurements. In: *IFAC-ADCHEM 2009*. Istanbul, Turkey. pp. 447-452
- Frau. A., R. Baratti and J. Álvarez (2010). Estimation model design for a multicomponent distillation column with temperature measurements. In: *ESCAPE 2010*. Napoli, Italy. pp. 1967-1972
- Frau. A., R. Baratti and J. Álvarez (2010). Estimation structure design for multicomponent distillation column with specific estimation objective. In: *IFAC-DYCOPS 2010*. Leuven, Belgium. pp. 779-784

Moreover, the contents of these chapters will be submitted for publication in journals.

During the PhD the author has also participated to the following conference paper which deals with a controller based on Control Lyapunov Functions for binary columns:

- Castellanos-Sahagún E., J. Álvarez, A. Frau and R. Baratti (2010). Two-point Lyapunov control of binary distillation columns with four temperature measurements. In: *IFAC-DYCOPS 2010*. Leuven, Belgium. pp. 55-60

Chapter 2

Control and estimation overview

In this Chapter, control and estimation problems are thoroughly illustrated. Such problems are adequately stated and motivated, and the respective states of the art are presented. Finally, our methodological approach is presented and compared with respect to the existing literature, with the summarization of the main contributions of the present Thesis.

2.1 Distillation control overview

Distillation columns are designed to separate a given stream into two or more effluent products where key component impurities are regulated around prescribed values. The related control problem consists in effectively performing this separation in spite of disturbances (mainly feed flow rate, composition and temperature), with the minimum waste of energy and the highest recovery of effluent products with the specified requirements. There exists a huge literature about distillation control, and therefore a chronological presentation of the topic would be very complicated and beyond the scopes of the present Thesis. Thus, only the most important papers are presented together with the different points covered, with the aim of motivating our work in the light of the existing literature.

2.1.1 State of the art

In order to obtain an offset-free online composition control, the use of composition analyzers would be needed. Unfortunately, such analyzers present high costs

of purchasing and maintenance, reliability problems, and measurement delays, which result in inadequacy for online composition control. Therefore, column effluent compositions are usually indirectly controlled through temperature measurements, which do not have the shortcomings associated to direct composition analysis. In binary distillation columns, compositions are uniquely related to temperature at same tray. On the other hand, this is not true for the multicomponent case, and these results in a composition offset, but temperature control at appropriate locations can provide efficient composition regulation. Furthermore, the use of multiple temperature measurements per section (cascade-type controllers) can often improve performance.

When using temperature control for indirectly regulating product compositions, a central issue is the sensor location. An appropriate selection of temperature control trays efficiently permits the attainment of the control objective. Different criteria have been employed in order to choose the best temperature sensor location, and some of most used require the selection of trays with: (i) the largest tray to tray temperature gradient (Rademaker *et al.*, 1975); (ii) the largest variation in temperature for a change in manipulated variables (Tolliver and McCune, 1980); (iii) the minimum condition number of the steady-state input-output gain matrix (Moore, 1992). The temperature selection task is more difficult for a multicomponent column, where non-key components can strongly influence the temperature: in this case Rademaker *et al.* (1975) suggested, in addition to the largest temperature gradient criteria, that sensors be located where non-key compositions are almost constant. Luyben (2006) compared five widely used criteria for selecting best control tray location for a five-component depropanizer (among many columns) and on the basis of steady-state performance, suggested that locations close to the bottom, the top, and the feed stages should be avoided, according to considerations in Rademaker *et al.* (1975). Same conclusions were derived for a seven-component depropanizer by Hori and Skogestad (2007), who combined considerations on temperature gradients, variations in temperatures for changes in manipulated variables and influence of non-key components. However, to our knowledge, it seems that a systematic steady-state method for the selection of the best temperature sensor location for control purposes that combines temperature sensitivity and component contributions considerations does not exist for the multicomponent case.

Once pressure, reboiler and condenser levels are fixed, two control inputs remain available. In single-end control structures, only one of the remaining manipulated inputs is used to control one temperature. The remaining one is either kept fixed or ratioed with some other flow, with this ratio kept constant, so that the minimum composition offset is achieved. Sometimes single-end control is not effective for the determined objectives, and the use of the two inputs for regulating two temperatures along the column is needed, that is, dual-end control is required. The effectiveness of each of these structures strongly depends on the control objective, especially on how many product compositions need to be regulated. When only one product composition needs to be regulated, single-

end control is sufficient for control purposes. On the other hand, when both product compositions need to be fixed, a simple rule which permits to decide between single-end or dual-end control has not been found yet (Luyben, 2006; Hori and Skogestad, 2007). The majority of columns is controlled with a single-end configuration since dual-end control is considered as a more difficult task. Moreover, when dual-end control is applied to the column, the possibility of using two-way, one-way, or no decoupling, must be investigated (Fagervik *et al.*, 1983; Castellanos-Sahagún *et al.*, 2006).

The use of virtual temperature outputs, that is, the combinations of different temperature sensors per control loop (cascade-type controllers) was stated to be more effective for disturbance rejection in some situations. Some examples are given in Yu and Luyben (1984) and Castellanos-Sahagún *et al.* (2005).

The problem of controlling product compositions in a distillation column has been extensively addressed with several algorithms. The majority of columns are successfully controlled with either PI or MPC schemes. Recently, fundamentals connections among passivity, optimality and robustness in nonlinear constructive control theory (Sepulchre *et al.*, 1997) have been applied to binary distillation columns, and it has been established that the nonlinear output-feedback SISO one-point (for single-end control) or MIMO two-point (for dual-end control) composition (Castellanos-Sahagún and Álvarez, 2006), temperature (Castellanos-Sahagún *et al.*, 2005) and cascade composition-to-temperature (Castellanos-Sahagún *et al.*, 2006) controller behaviors can be recovered by means of observer-based controllers with linear-decentralized PI components, leading to a control algorithm with: (i) systematic tuning design valid for any structure, ensuring that results are due to the structure itself and not to the tuning, and (ii) anti-windup capability due to the observer integrated in the controller.

2.2 Distillation estimation overview

In order to guarantee the effectiveness of control schemes, product effluent compositions to be controlled should be online monitored. Unfortunately, this is not often possible since this would require the use of dedicate composition analyzers that, because of previously discussed shortcomings, is not usually possible. A possible method for solving this problem is the employment of composition estimators which employ temperature measurements and allow the online estimate of the compositions of interest. Such estimates must lie within a range determined by the admissible control variability for the component and by the uncertainty of the available experimental concentration measurements. Besides the monitoring purposes, composition estimates can be also used (i) for advisory temperature control, implying a set-point adjustment according to composition error, and (ii) for inferential control, in both conventional and composition-temperature parallel cascade (with a master composition loop in conjunction with a slave temperature one) form.

Compared to control case, estimation is a more recent area of interest, and therefore a chronological state of the art can be presented. After listing the most important literature in estimation, our contributions are presented and motivated in the light of the existing works.

2.2.1 State of the art

The first attempt to develop a composition estimator was made in Joseph and Brosilow (1978), where product compositions were inferred by means of temperature and flow measurements, which are chosen on the basis of a trade-off between measurement error and condition number, with a linearized model, yielding the so-called Brosilow's estimator.

Yu and Luyben (1987) extended the Brosilow's estimator to a rigorous nonlinear estimator, and used it for a multicomponent distillation case, finding that $C-1$ temperature measurements are needed for a column that separates a mixture with C components. Such temperature measurements are chosen with the Singular Value Decomposition (SVD) criteria.

Quintero-Marmol *et al.* (1991) stated that even though the column is observable with $C-1$ temperature measurements, at least C sensors are necessary to the estimator for effectiveness, and $C+2$ measurements are needed for robust convergence.

Mejdell and Skogestad (1993) compared the use of Brosilow's estimator, Kalman filter, Principal control regression (PCR) and Partial least squares (PLS) techniques. They found that the Brosilow's estimator is not good for ill-conditioned plants ans recommended the use of the simple PCR estimator. Furthermore, they recommended not to use flow measurements for estimation purposes.

Baratti *et al.* (1995) and Baratti *et al.* (1998) employed an Extended Kalman Filter (EKF) for inferring product compositions in experimental binary and ternary columns, using temperature measurements. They stated that an accurate description of the vapor-liquid equilibrium (VLE) is very important for obtaining good performance.

Kano *et al.* (2000) developed a dynamic PLS for the inferential control of a multicomponent column using temperature measurements and other input variables as flows and pressures.

Shin *et al.* (2000) proposed a nonlinear profile observer based on wave theory using temperature measurements.

An EKF for inferring effluent compositions in multicomponent batch distillation was implemented by Oisiovici and Cruz (2000; 2001) for ternary columns and by Venkateswarlu and Avantika (2001) for a 4-component column.

Zamprogna *et al.* (2005) developed a composition estimator for a ternary batch column with temperature measurements selected on the basis of the PCA technique, and PLS and Artificial Neural Network (ANN) as algorithms for inferring compositions.

Tronci *et al.* (2005) presented a nonlinear Geometric Estimator (GE) (Álvarez and López, 1999) based on the differential geometry theory. Temperature measurements were used for innovating composition states.

Venkateswarlu and Kumar (2006) used the PCA for selecting temperature measurements to be used together with an EKF for inferring compositions in a 4-component reactive batch distillation column.

Álvarez and Fernandéz (2009) employed the GE with truncated models (i.e. with only some of the trays modeled) and data assimilation structure (states to be innovated through temperature measurements) chosen through detectability measurements according to the estimation objective for a binary column.

As it can be seen from the previous state of the art, distillation column composition estimation task has been addressed with a variety of techniques. The EKF with full-order innovation (Jazwinsky, 1970) is by far the most widely used estimation technique. Unfortunately, it requires the integration of a large set of nonlinear Ordinary Differential Equations (ODEs) and the tuning must be made via trial-and-error, leading to a procedure that can be very time consuming. GE and EKF with partial innovation were used in order to obtain a considerable reduction of the number of the ODEs to be integrated for binary (Fernandéz, 2007) and ternary (Pulis, 2007) columns. Moreover the GE, differently from the EKF, has a systematic and simple tuning procedure for any admissible estimation structure.

Like in control case, compositions cannot be online monitored through composition analyzers because of the associated delays, together with maintenance and reliability problems. The inference can be made online by using data available from temperature sensors. Another important issue is therefore the number and location of temperature measurements to be used for estimation purposes. Only few works (Joseph and Brosilow, 1978; Yu and Luyben, 1987; Quintero-Marmol *et al.*, 1991; Zamprogna *et al.*, 2005; Venkateswarlu and Kumar, 2006; Álvarez and Fernandéz, 2009) dealt with this matter, which on the contrary has been more widely considered for the control case.

Regarding the model reduction, the three most used methods that have been proposed are tray aggregation, wave propagation theory and orthogonal collocation. Tray aggregation (Benallou *et al.*, 1986; Levine and Rouchon, 1991; Linhart and Skogestad, 2009; Linhart and Skogestad, 2010) consists in partitioning the column into compartments composed by a dynamic aggregation tray and other steady-state trays, in such a way that a reduced-order model is obtained. Wave propagation theory (Balasubramhanya and Doyle III, 1997; Shin *et al.*, 2000; Hankins, 2007) approximates the column dynamics through traveling wave profiles.

Orthogonal collocation (Huss and Westerberg, 1996; Dalaouti and Seferlis, 2006) is used for the approximation of state variable profiles as sums of orthogonal polynomials.

Recently, the entire estimation structure (i.e., the model reduction, the number and location of temperature sensors, the states to be innovated) has been considered as a degree of freedom in the design of the observer, on the basis of the given estimation objective (Fernandéz, 2007; Álvarez and Fernandéz, 2009). Detectability measurements were used for the selection of the estimation structure, leading to the employment of complete and truncated models with complete or partial innovation.

2.3 Contributions

The main contribution of the present Thesis with respect to the abovementioned state of the art, is the construction of a *methodology* that consists in the *partition of both control and estimation problem into a structural and an algorithmic part*, permitting a more *systematic joint design* through a *unified approach*. Such methodology puts together techniques already employed and new ideas. Its main tool is the *temperature gradient with per-component contribution diagram*, which is based on the temperature slope criterion (Rademaker *et al.*, 1975), and consists in plotting the temperature gradient profile at a nominal steady-state, together with the contributions due to each component. This diagram only requires steady-state information, and will be extensively used in this Thesis in conjunction with systematic procedures for the selection of part of the control structure and the entire estimation one.

In the following, the other contributions for solving the control and estimation problem are listed.

Control problem contributions

- The selection of temperature sensor locations is made through the temperature gradient with per-component contribution diagram in conjunction with a systematic procedure. Temperature sensors for control purposes must be placed in stages with (i) quite large temperature gradients and (ii) small contribution of non-key components to these gradients. Furthermore, sensors must be located according to the control objective, that is, they must be placed in the column section that contains the product impurity to be regulated.

- On the basis of nonlinear constructive control theory (Sepulchre *et al.*, 1997) and passivity concepts, observer-based controllers with linear-decentralized PI components with anti-windup protection are developed for indirect com-

position regulation through temperature measurements. This approach was used by Castellanos-Sahagún *et al.* (2005) for a binary column, and is here employed for a multicomponent case. Furthermore, a conventional parallel cascade observer-based controller is developed on the basis of the same ideas.

- In addition to the conventional and cascade controllers, nonlinear constructive control theory allows the construction of a parallel cascade-type observer-based temperature controller based on Lyapunov stability theorem. A control function is built such that a given system Lyapunov function be positive definite and its time derivative be negative definite. Such control function is defined as Control Lyapunov Function (CLF). This cascade-type controller is based on a virtual temperature output combination of a primary and a secondary temperature measurement. Castellanos-Sahagún *et al.* (2010) used this approach for developing a controller for a binary column; in this Thesis the approach is extended to the multicomponent case.

Estimation problem contributions

- The model reduction task is addressed for a multicomponent column following the ideas for column model reduction given in Fernandéz (2007) and Álvarez and Fernandéz (2009). Since detectability measures method becomes intractable for multicomponent columns, the removal task is here performed with a simpler criterion which consists of the employment of the temperature gradient with per-component contribution diagram in conjunction with a systematic procedure. According to this method, components are retained in the model if their contribute to the gradients is significant in the section of interest, according to the estimation objective. On the other hand, a further reduction is performed with the assistance of the temperature gradient with per-component contribution diagram following aggregation tray ideas, but in a different way: the temperature has been assumed as constant and equal to the average one, in the regions where gradients are small.

- As for the control case, the temperature gradient with per-component contribution diagram is used for selecting sensor locations for estimation purposes, differently from Fernandéz (2007) where detectability measure methods (intractable for multicomponent columns) were used for a binary case. In this case, gradients are used according to a systematic criterion which consists in placing temperature sensors in stages with (i) large temperature gradients and (ii) small contribution of unmodeled components to these gradients. Furthermore, sensors must be located according to the estimation objective, that is, they must be placed in the column section that contains product impurity to be monitored.

- The temperature gradient with per-component contribution diagram is also used for selecting states to be innovated, in a simpler manner compared to

the detectability measure method used in Fernandéz (2007). According to the gradient profiles, the composition to be innovated in a tray where the sensor is placed, is the one that mostly contributes to the temperature gradient of that tray.

2.4 Chapter summary

In this Chapter, control and estimation problems of the present Thesis have been introduced and motivated on the basis of the existing literature, which has been listed and described. Our methodological approach is based on the partition of both problems in a structural and an algorithmic part. Finally the main contributions of this Thesis are summarized: here it is sufficient to mention that (i) the temperature gradient with per-component contribution diagram is presented and used in this Thesis for solving most of the structural parts of the problems, since it is simpler and more intuitive compared to other well known methods and can be easily used by process engineers, and that (ii) observed-based controllers based on passivity concepts are developed and used.

Chapter 3

Distillation Columns

The methodology adopted in this work is intended for composition control and estimation with temperature measurements of the entire class of columns including the six-component depropanizer column subject of this study. Therefore, the complete model (i.e., where all stages and components are modeled) used for simulating the dynamics of a column with any number of stages and components is illustrated, after the description of the general distillation model features. Next, the six-component depropanizer is described, and control and estimation problems are introduced, together with the objectives to be attained. Finally, the temperature gradient with per-component contribution diagram is presented and used for a thermodynamic analysis of the column.

3.1 Introduction

Distillation columns are used in order to separate an inlet stream with more components into two or more outlet products with specified impurity compositions. Separation takes place in the column because of the difference in volatility of the components: a vapor stream, produced in the reboiler by heat supply rises through the column while a liquid stream coming from the reflux drum and the feed stage goes downwards. Vapor-liquid equilibrium is assumed on each stage, and the liquid and vapor streams leaving the stage have different compositions: liquid is enriched with the least volatile components, while vapor is enriched with the most volatile components.

Dynamical distillation models are widely used since they are powerful tools for flexibly handling different processes and operations (e.g., closed-loop responses, start-up and shutdown procedures, etc.). The state of the art can be seen elsewhere (e.g., Gani *et al.* (1986), Luyben (1989)): here it suffices to mention that

distillation models able to capture the main behavior of a column usually present the following features:

- *High order*, which is due to the large set of ODEs that arises from the material (composition and holdup) and enthalpy balances on each tray. The number of each kind of balance equations increases with the number of trays, since one equation per tray is needed; moreover, the number of composition balance equations rises with the number of components as well, since one equation per tray and component (all but one) is required.
- *Strong nonlinearity*, which is present because of the vapor-liquid equilibrium (VLE), which is described by a nonlinear function.
- *Ill-conditioning or high directionality*, caused by the fact that the outputs are much more sensitive to certain combinations of inputs than to others (Skogestad and Morari, 1988).
- *Stiffness*, determined by the separation between large and small time constants related to slow and fast column dynamics (Tyreus *et al.*, 1975).

Distillation models can be classified in several ways. On the basis of the balances taken into account, they are often divided in (i) EMC, (ii) MC and (iii) C models, where E, M and C stand for enthalpy, mass and composition balances respectively (Levy *et al.*, 1969). EMC models are the most rigorous, since both enthalpy, holdup and composition balances are included. MC models do not take energy balances into account, mainly because of almost equal vaporization heats which imply constant molar flows along the column. Finally, C models only include composition balances since constant holdups are assumed. Models can also be denoted as *complete* if balances are modeled for each tray and component, and as *reduced* if some tray or composition balance is neglected or lumped.

The kind of model adopted strongly depends on its purpose: when a model is used for simulation and analysis a quite detailed model is usually required; on the other hand, models adopted for online control or estimation aims do not have to be complex in order to avoid large computing times.

3.2 Column model

The *complete model* that is going to be described can be used for simulating the dynamics of a multicomponent column with any number of stages and components, under the following standard assumptions (Skogestad, 1997; Baratti *et al.*, 1998):

- Energy balances neglected on each tray and constant liquid and vapor flow rates for each column section. Changes in flow rates are only due to feed, reflux and vapor streams, and to feed and reflux subcoolings.

- Holdup dynamics are neglected, meaning they are assumed to be constant. It can equivalently be assumed that reboiler and condenser holdups are tight controlled. This means that fast column dynamics are not described. Since level controllers act on holdup volume, here it is assumed that the volumetric holdup is constant while the molar one is updated on the basis of the composition at that tray.

- Linear pressure drop is assumed along the column.

- The reboiler is modeled as an ideal separation stage (partial reboiler), while the condenser is total.

If previous assumptions hold, a column with N stages, C components and m temperature sensors can be modeled through the following equations:

Composition states ($i = 1, \dots, N$, $j = \rho_1, \dots, \rho_{C-1}$)

$$\dot{c}_i^j = f_i^j(\mathbf{c}_{i-1}, \mathbf{c}_i, \mathbf{c}_{i+1}, Q, R, F, \mathbf{c}_F, T_F) \tag{3.1a}$$

Temperatures ($k = 1, \dots, m$)

$$T_{s_k} = \beta_{s_k}(\mathbf{c}_{s_k}) \tag{3.1b}$$

According to previous model classification, Eq. (3.1) is a C model (Levy *et al.*, 1969), since only composition balances are modeled; furthermore, Eq. (3.1) is a *complete* model since balances are present for each component at each stage.

In Eq. (3.1), c_i^j is the liquid mole fraction of the component j at stage i, Q is the reboiler duty, R is the reflux, F is the feed flow, T_F and T_{s_k} are feed and s_k-th stage temperatures, with s_k denoting the stage where the k-th sensor is placed. ρ_j is the tag associated to the j-th component. $\mathbf{c}_i$ and $\mathbf{c}_F$ represent the composition vectors at i-th and feed stage respectively. The components $c_i^{\rho_C}$ for $i = 1, \dots, N$ are not modeled, being uniquely determined by the mass conservation condition $\sum_{j=1}^{C} c_i^{\rho_j} = 1$.

f_i^j and β_{s_k} are the mole balance (for component j at i-th stage) and the bubble-point (at s_k-th stage) functions: their expressions are given by the next equations:

Reboiler ($i = 1$, $j = \rho_1, \dots, \rho_{C-1}$)

$$\dot{c}_1^j = \frac{L_S(c_2^j - c_1^j) - V_S v_1^j}{H_1} := f_i^j(\mathbf{c}_1, \mathbf{c}_2) \tag{3.2a}$$

Generic stage i in the stripping section ($i = 2, \ldots, N_F - 1$, $j = \rho_1, \ldots, \rho_{C-1}$)

$$\dot{c}_i^j = \frac{L_S(c_{i+1}^j - c_i^j) - V_S(v_i^j - v_{i-1}^j)}{H_i} := f_i^j(\mathbf{c}_{i-1}, \mathbf{c}_i, \mathbf{c}_{i+1}) \tag{3.2b}$$

Feed tray ($i = N_F$, $j = \rho_1, \ldots, \rho_{C-1}$)

$$\dot{c}_{N_F}^j = \frac{L_E c_{i+1}^j - L_S c_i^j - V_E v_i^j + V_S v_{i-1}^j + F c_F^j}{H_{N_F}} := f_{N_F}^j(\mathbf{c}_{N_F-1}, \mathbf{c}_{N_F}, \mathbf{c}_{N_F+1}, \mathbf{c}_F) \tag{3.2c}$$

Generic stage i in the enriching section ($i = N_F + 1, \ldots, N - 2$, $j = \rho_1, \ldots, \rho_{C-1}$)

$$\dot{c}_i^j = \frac{L_E(c_{i+1}^j - c_i^j) - V_E(v_i^j - v_{i-1}^j)}{H_i} := f_i^j(\mathbf{c}_{i-1}, \mathbf{c}_i, \mathbf{c}_{i+1}) \tag{3.2d}$$

Top tray ($i = N - 1$, $j = \rho_1, \ldots, \rho_{C-1}$)

$$\dot{c}_{N-1}^j = \frac{L_T c_N^j - L_E c_{N-1}^j - V_T v_{N-1}^j - V_E v_{N-2}^j}{H_{N-1}} := f_{N-1}^j(\mathbf{c}_{N-2}, \mathbf{c}_{N-1}, \mathbf{c}_N) \tag{3.2e}$$

Condenser ($i = N$, $j = \rho_1, \ldots, \rho_{C-1}$)

$$\dot{c}_N^j = \frac{V_T v_{N-1}^j - L_T c_N^j}{H_N} := f_N^j(\mathbf{c}_{N-1}, \mathbf{c}_N) \tag{3.2f}$$

Implicit bubble-point function β_{s_k} ($k = 1, \ldots, m$)

$$\sum_{j=\rho_1}^{\rho_C} c_{s_k}^j P_{s_k}^j(T_{s_k}) - P_{s_k} = 0 \tag{3.2g}$$

The state of the i-th stage is described by the $(C-1)$-dimensional composition vector $\mathbf{c}_i = \begin{bmatrix} c_i^{\rho_1} & \ldots & c_i^{\rho_{C-1}} \end{bmatrix}^T$. H_i is the molar holdup at i-th stage.

Each vapor composition $v_i^{j,*}$ in equilibrium with the corresponding liquid one c_i^j is given by the ideal liquid-vapor equilibrium equation:

$$v_i^{j,*} = c_i^j \frac{P_i^j(T_i)}{P_i}$$

where P_i^j is the partial pressure at i-th stage due to the component j and P_i is the total pressure at i-th stage.

The partial pressures P_i^j are computed by the following Extended Antoine Equation, which is a 7-constant extension of the standard Antoine Equation:

$$P_i^j = \exp\left(A_j - \frac{B_j}{C_j + T_i} + D_j T_i + E_j \ln(T_i) + F_j T_i^{G_j}\right)$$

The composition of vapor leaving the i-th stage for the component j is computed from the corresponding equilibrium value $v_i^{j,*}$ through the Murphree efficiency E as follows:

$$E = \frac{v_i^j - v_{i-1}^j}{v_i^{j,*} - v_{i-1}^j}$$

L and V are the liquid and vapor molar flows along the column, and their subindices S, E, and T stand for stripping section, enriching section, and top tray respectively. They are computed according to following equations:

$$\begin{aligned} L_T &= R & V_S &= V \\ L_E &= L_T + \Delta V_R & V_E &= V_S - \Delta V_F \\ L_S &= L_E + F + \Delta V_F & V_T &= V_E - \Delta V_R \end{aligned}$$

F, R and V are the feed, reflux and vapor (leaving the bottom) molar flows respectively. ΔV_F and ΔV_R are the molar flow variations due to feed and reflux subcoolings, given by

$$\Delta V_F = \frac{F C_{p,N_F}(T_{N_F} - T_F)}{\lambda_{v,N_F}} \qquad \Delta V_R = \frac{R C_{p,N}(T_N - T_R)}{\lambda_{v,N}}$$

Reflux temperature T_R is smaller than equilibrium temperature at condenser stage T_N due to subcooling. $C_{p,i}$ and $\lambda_{v,i}$ are respectively the heat capacity and heat of vaporization at i-th stage.

Input and disturbances flows entering the model are given in volumetric units, while the reboiler duty is given in caloric units. The volumetric flows are subsequently converted in mole units on the basis of the current composition, while the reboiler duty Q is converted into the respective vapor molar flow V (Reid *et al.*, 1998).

3.3 Case study

The multicomponent column subject of the present work is a prototype of an *industrial six-component C3-C4 splitter*, whose dynamics are simulated by Eq. (3.2). The column is mainly fed with a flow which presents significant concentrations of propane (C3), iso-butane (iC4) and n-butane (nC4), while ethane (C2), iso-pentane (iC5) and n-pentane (nC5) are there in much smaller amounts. The

column has 35 Nutter Float Valve trays (with a diameter of 2 m and a spacing of 610 mm), a kettle reboiler (1-st stage) and a total condenser (37-th stage), for a total of $N = 37$ stages. Feed stage is located at 19-th stage ($N_F = 19$). The condenser subcooling ($T_R - T_N$) is equal to 5 K, and the efficiency E is equal to 0.8.

Such column is designed to perform the separation of the two key components: the C3 (light key-component, i.e., heaviest among light components) and the iC4 (heavy key-component, i.e., lightest among heavy components). In order to obtain the desired separation, one or two key impurities, that is, C3 in the bottom (c_1^{C3}) and iC4 in the distillate (c_N^{iC4}), must be regulated around their nominal SS values.

In this Thesis, two different nominal SS operating conditions denoted as SS1 (steady-state 1) and SS2 (steady-state 2) are considered. Such conditions are listed in the following, and the values of key impurities at these conditions are emphasized. Each of the steady-states considered will be subsequently related to a control objective, which consists in the regulation of one or two key impurities around their nominal value. Then, for each control objective considered, the related estimation objective will be the monitoring of the controlled key impurities. From now on, the symbol $(\bar{\cdot})$ will stand for the nominal value or the set-point of a variable.

Nominal Steady-state (SS1)

The SS nominal conditions denoted as SS1 are reported in Table 3.1.

F	$\bar{c}_F^{C2}$	$\bar{c}_F^{C3}$	$\bar{c}_F^{iC4}$	$\bar{c}_F^{nC4}$	$\bar{c}_F^{iC5}$	T_F
88.2 $\mathrm{m^3\,h^{-1}}$	0.0036	0.281	0.236	0.4746	0.0004	320 K
Q			R			
3876645 $\mathrm{kcal\,h^{-1}}$			61.62 $\mathrm{m^3\,h^{-1}}$			

Table 3.1: Operating conditions for SS1

As it can be seen from Figure 3.1, where composition and temperature profiles at SS1 are shown, key impurities present the following values:

$$\bar{c}_D^{iC4} = \bar{c}_N^{iC4} \approx 0.02 \tag{3.3a}$$

$$\bar{c}_B^{C3} = \bar{c}_1^{C3} \approx 10^{-5} \tag{3.3b}$$

In SS1 case, column is working at high-purity conditions in the bottom section, as it can be seen from the very small amount of C3 (see Eq. (3.3b)). This will influence the control objective related to these operating conditions, as will be illustrated later.

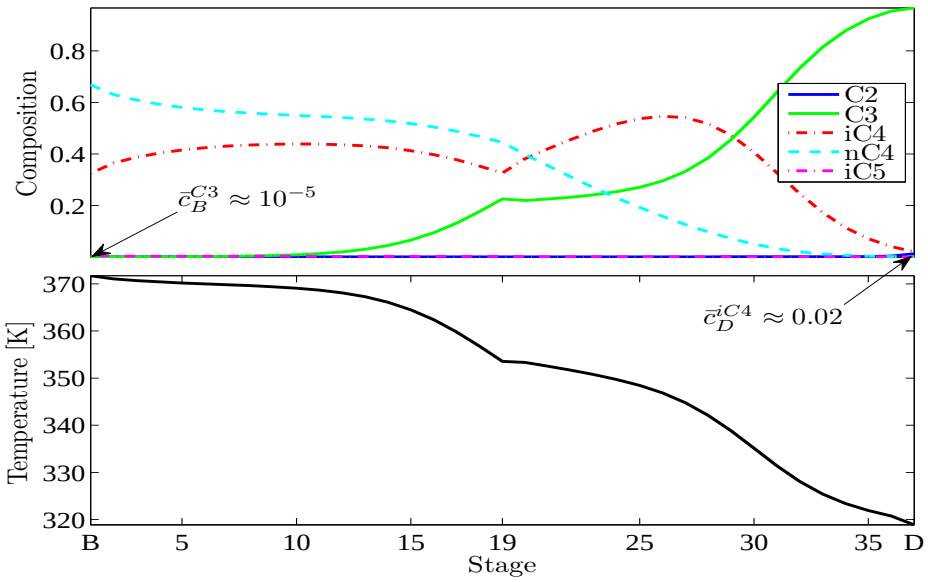

Figure 3.1: Steady-state composition and temperature profiles for SS1

Nominal Steady-state (SS2)

In Table 3.2, nominal conditions of SS2 are listed.

$\bar{F}$	$\bar{c}_F^{C2}$	$\bar{c}_F^{C3}$	$\bar{c}_F^{iC4}$	$\bar{c}_F^{nC4}$	$\bar{c}_F^{iC5}$	$\bar{T}_F$
88.2 $m^3\,h^{-1}$	0.0036	0.281	0.236	0.4746	0.0004	320 K
$\bar{Q}$			$\bar{R}$			
2665688 Kcal·h^{-1}			34.99 $m^3\,h^{-1}$			

Table 3.2: Operating conditions for SS2

Composition and temperature profiles at SS2 are depicted in Figure 3.2, where it can be seen that key impurity values are the following:

$$\bar{c}_D^{iC4} = \bar{c}_N^{iC4} \approx 0.02 \tag{3.4a}$$

$$\bar{c}_B^{C3} = \bar{c}_1^{C3} \approx 0.02 \tag{3.4b}$$

In this case, no section of the column is working at high-purity conditions, and therefore the nominal reboiler heat duty $\bar{Q}$ and the reflux rate $\bar{R}$ are smaller than in SS1 case, implying a larger amount of effluent products and a smaller amount of energy needed for performing the separation. The control objective for the column operating at SS2 conditions will be different from SS1 case, as will be shown afterwards.

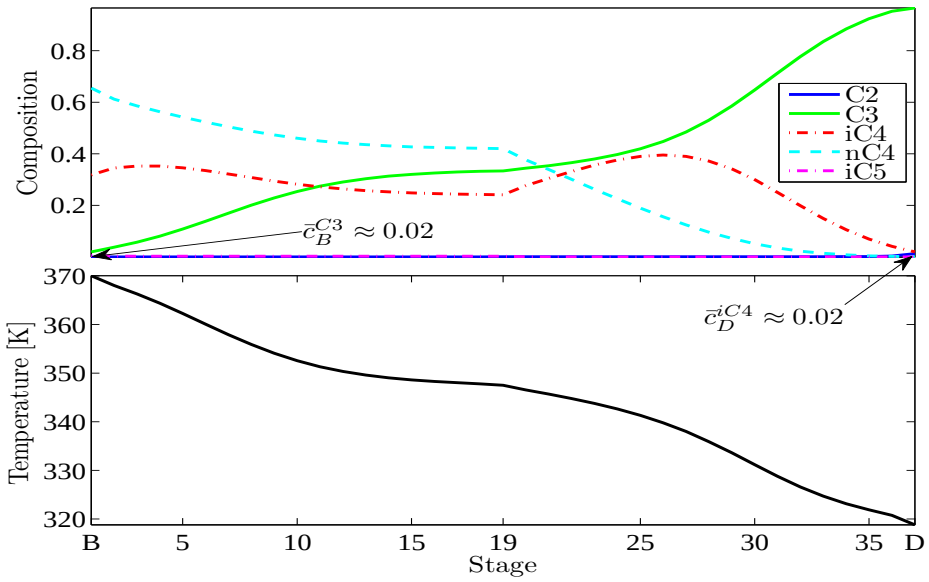

Figure 3.2: Steady-state composition and temperature profiles for SS2

3.4 Control problem

The control problem for a distillation column consists in performing the required separation in spite of the disturbances entering the column, possibly with the maximum quantity of effluent products with the specified requirements and the minimum consumption of energy. Typical disturbances are changes in feed flow rate, composition and temperature, generally due to outlet flows which stem from upstream units.

In order to perform such separation, generally one or two key impurities (i.e., C3 in the bottom and the iC4 in the distillate, for the present case) have to be fixed around their nominal SS values, meaning that compositions have to be regulated within a prescribed range. Due to common unavailability of composition analyzers for control purposes, in this Thesis key impurities are indirectly regulated through one or more appropriate temperature measurements for each control loop, by manipulating reboiler heat duty and/or reflux flow rate.

On the basis of the different SS nominal conditions SS1 (see Eq. (3.3)) and SS2 (see Eq. (3.4)), two different control objectives are here considered:

Control Objective 1 (CO1). This objective is the regulation of iC4 in the distillate (heavy-key impurity) around the nominal value (0.02) within a certain range (0.005), and has to be achieved at the nominal conditions SS1 (stripping

section working at high-purity conditions) listed in Table 3.1.

$$c_D^{iC4} \in \bar{c}_D^{iC4} \pm \Delta c = 0.02 \pm 0.005 \tag{3.5}$$

Control Objective 2 (CO2). This objective is the joint regulation of iC4 in the distillate (heavy-key impurity) and of C3 in the bottom (light-key impurity) around the nominal value (0.02) within a certain range (0.005), and has to be achieved when nominal conditions are the ones at SS2 (no section working at high-purity conditions), listed in Table 3.2.

$$c_D^{iC4} \in \bar{c}_D^{iC4} \pm \Delta c = 0.02 \pm 0.005 \tag{3.6a}$$

$$c_B^{C3} \in \bar{c}_B^{C3} \pm \Delta c = 0.02 \pm 0.005 \tag{3.6b}$$

$$\tag{3.6c}$$

The maximum composition offset allowed is $\Delta c = 0.005$, and this is equivalent to say that the maximum relative error has to lie within $\pm 25\%$. Impurity values larger than 0.025 would imply the reprocessing of the product, since the quality is smaller than required; on the other hand, values smaller than 0.015 mean that the product purity and the consumption of energy are higher than necessary.

Note that the objective CO1 only consists in regulating the compositions of iC4 in the distillate, due to the fact that effluent bottom product is overpurified and therefore C3 composition does not need to be regulated since it is self-regulating. On the other hand, both key impurity compositions need to be regulated in CO2 case.

The control problem is solved through its partition into a structural and an algorithmic part. The control structural problem consists in (i) the selection of the location where temperature sensors are placed (one or more, according to the employed algorithm), (ii) the manipulated variables, and (iii) their pairing when dual-end configurations are considered. On the other hand, the control algorithmic problem is separately addressed with 3 control algorithms based on passivity concepts and nonlinear constructive theory (Sepulchre *et al.*, 1997): (i) a conventional controller; (ii) a cascade controller; (iii) a CLF controller (a cascade-type controller based on Lyapunov stability theorem).

3.5 Composition estimation from an industrial perspective

In industrial situations, compositions to be regulated have to stay within a composition range in order to satisfy quality and energy saving requirements. Consider, for instance, the regulation of one of the key impurities, the iC4 in the distillate, when the column is working at SS1 conditions (3.3): in such case the controller has to maintain that composition around its nominal value $\bar{c}_D^{iC4} = 0.02$. Suppose, as done in Section 3.4, that variations be only permitted within a ± 0.005 range

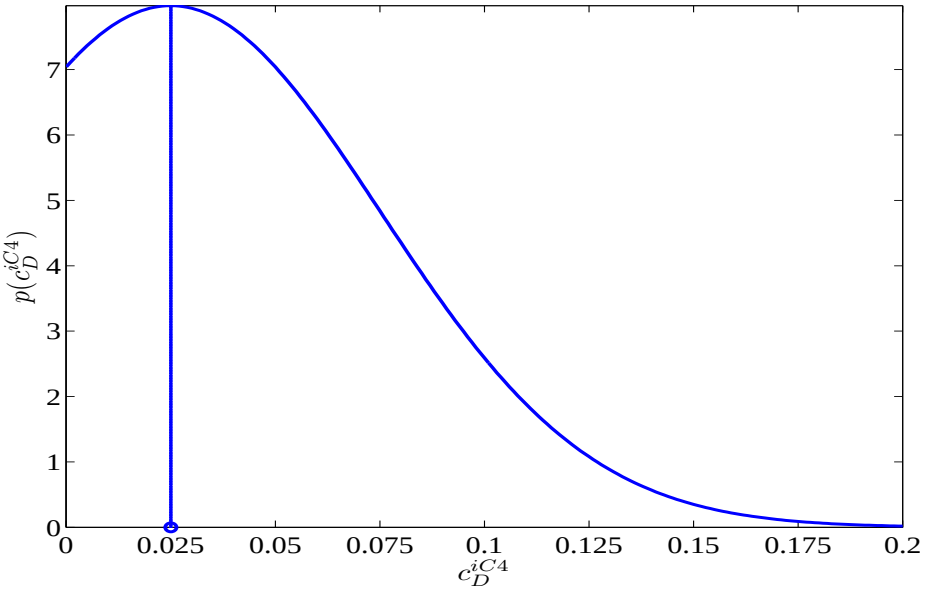

Figure 3.3: Possible yearly trend for iC4 distillate composition

(i.e. relative error equal to ±25% is allowed). In typical industrial processes, such composition presents large fluctuations during a long period even though a control action is performed: a possible behavior during a year is summarized by the probability density function (assumed to be Gaussian for sakes of simplicity) in Figure 3.3, where it can be noted that c_D^{iC4} frequently lies between 0 and 0.05, and (ii) its yearly average 0.025 is different from the given set-point. This means that often, in industrial situations, the product does not satisfy prescribed requirements.

Because of the unavailability of direct composition analyzers, a composition estimator driven by temperature measurements is needed. With such estimator, it is possible to improve the separation performance through (i) advisory control, (ii) inferential control, and (iii) composition-temperature cascade control. Even if these control options will not be explored in the present Thesis, it is important to illustrate as the employment of such estimator has a positive effect on controller behavior.

A possible c_D^{iC4} yearly trend to be obtained through the use of an estimator is shown in Figure 3.4, where it is also compared to the actual trend without the assistance of the estimator.

The objective can be achieved through an online composition estimator whose c_{iC4}^D estimate distribution (assumed to be gaussian as well) is illustrated in Figure 3.5, and compared to the desired composition trend.

It must be noted that the estimation error distribution has to be sufficiently

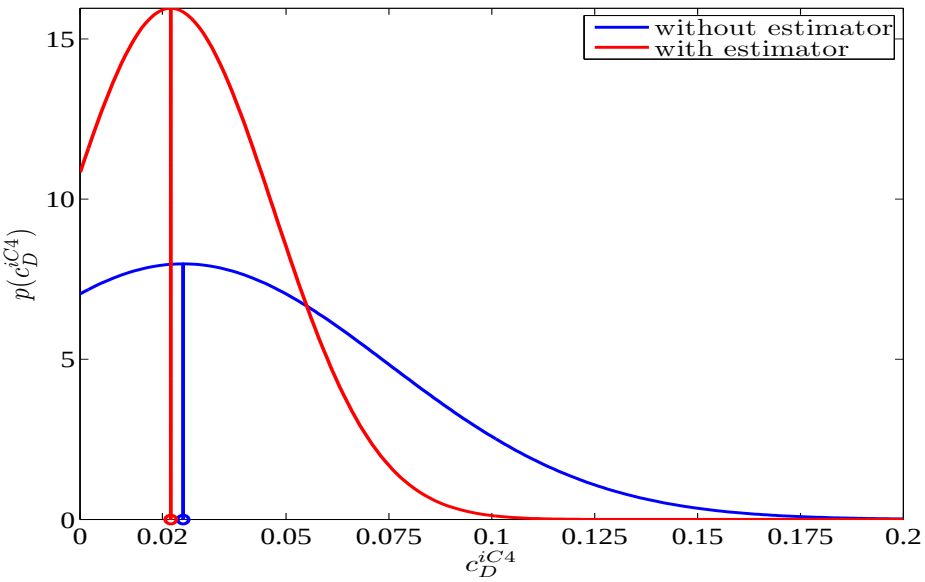

Figure 3.4: Possible yearly trend for iC4 distillate composition with the assistance of a composition estimator, and comparison with trend without estimator assistance.

smaller than the one of the desired composition trend, but it is not necessary that composition values lie in a range smaller than the typical composition measurement error one. Indeed it is impossible to assess controller performance with more accuracy than a composition analyzers, because it is impossible to appreciate a composition error smaller than analyzer accuracy.

In the following sections, the estimation problem will be introduced with the statement of the estimation objective, and the estimation range will be given according to the considerations of this section.

3.6 Estimation problem

The estimation problem addressed in this Thesis is the online composition inferring of one or two key impurities around the prescribed range, according to the control objective to be achieved, meaning that the impurities to be estimated are the controlled ones. Indeed, such impurities need to be estimated in order to monitor the desired separation; however, because of the unavailability of means for online measuring such compositions, estimators driven by available measurements need to be used. In this Thesis, two estimation objectives are considered,

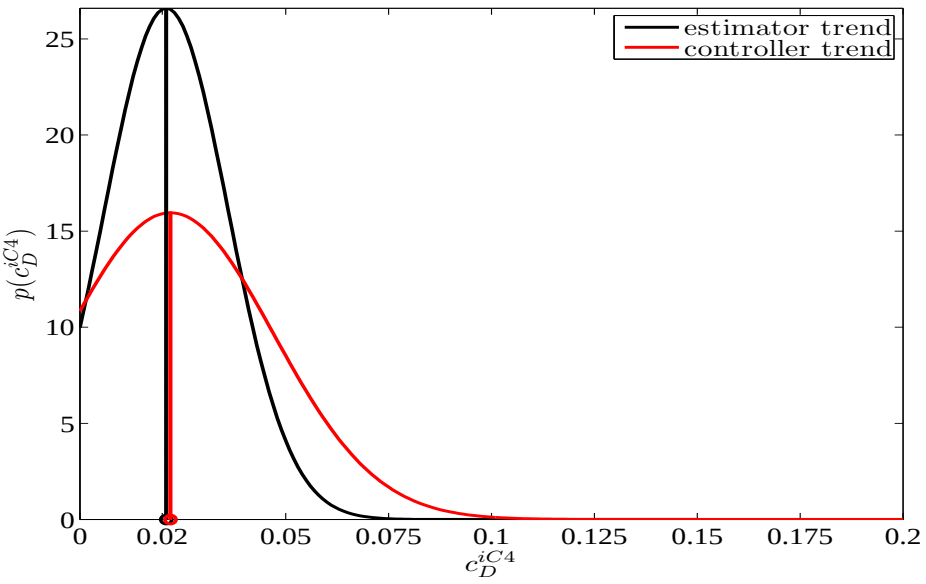

Figure 3.5: Comparison of yearly trend for iC4 distillate composition controlled with the assistance of a composition estimator, and necessary estimation trend.

with each of them related to one of the control objectives CO1 (see Eq. (3.5)) and CO2 (see Eq. (3.6)):

Estimation Objective 1 (EO1). This objective consists in the estimation of distillate iC4 dynamics within the prescribed range when the control objective CO1 (regulation of distillate iC4) is achieved, and has to be attained with nominal conditions SS1 (stripping section working at high-purity conditions), listed in Table 3.1

$$\hat{c}_D^{iC4}(t) \in c_D^{iC4}(t) \pm \Delta\hat{c} = c_D^{iC4}(t) \pm 0.015 \tag{3.7}$$

Estimation Objective 2 (EO2). This objective consists in the joint estimation of distillate iC4 and bottom C3 dynamics within the prescribed range when the control objective CO2 (joint regulation of distillate iC4 and bottom C3) is achieved, and has to be attained with nominal conditions SS2 (no section working at high-purity conditions), listed in Table 3.2

$$\hat{c}_D^{iC4}(t) \in c_D^{iC4}(t) \pm \Delta\hat{c} = c_D^{iC4}(t) \pm 0.015 \tag{3.8a}$$

$$\hat{c}_B^{C3}(t) \in c_B^{C3}(t) \pm \Delta\hat{c} = c_B^{C3}(t) \pm 0.015 \tag{3.8b}$$

In Eq. (3.7) and (3.8), and in the following, the symbol $(\hat{\cdot})$ stands for estimate. According to the estimation objectives, impurities of interest must be online in-

ferred within an admissible range ($\Delta\hat{c} = 0.015$), and determined both by the admissible control variability for the component and by the uncertainty of the infrequent and delayed experimental concentration determinations, as illustrated in Section 3.5. The estimators must be assessed as a compromise among speed, robustness and simplicity. In this Thesis, in order to obtain a simple and fast estimator, a *reduced model* is used. Such model has a smaller number of ODEs compared to the $N(C-1)$ ones necessary for modeling the actual columns as in Eq. (3.1), and is driven by temperature measurements, through the innovation of some appropriate composition states, in order to infer the compositions of interest. A further model reduction can be obtained by approximating the temperature in a column region (to be determined) as the average one. The joint selection of (i) the components to be modeled, (ii) the number and location of temperature measurements along the column, (iii) the composition states to be innovated, and (iv) the regions where temperature is approximated as the average one, form the *estimation structure* problem.

The whole structural problem is now addressed in mathematical terms. The column system (3.1) can be written in compact form as:

$$\dot{\mathbf{c}} = \mathbf{f}_c(\mathbf{c}, \mathbf{u}, \mathbf{w}) \tag{3.9a}$$

$$\mathbf{y} = \boldsymbol{\beta}(\mathbf{c}) \tag{3.9b}$$

In Eq. (3.9), $\mathbf{c} = [{\mathbf{c}_1}^T \cdots {\mathbf{c}_N}^T]^T \in \mathbb{R}^n$ is the state vector and includes all compositions for each component and stage along the column; $\mathbf{u} = [R\, Q]^T$ is the input vector; $\mathbf{w} = [F\, \mathbf{c}_F\, T_F]^T$ is the disturbance vector; $\mathbf{y} = [T_{s_1} \cdots T_{s_m}]^T \in \mathbb{R}^m$ is the output vector that includes all measured temperatures; $\mathbf{f}_c = [{\mathbf{f}_1}^T \cdots {\mathbf{f}_N}^T]^T$, with $\mathbf{f}_i = [f_i^{\rho_1} \ldots f_i^{\rho_{C-1}}]^T$, includes the mass balance functions for all compositions (minus one) at each stage; $\boldsymbol{\beta} = [\beta_{s_1} \cdots \beta_{s_m}]^T$ is the bubble-point function vector.

In the case in exam, the order of the model which describes the actual column is $n = N(C-1) = 185$, that is, 185 ODEs need to be integrated in order to simulate column dynamics. The estimation problem consists in designing a composition estimator according to the specific estimation objective, and can be split into the *estimation structure* design and the *estimation algorithm* selection.

As regards the estimation structural problem, the first task addressed in this Thesis is the development of a reduced estimator model where only $C_M < C$ components are modeled: in compact notation such model is described as

$$\dot{\hat{\mathbf{x}}} = \hat{\mathbf{f}}(\hat{\mathbf{x}}, \hat{\mathbf{u}}, \hat{\mathbf{d}}) \tag{3.10a}$$

$$\hat{\mathbf{y}} = \hat{\boldsymbol{\beta}}(\hat{\mathbf{x}}) \tag{3.10b}$$

The estimated state vector $\hat{x} = [\hat{\mathbf{x}}_1^T \cdots \hat{\mathbf{x}}_N^T]^T \in \mathbb{R}^{n_M}$ in Eq. (3.10) has a smaller dimension ($n_M < N$) than the system state vector in Eq. (3.9). Indeed, the dimension of each vector $\hat{\mathbf{x}}_i = [\hat{c}_i^{\phi_1} \cdots \hat{c}_i^{\phi_{C_M-1}}]$, where ϕ_j is the tag associated to the j-th component of the reduced model, is $C_M - 1$, meaning that the order of the

system is $n_M = N(C_M - 1) < n$. For the same reason, the estimated disturbance vector $\hat{\mathbf{d}} = [\hat{F}\, \hat{\mathbf{x}}_F^T\, \hat{T}_F]^T$ has a smaller dimension than the disturbance vector w in Eq. (3.9a). The subsequent task is the selection of m measured temperatures together with their locations $s_1, \cdots, s_m$ for estimation purposes. Subsequently, the innovated-noninnovated state partition $[\hat{x}_I, \hat{x}_{II}]$ must be suitably selected, meaning that the composition states which must be innovated with temperature measurement injection must be chosen. Finally, the temperature is approximated as the average one in some regions to be determined, leading to a further model approximation (change in function approximation $\hat{f}$) and reduction (number of states smaller than n_M). The entire estimation structural problem will be addressed later in Chapter 6.

On the other hand, the other part of the estimation problem is the determination of the *estimation algorithm*, which is the dynamic data processor that performs the estimation task, and will be discussed afterwards: here it is sufficient to say that the focus is on Geometric Estimator (GE) algorithm with partial innovation, while the well-known Extended Kalman Filter (EKF) with partial and complete innovation will be used for sakes of comparison.

3.7 The temperature gradient with per-component contribution diagram

In order to obtain a good control and estimate of the components of interest with temperature measurements only, it is necessary to understand the behavior of the column, meaning that some thermodynamic considerations are needed. The main goal is the comprehension of the relationship between the temperature in one tray and the corresponding mixture compositions at the same trays. It is also important to analyze the sensitivity along the column, by finding the trays where most of the separation takes place.

For a binary column, the correspondence between the temperature and the composition in the same tray is uniquely determined when the pressure is constant. Therefore, in that case, the only knowledge of the temperature profile suffices to obtain compositions along the column. On the other hand, the same relation is not straightforward when multicomponent cases are considered, since compositions can not be determined once the temperature and pressure in the tray are known.

In this work, we propose the *temperature gradient with per-component contribution diagram* as a new tool to be used in order to analyze thermodynamics in a multicomponent column. This diagram derives from the well-known temperature-slope technique (Rademaker *et al.*, 1975), where temperature profile is computed at the nominal SS conditions and temperature measurement sensors for control purposes are placed at the stages with the largest stage-to-stage variation. In a

multicomponent column, temperature gradients would not be sufficient for determining per-component contributions, and therefore the related diagram can be refined through the addition of such contributions.

Per-component contributions are computed as follows: starting from a nominal operating conditions where temperature and composition profiles are known, and motivated by the preceding considerations, consider the bubble point expression (3.1b) at stage i, approximate the temperature gradient over the column (3.1), and obtain the following relationship between the stage-to-stage temperature and the per-component gradients

$$\Delta\bar{T}_i \approx \sum_{j=\rho_1}^{\rho_C} \bar{\beta}'_{i,j}\Delta\bar{c}_i^j = \sum_{j=\rho_1}^{\rho_C} \Delta\bar{T}_{c_i^j} \tag{3.11}$$

$$\Delta\bar{T}_i = \bar{T}_{i+1} - \bar{T}_i, \qquad \Delta\bar{c}_i^j = \bar{c}_{i+1}^j - \bar{c}_i^j, \qquad \bar{\beta}'_{i,j} = \left.\frac{\partial T_i}{\partial c_i^j}\right|_{\bar{\mathbf{c}}_i}$$

In Eq. (3.11), the quantity $\Delta\bar{T}_{c_i^j}$ is the approximated contribution of the component j to the temperature gradient at i-th stage, and consists in the product of the composition gradient $\Delta\bar{c}_i^j$ by a term that represents the sensitivity of $\bar{T}_i$ with respect to $\bar{c}_i^j$. This means that the combination of a large component sensitivity with large concentration gradients yields the largest contribution to the overall temperature gradient. Such sensitivity term is computed analytically, on the basis of Eq. (3.2g).

Once component contributions are computed, two plots are constructed in order to obtain an easy to read representation: the first one shows the temperature gradients along the column (same plot of temperature-slope technique), while the second one shows the additive per-component contributions to the temperature gradients. The plot for nominal operating conditions of case SS1 (Table 3.1) is shown in Figure 3.6 and the same plot for case SS2 (Table 3.2) is shown in Figure 3.7.

In the following, such diagram will also be referred as gradient diagram. Let now analyze it for the two operating conditions SS1 ans SS2.

SS1. It can be noted from Figure 3.6 that largest temperature gradients lie in the enriching section, and more specifically around the 30-th stage. On the contrary, gradients in the stripping section are considerably smaller, except for the trays immediately below the feed stage. This means that enriching section shows a larger sensitivity than the stripping one, and this is due to the high-purity conditions in the bottoms. In general the component which mostly contributes to the overall gradients along the column is the C3, since it presents the largest contributions, and these have the same sign of the temperature gradient. iC4 and nC4 also present a significant contribution, but note that iC4 gradient frequently changes direction (at feed tray and in the middle of both sections), while nC4

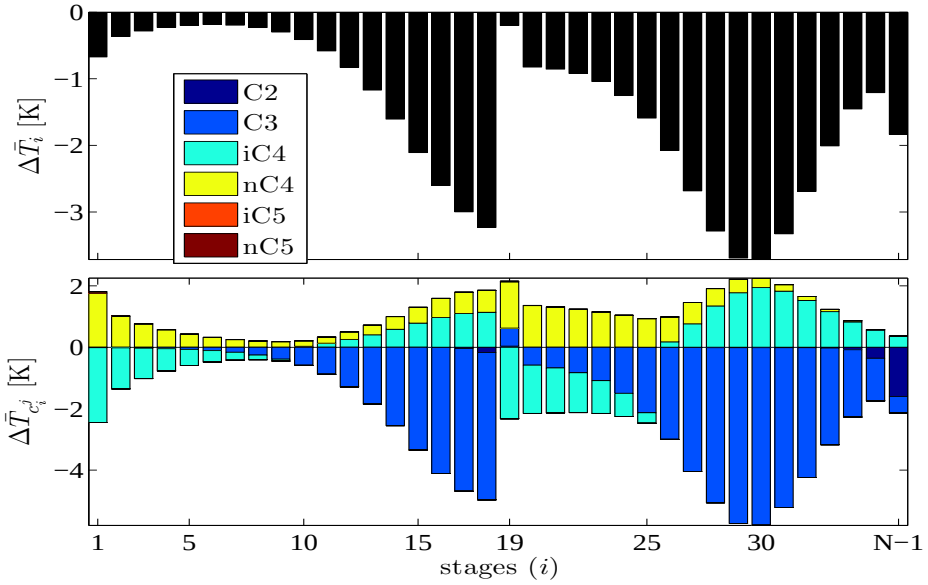

Figure 3.6: Steady-state temperature gradient with per-component contribution diagram for case SS1

contribution is always opposite to the one of the temperature gradient. C2 is not negligible only in the top trays, while iC5 and nC5 only have a very small contribution in bottom stage.

SS2. Differently from SS1 case, it can be seen in Figure 3.6 that a region with large gradients can be found in both stripping and enriching sections, around 5-th and 30-th trays respectively, meaning that both sections are quite sensitive. Note also that temperature gradients at the most sensitive area of the enriching sections are around 1 K smaller than in SS1 case. For the rest, the same considerations of SS1 case hold.

In this Thesis, the temperature gradient with per-component contribution diagram together with systematic procedures is used is used for selecting part of control structure (the selection of temperature sensor locations), and the entire estimation one (selection of (i) the reduced number of components for the estimation model, (ii) number and location of temperature measurements, (iii) composition states to be innovated) and (iv) regions where temperature can be approximated as the average one. The gradient diagram and the procedures for the structure selection are considerably simpler and more intuitive than the majority of well-known methods, and moreover, can be easily used by process engineers. Their use for the control and estimation structural task will be analyzed in the corresponding Chapter.

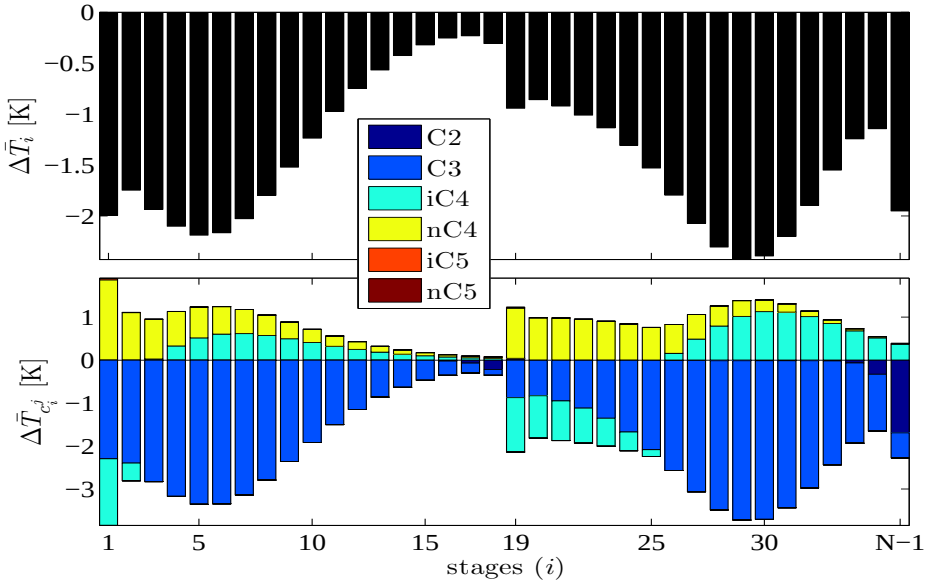

Figure 3.7: Steady-state temperature gradient with per-component contribution diagram for case SS2

3.8 Chapter summary

This Chapter starts with the description of the complete model used in order to simulate the actual dynamics of the six-component C3-C4 splitter considered in this Thesis. Such multicomponent column is subsequently described. Next, the control and the estimation problem are introduced, together with the methodology employed for solving them. The methodology is general, and consists in the partition of each problem in a structural and an algorithmical part. The main tool of such methodology is the temperature gradient with per-component contribution diagram, which is proposed as a simple mean to study thermodynamics in a multicomponent column, and introduced. Part of the control structure and the entire estimation one will be selected on the basis of the gradient gradient in conjunction with systematic procedures.

Part I

Distillation column control

Control part overview

The control problem task has been introduced in Section 3.4: here it must only be recalled that the objectives consist in indirectly regulating one or two key impurities of the multicomponent C3-C4 splitter described in Section 3.3, that is, the iC4 in the distillate and the C3 in the bottom, in order to perform the desired separation in spite of disturbances entering the column. The problem is solved by partitioning it into a structural and an algorithmical part.

The control Part is organized as follows:

Chapter 4. In this Chapter, the control algorithms, that is, the dynamic processors that perform the control task, are illustrated. These algorithms are based on the nonlinear constructive theory and passivity concepts, which are employed in this Thesis in order to develop observer-based temperature controllers with anti-windup protection for indirectly regulating key impurities. Such controllers are the following: (i) a conventional controller; (ii) a parallel cascade controller; (iii) a cascade-type controller based on Control Lyapunov Functions (CLF).

Chapter 5. In this Chapter, the control structure analysis made in order to select the best control structure for the given control objective is presented. The structural problem consists in selecting (i) the location of temperature sensors, (ii) the manipulated variable, and (iii) their pairing (for dual-end controllers). Part of the control structure, that is, the selection of temperature measurement locations, is chosen through the temperature gradient with per-component contribution diagram in conjunction with a systematic procedure. Once the candidate structures are chosen, the concerning results are shown and assessed.

Chapter 4

Control algorithm

In this Chapter, the development of the control algorithms (i.e., the dynamic data processors) used in order to carry out the control task is addressed. Such algorithms are based on the nonlinear constructive control theory and passivity concepts, which have been here used for developing observer-based temperature controllers with anti-windup protection for the indirect composition regulation of the key impurities of the multicomponent C3-C4 splitter illustrated in Section 3.3. The algorithms are the following: (i) a conventional controller; (ii) a parallel cascade controller; (iii) a cascade-type controller based on Control Lyapunov Functions (CLF).

4.1 Introduction

The control problem for a distillation column has been addressed with a lot of different algorithms. The majority of columns are successfully controlled with either PI schemes or MPC ones, and in literature there exists a large number of studies which deals about these specific control algorithms.

A recent approach in the field of nonlinear control theory is represented by the *nonlinear constructive control theory* (Sepulchre *et al.*, 1997). This framework is based on fundamental connections among passivity, optimality and robustness, and is denoted in this way according to the fact that the controller is *constructed* on the basis of given system properties and nonlinear tools.

The nonlinear constructive methods have recently been used in distillation column control, and it has been established that the nonlinear output-feedback SISO one-point (for single-end control) or MIMO two-point (for dual-end control) composition (Castellanos-Sahagún and Álvarez, 2006), temperature (Castellanos-Sahagún *et al.*, 2005) and cascade composition-to-temperature (Castellanos-Sahagún

et al., 2006) controller behaviors can be recovered by means of observer-based controllers with linear-decentralized PI components, leading to a control algorithm with: (i) systematic tuning design valid for any structure, ensuring that results are due to the structure itself and not to the tuning, and (ii) anti-windup capability due to the observer integrated in the controller.

Due to the intrinsic problems in direct composition measurements already discussed in Chapter 2, only temperature controllers are developed in this Thesis, in order to indirectly regulate compositions of interest. Three kind of temperature controllers constructed on the basis of the abovementioned concepts are illustrated. Such controllers are the following:

- a *conventional controller* (1 input - 1 output);
- a *cascade controller* (2 inputs - 1 output);
- a cascade-type controller based on Control Lyapunov Functions (CLF) (2 inputs - 1 output), which will be denoted as *CLF controller*.

In the following, such controllers will also be denoted as *controllers in IMC form*, since their derivation is based on an explicit model of the system. Note that previous input-output classification is here made from the point of view of the control system and not according to the process, meaning that temperatures are classified as controller inputs (while they are process outputs) and flows are classified as controller outputs (while they are process inputs).

The built controllers are decoupled, signifying that each MIMO controller (conventional, cascade or CLF) is made by two decentralized SISO ones. Then, only the description of SISO control algorithms is necessary for describing both SISO and MIMO decoupled controllers afterwards illustrated.

In this Chapter, firstly some key concepts about passivity are introduced, and then the control algorithms are presented.

4.2 Passivity concepts

In this section, the crucial properties of *dissipativity* (Willems, 1972) and *passivity* are briefly illustrated for nonlinear system. Such introduction is based on Sepulchre *et al.* (1997), where a wider and more detailed description of these concepts can also be found.

Intuitively, a system is dissipative if its energy increase is not larger than the amount of supply given by external sources. More formally, consider a system H in deviation variables (i.e., around an equilibrium point) with state x, input u and output y: such system is said to be dissipative if there exists a positive

semidefinite storage function $S(x)$ and a supply rate $w(u, y)$ such that

$$S(x(T)) - S(x(0)) \leq \int_0^T w(u(t), y(t))\, dt \qquad \forall\, u, \quad T > 0 \tag{4.1}$$

The storage function S can be seen as the amount of energy owned by the system, while the supply rate w represents the power entering the system. Such dissipative system is also passive if the following condition holds:

$$w(u(t), y(t)) = u^T y \tag{4.2}$$

Passivity is the base concept in nonlinear constructive theory. But why passivity concepts are so important? From Sepulchre *et al.* (1997) it can be seen that under determined conditions, *passivity implies stability*. Since stability is the property desired for the system, therefore the interest is in finding the necessary and sufficient conditions under which such system can be rendered passive by means of a feedback action. If a system has such properties, it is defined as *feedback passive*. These properties are *relative degree one* and *weakly minimum phase*, and are listed in the following.

Relative degree 1. A system H has relative degree r if the input u explicitly appears in the equation of output y, when the latter is derived with respect to time r times. Therefore, this means that the relative degree is one when the equation for the first time derivative of y (i.e., the equation for $\dot{y}$) explicitly contains a dependence on u, while the equation for y does not.

Weakly minimum phase. A system is weakly minimum phase if zero-dynamics (i.e., system dynamics when $y = 0$) are stable.

These two properties can not be modified by feedback, and therefore are needed for obtaining the system passivity, and thus its stability. As will be shown later, the distillation column system satisfies such properties and therefore nonlinear constructive approach can be used.

4.3 Conventional controller

The *conventional controller* discussed in this Section was introduced for distillation purposes in Castellanos-Sahagún *et al.* (2005) for a binary column, and was developed on the basis of nonlinear constructive theory (Sepulchre *et al.*, 1997), and passivity concepts. Such controller is here extended to the multicomponent case, and consists in an observer-based temperature controller with either reboiler heat duty Q and/or reflux rate R as manipulated variables. Some possible configurations for single-end and dual-end conventional controllers are reported in Figure 4.1.

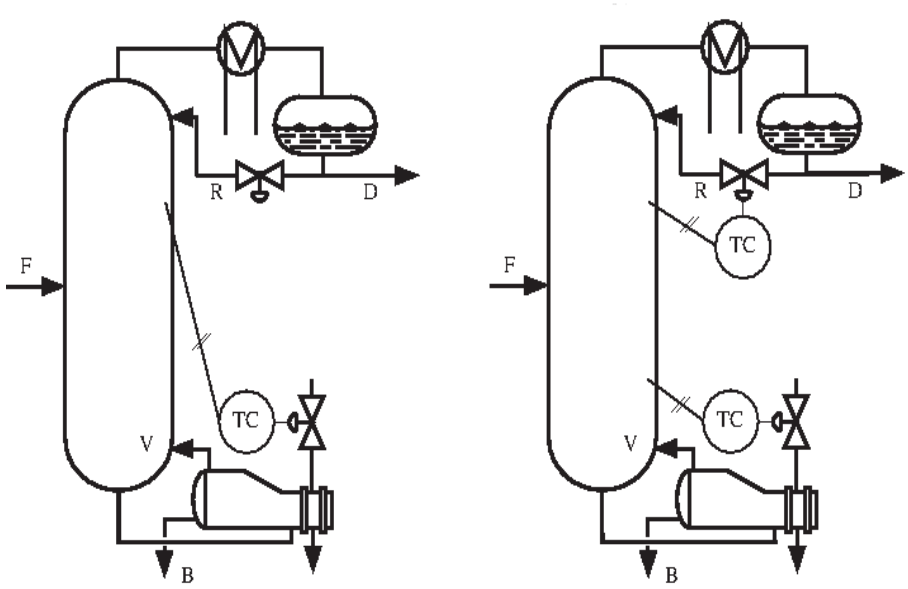

Figure 4.1: Scheme of a conventional temperature controller for single-end (left) and dual-end (right) configurations.

4.3.1 Derivation

Consider the dynamic of a temperature T_k to be controlled, driven by a manipulated input u_l (either Q or R). As it can be seen from column equations (3.2), the *conventional controller* discussed in this Section was introduced for distillation purposes in Castellanos-Sahagún *et al.* (2005), and was developed on the basis of nonlinear constructive theory (Sepulchre *et al.*, 1997), and passivity concepts. Such controller is here extended to the multicomponent case, and consists in an observer-based temperature controller with either reboiler heat duty Q or reflux rate R as manipulated variables. The relation between the first time derivative of T_k and u_l is affine, and therefore the temperature dynamics in deviation variables can be written as:

$$\dot{y} = \overset{*}{a}u + \overset{*}{b} \tag{4.3}$$

where the deviated variables $y = T_k - \bar{T}_k$ and $u = u_l - \bar{u}_l$ are used, and the symbol $(\bar{\cdot})$ stands for the nominal value or the set-point of the variable. Note that, differently from the Chapter introduction, the input-output classification is here made on the basis of the process system, meaning that u is the input and y is the output.

The control model (4.3) has relative degree 1, since the input u explicitly appears in the equation of the first time-derivative of the output y. Moreover, it is known

from distillation theory that zero-dynamics are stable (Castellanos-Sahagún *et al.*, 2005), meaning that the system represented by Eq. (4.3) is passive, and therefore nonlinear constructive methods can be used.

Instead of computing the real value of $\overset{*}{a}$ step by step, an approximation a computed at nominal conditions can be suitably used if the condition $a = \text{sign}(\overset{*}{a})$ holds; otherwise, a positive feedback loop would result, yielding an unstable system. Eq. (4.3) can therefore be manipulated as follows:

$$\begin{aligned} \dot{y} &= \overset{*}{a}u + \overset{*}{b} = au + (\overset{*}{a} - a)u + \overset{*}{b} \\ &= au + b \end{aligned} \tag{4.4}$$

where $b = (\overset{*}{a} - a)u + \overset{*}{b}$. In this work, the value of a has been computed at nominal value and approximated on the basis of column model (3.2) as follows:

Q as manipulated input, T_k as controlled temperature

$$a = -\frac{\Delta\bar{T}_k}{\bar{H}_k\bar{\lambda}_{v,k}} \sum_{j=\rho_1}^{\rho_C} \frac{\Delta\bar{v}_k^j}{\Delta\bar{c}_k^j} \tag{4.5a}$$

R as manipulated input, T_k as controlled temperature

$$a = C\frac{\Delta\bar{T}_k}{\bar{H}_k} \tag{4.5b}$$

where C is the number of components, $\Delta\bar{T}_k = \bar{T}_{k+1} - \bar{T}_k$, $\Delta\bar{c}_k^j = \bar{c}_{k+1}^j - \bar{c}_k^j$ and $\Delta\bar{v}_k^j = \bar{v}_k^j - \bar{v}_{k-1}^j$ are the temperature, liquid composition and vapor composition gradients at stage k for component j, H_k is the holdup at k-th stage and $\lambda_{v,k}$ is the heat of vaporization at stage k, with all the variables being at nominal conditions. On the other hand, the value of b will be estimated as later explained.

In order to build the controller, the temperature dynamics are forced with the following closed-loop first order dynamics:

$$\dot{y} = -K_c y \tag{4.6}$$

K_c is the controller gain, and has the dimension of a frequency: in fact, it is the inverse of the time constant of Eq. (4.6). If the dynamics given in Eq. (4.6) are imposed in Eq. (4.4), then the following controller action is obtained:

$$-K_c y = au + b, \qquad \Rightarrow \qquad u = -\frac{(K_c y + b)}{a} \tag{4.7}$$

On the other hand, the parameter b is unknown, because of modeling errors (due to the approximation used), unmeasured disturbances, and so on. However, b

is instantaneously observable since it is uniquely determined by the measurable input-output pair given by u and y, meaning that it can be reconstructed through the following first order observer (Hermann and Krener, 1977):

$$\dot{\hat{b}} = K_o(b - \hat{b}) = K_o(\dot{y} - au - \hat{b}) \tag{4.8}$$

In Eq. (4.8), K_o denotes the observer gain and represents the inverse of the time constant of Eq. (4.9).

The use of the temperature time-derivative $\dot{y}$ in Eq. (4.8) should be avoided to eliminate problems due to differentiator noise sensitivity. This can be done firstly rewriting the observer (4.8) as follows:

$$\dot{\hat{b}} - K_o\dot{y} = -K_o(au + \hat{b})$$

If the coordinate change $\chi = \hat{b} - K_o y$ is used, a new form of (4.9) is obtained as

$$\dot{\chi} = -K_o\chi - K_o(au + K_o y) \tag{4.9}$$

where the use of the time derivative $\dot{y}$ is not needed anymore.

From the combination of Eq. (4.7) and Eq. (4.9), the following *Conventional controller in IMC open-loop form* is derived

$$u = -\frac{K_c y + b}{a} = -\frac{(K_c + K_o)y + \chi}{a} \tag{4.10a}$$

$$\dot{\chi} = -K_o\chi - K_o(au + K_o y) \tag{4.10b}$$

The controller (4.10) is formed by a static part (the controller u given in Eq. (4.10a)) and a dynamic part (the observer for estimating χ, and therefore b, given in Eq. (4.10b)). Such controller form is the one which will be implemented in order to achieve control objectives.

Another controller form can be derived considering the following expression for au obtained from Eq. (4.10a)

$$au = -(K_c + K_o)y - \chi$$

Inserting the expression above in Eq. (4.10b) the following expression for χ is obtained:

$$\begin{aligned}\dot{\chi} &= -K_o\chi - K_o(au + K_o y) = -K_o\chi - K_o(-K_c y - K_o y - \chi + K_o y) \\ &= K_c K_o y \\ &\Downarrow \\ \chi &= K_c K_o \int y\, dt\end{aligned} \tag{4.11}$$

Combining Eq. (4.10a) and Eq. (4.11), the following *Conventional controller in closed-loop form* is obtained

$$\begin{aligned} u &= -\frac{(K_c + K_o)y + \chi}{a} \\ &= -\frac{(K_c + K_o)y + K_c K_o \int y\,dt}{a} \end{aligned} \tag{4.12}$$

Remark 4.1 *The controller* (4.12) *can be written in state-space form as follows:*

$$\begin{aligned} \dot{\chi} &= A\chi + By = K_c K_o y \\ u &= C\chi + Dy = -\frac{1}{a}\chi - \frac{K_c + K_o}{a} y \end{aligned}$$

The controller system is at the limit of stability, as can be seen by the fact that $\det A = 0$. *This is normal since* $u \neq 0$ *when the controller is acting, but remains bounded.*

4.3.2 Equivalence with conventional PI

After reorganization, Eq. (4.12) can be rewritten in a standard PI form

$$\begin{aligned} u &= -\frac{(K_c + K_o)y + K_c K_o \int y\,dt}{a} = -\frac{K_c + K_o}{a}\left(y + \frac{K_c K_o}{K_c + K_o}\int y\,dt\right) \\ &= -K_p\left(y + \frac{1}{\tau_I}\int y\,dt\right) \end{aligned} \tag{4.13}$$

The controller (4.13) is clearly expressed in PI form, where K_p is the proportional gain and τ_I is the integral time, according to the following relationships

$$K_p = \frac{K_c + K_o}{a}, \qquad \tau_I = \frac{K_c + K_o}{K_c K_o}$$

Note that the controller gain K_c and the observer gain K_o are interchangeable since the same values for K_p and τ_I are obtained.

4.3.3 Anti-windup feature

Due to the constraints imposed by the actuators, the saturation phenomena can happen. When the controller is under saturation, the windup problem causes an inadequate control action. A controller expression which includes the saturation is the following:

$$u_S = \mathrm{sat}(u, u_-, u_+) = u + \Delta u_S \tag{4.14}$$

In Eq. (4.14) u_- and u_+ are the minimum and maximum saturation limits, u_S is the real control action due to the actuator constraints and Δu_S is the difference between the real control action and the computed one.

If the controller is not under saturation, i.e., when the condition $u_- \leq u \leq u_+$ is verified, the condition $u_S = u$ holds since the real control action coincides with the computed one. If $u > u_+ = u_S$, it means that the computed control action is larger than the real one and therefore $\Delta u_S = u_+ - u < 0$. On the contrary, if $u < u_- = u_S$ the real control action is smaller than the computed one and therefore the condition $u < u_S = u_-$ is verified, with $\Delta u_S = u_- - u > 0$.

One of the most important features of the conventional controller in IMC form (and of all observer-based controllers based on nonlinear constructive theory) is the automatic inclusion of an anti-windup action. When saturation occurs, the conventional controller in IMC open-loop form (4.10) changes as follows:

$$u = -\frac{(K_c + K_o)y + \chi}{a} \qquad u_S = \mathrm{sat}(u, u_-, u_+) \tag{4.15a}$$

$$\dot{\chi} = -K_o\chi - K_o(au_S + K_o y) = -K_o\chi - K_o(au + K_o y) + K_o a\Delta u_S \tag{4.15b}$$

An expression for χ can therefore derived as follows:

$$\begin{aligned}
\dot{\chi} &= -K_o\chi - K_o(au + K_o y) + K_o a\Delta u_S \\
&= -K_o\chi - K_o(-K_c y - K_o y - \chi + K_o y) + K_o a\Delta u_S \\
&= K_c K_o y + K_o a\Delta u_S \\
&\Downarrow \\
\chi &= K_c K_o \int y\,dt + K_o a \int \Delta u_S\,dt
\end{aligned} \tag{4.16}$$

The closed-loop form equivalent to Eq. (4.15) is thus obtained through the combination of 4.16:

$$\begin{aligned}
u &= -\frac{(K_c + K_o)y + \chi}{a} \\
&= -\frac{(K_c + K_o)y + K_c K_o \int y\,dt}{a} + K_o \int \Delta u_S\,dt
\end{aligned} \tag{4.17}$$

Remark 4.2 *The controller* (4.17) *can be written in state-space form as follows:*

$$\dot{\chi} = A\chi + By^A = \begin{bmatrix} K_c K_o y & K_o a \end{bmatrix} \begin{bmatrix} y \\ \Delta u_S \end{bmatrix}$$

$$u = C\chi + Dy^A = -\frac{1}{a}\chi - \begin{bmatrix} \frac{K_c + K_o}{a} & 0 \end{bmatrix} \begin{bmatrix} y \\ \Delta u_S \end{bmatrix}$$

The anti-windup feature results very clear when considering the controller (4.15)

in the equivalent PI form. After reorganization, Eq. (4.15) can be rewritten as:

$$\begin{aligned} u &= -\frac{(K_c + K_o)y + K_c K_o \int y\,dt - K_o a \int \Delta u_S\,dt}{a} \\ &= -\frac{K_c + K_o}{a}\left(y + \frac{K_c K_o}{K_c + K_o}\int y\,dt\right) - K_o \int \Delta u_S\,dt \\ &= -K_p\left(y + \frac{1}{\tau_I}\int y\,dt\right) - \frac{1}{\tau_\tau}\int \Delta u_S\,dt \end{aligned} \tag{4.18}$$

which is a classical anti-reset windup form (Kothare *et al.*, 1994) where τ_τ is the reset time of the anti-windup term. Note that K_c and K_o are not interchangeable, differently from the case without saturation.

4.3.4 Tuning

The Conventional controller (4.10) can be easily tuned on the basis of the following rules based on Castellanos-Sahagún *et al.* (2005):

$$K_c \approx 1\text{-}2\omega, \qquad K_o \approx 5\text{-}10K_c \tag{4.19}$$

The tuning rules given in Eq. (4.19) can be easily interpreted as follows: (i) the controller gain K_c represents the characteristic frequency of the controller, which must be forced to be equal or at most twice larger of the characteristic frequency of the system ω; (ii) the estimator gain K_o represents the characteristic frequency of the estimator, and it is desired that the estimation error decay much faster than the regulation error (from 5 to 10 times quicker).

Remark 4.3 *Even if in this work the holdup dynamics have been neglected, it is worth recalling that the estimator frequency K_o should not exceed $\frac{1}{3}$ of the holdup characteristic frequency ω_H, in order to keep the system stable. Since a typical value for the latter is $\omega_H \approx 100\omega$, the previous requirement is satisfied.*

Note that the controller (4.10) can be simply tuned once the characteristic frequency of the system is known. In this specific case, it is known from distillation theory (Skogestad and Morari, 1988) that a column has a main time constant. The latter can be easily computed with open-loop input step variations to reboiler heat or reflux, by looking at the characteristic frequency of the resulting temperature dynamic responses for the trays of interest.

Compared to typical tuning criteria of PI controllers (Ziegler-Nichols, etc.), these rules are much simpler to apply. It will be shown in Chapter 5 that these rules also lead to very good performance.

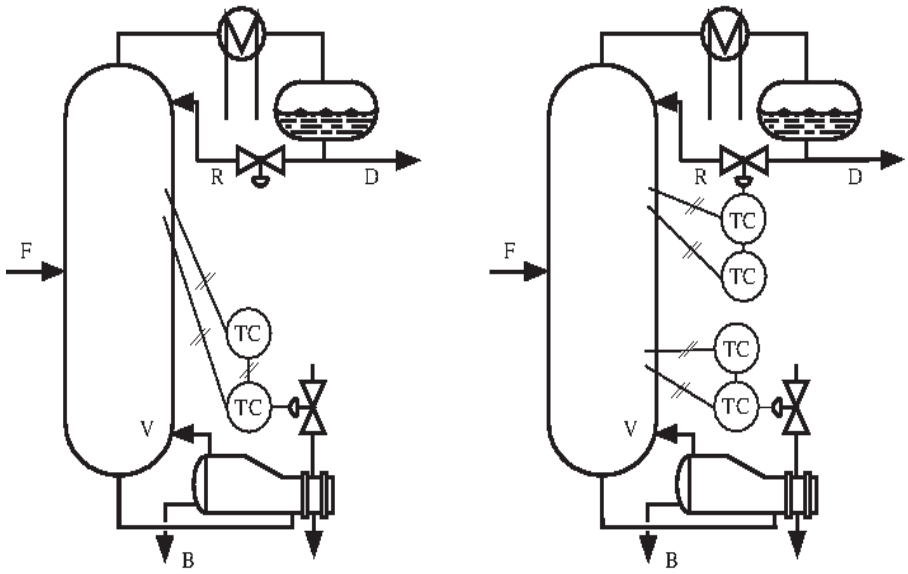

Figure 4.2: Scheme of a cascade temperature controller for single-end (left) and dual-end (right) configuration.

4.4 Cascade controller

In this Section, a parallel cascade temperature controller is developed for a multicomponent column on the basis of the nonlinear constructive theory (Sepulchre *et al.*, 1997) and passivity concepts. Composition is indirectly controlled through a manipulated input which regulates a primary temperature through the assistance of a secondary temperature control loop. The role of the secondary temperature in the cascade is the fast rejection of feed disturbances. Such controller is parallel since the manipulated input affects both primary and secondary temperatures through parallel first-order equations (Luyben, 1973). Some possible configurations for single-end and dual-end cascade controllers are reported in Figure 4.2.

4.4.1 Derivation

In order to obtain the derivation of the cascade controller according to the nonlinear constructive theory (Sepulchre *et al.*, 1997), consider the dynamic of a primary temperature T_{k_1} and a secondary temperature T_{k_2} driven by a manipulated input u_l (either Q or R):

$$\dot{y_1} = a_1 u + b_1 \tag{4.20a}$$

$$\dot{y_2} = a_2 u + b_2 \tag{4.20b}$$

where the deviated variables $y_1 = T_{k_1} - \bar{T}_{k_1}$, $y_2 = T_{k_2} - \bar{T}_{k_2}$ and $u = u_l - \bar{u}_l$ are used. As already stated in Section 4.3.1, the relationships between the first time derivative of a generic temperature and a manipulated input is affine, and therefore dynamics can be written as in Eq. (4.20). Moreover, Eq. (4.20) is passive, and therefore nonlinear constructive theory can be used for developing the proposed controller. Note that Eq. (4.20) has been already manipulated as in Eq. (4.4), meaning that the actual parameters $\overset{*}{a}_1$, and $\overset{*}{a}_2$ have already been substituted with suitable approximations with the same sign a_1 and a_2, and therefore the procedure is not reported again.

In cascade-type temperature controllers, the primary temperature regulation is needed for reducing the composition offset, while the secondary temperature control is useful for a fast rejection of disturbances. The entire control action can be split into two parts: a primary control action u^* and a secondary control action $\tilde{u}$.

For obtaining the primary controller action u^*, primary temperature dynamics has to be forced as in Eq. (4.6), resulting in the following expression:

$$u^* = -\frac{(K_{c,1} y_1 + b_1)}{a_1} \tag{4.21}$$

The primary controller u^* generates the set-point of the secondary loop y_2^* as follows:

$$\dot{y}_2^* = a_2 u^* + b_2 \tag{4.22}$$

Secondary temperature dynamics are forced according to the following first order dynamics

$$\dot{y}_2 - \dot{y}_2^* = -K_{c,2}(y_2 - y_2^*) \Rightarrow \dot{e}_2 = -K_{c,2} e_2 \tag{4.23}$$

where $e_2 = y_2 - y_2^*$ denotes the difference between the actual secondary temperature and its (dynamic) set-point (both in perturbation variables).

The entire controller is formed by the primary and the secondary part as

$$u = u^* + \tilde{u} \tag{4.24}$$

and its expression can be derived as follows making use of Eq. (4.21), (4.22) and (4.23):

$$\begin{aligned}
\dot{y}_2 &= \dot{y}_2^* - K_{c,2}(y_2 - y_2^*) \\
&= a_2 u^* + b_2 - K_{c,2}(y_2 - y_2^*) \\
&= -\frac{a_2}{a_1}(K_{c,1} y_1 + b_1) + b_2 - K_{c,2}(y_2 - y_2^*) \\
&\Downarrow
\end{aligned}$$

$$
\begin{aligned}
a_2u + b_2 &= -\frac{a_2}{a_1}(K_{c,1}y_1 + b_1) + b_2 - K_{c,2}(y_2 - y_2^*) \\
&\Downarrow \\
u = u^* + \tilde{u} &= -\frac{K_{c,1}y_1 + b_1}{a_1} - \frac{K_{c,2}(y_2 - y_2^*)}{a_2}
\end{aligned} \tag{4.25}
$$

The first order observers for indirectly estimating b_1 and b_2 can be obtained as done for the conventional case in Eq. (4.9) as follows:

$$\dot{\chi}_1 = -K_{o,1}\chi_1 - K_{o,1}(a_1u + K_{o,1}y_1), \qquad \hat{b}_1 = \chi_1 + K_{o,1}y_1 \tag{4.26a}$$

$$\dot{\chi}_2 = -K_{o,2}\chi_2 - K_{o,2}(a_2u + K_{o,2}y_2), \qquad \hat{b}_2 = \chi_2 + K_{o,2}y_2 \tag{4.26b}$$

Finally, the *Cascade controller in IMC open-loop form* can be expressed as

$$u = u^* + \tilde{u}, \qquad u^* = -\frac{(K_{c,1} + K_{o,1})y_1 + \chi_1}{a_1}, \qquad \tilde{u} = -\frac{K_{c,2}(y_2 - y_2^*)}{a_2} \tag{4.27a}$$

$$\dot{y}_2^* = a_2u^* + \chi_2 + K_{o,2}y_2 \tag{4.27b}$$

$$\dot{\chi}_1 = -K_{o,1}\chi_1 - K_{o,1}(a_1u + K_{o,1}y_1) \tag{4.27c}$$

$$\dot{\chi}_2 = -K_{o,2}\chi_2 - K_{o,2}(a_2u + K_{o,2}y_2) \tag{4.27d}$$

The expression for closed-loop primary temperature dynamics can be derived as:

$$
\begin{aligned}
\dot{y}_1 &= a_1u + b_1 \\
&= -(K_{c,1} + K_{o,1})y_1 - \chi_1 - K_{c,2}\frac{a_1}{a_2}(y_2 - y_2^*) + \chi_1 + K_{o,1}y_1 \\
&= -K_{c,1}y_1 - K_{c,2}\frac{a_1}{a_2}(y_2 - y_2^*)
\end{aligned} \tag{4.28}
$$

It is worth noting as primary temperature dynamics are influenced by the secondary temperature error: once the latter decays to zero, the expression for the dynamics is equivalent to the primary temperature closed-loop dynamic equation (4.6).

Remark 4.4 *The state variables for the cascade controller are the two estimated variables χ_1 and χ_2 and the secondary set-point y_2. In order to get the state-space representation, manipulate their time derivative expressions as follows:*

$$
\begin{aligned}
\dot{\chi}_1 &= -K_{o,1}\chi_1 - K_{o,1}(a_1u + K_{o,1}y_1) \\
&= -K_{o,1}\chi_1 - K_{o,1}\left((K_{c,1} + K_{o,1})y_1 + \chi_1 - K_{c,2}\frac{a_1}{a_2}(y_2 - y_2^*) + K_{o,1}y_1\right) \\
&= -K_{c,2}K_{o,1}\frac{a_1}{a_2}y_2^* + K_{c,1}K_{o,1}y_1 + K_{c,2}K_{o,1}\frac{a_1}{a_2}y_2 \\
\dot{\chi}_2 &= -K_{o,2}\chi_2 - K_{o,2}(a_2u + K_{o,2}y_2)
\end{aligned}
$$

$$
\begin{aligned}
&= -K_{o,2}\chi_2 - K_{o,2}\left(-\frac{a_2}{a_1}(K_{c,1}y_1 + b_1) - K_{c,2}(y_2 - y_2^*) + K_{o,2}y_2\right) \\
&= -K_{o,2}\frac{a_2}{a_1}\chi_1 - K_{o,2}\chi_2 - K_{c,2}K_{o,2}y_2^* + K_{o,2}(K_{c,1} + K_{o,1})\frac{a_2}{a_1}y_1 \\
&\quad + K_{o,2}(K_{c,2} - K_{o,2})y_2 \\
\dot{y}_2^* &= a_2u^* + \chi_2 + K_{o,2}y_2 = -\frac{a_2}{a_1}\left((K_{c,1} + K_{o,1})y_1 + \chi_1\right) + \chi_2 + K_{o,2}y_2 \\
&= -\frac{a_2}{a_1}\chi_1 + \chi_2 - \frac{a_2}{a_1}(K_{c,1} + K_{o,1})y_1 + K_{o,2}y_2
\end{aligned}
$$

The cascade controller (4.27) *can then be written in state-space form as:*

$$
\begin{bmatrix} \dot{\chi}_1 \\ \dot{\chi}_2 \\ \dot{y}_2^* \end{bmatrix} = \begin{bmatrix} 0 & 0 & -K_{c,2}K_{o,1}\frac{a_1}{a_2} \\ K_{o,2}\frac{a_1}{a_2} & -K_{o,2} & -K_{c,2}K_{o,2} \\ -\frac{a_1}{a_2} & 1 & 0 \end{bmatrix} \begin{bmatrix} \chi_1 \\ \chi_2 \\ y_2^* \end{bmatrix} + \begin{bmatrix} -K_{c,1}K_{o,1} & -K_{c,2}K_{o,1}\frac{a_1}{a_2} \\ -K_{c,2}(K_{c,1} + K_{o,1})\frac{a_2}{a_1} & K_{o,2}(K_{c,2} + K_{o,2}) \\ -\frac{a_2}{a_1}(K_{c,1} + K_{o,1}) & K_{o,2} \end{bmatrix} \begin{bmatrix} y_1 \\ y_2 \end{bmatrix}
$$

$$
\begin{bmatrix} u^* \\ \tilde{u} \end{bmatrix} = \begin{bmatrix} -\frac{1}{a_1} & 0 & 0 \\ 0 & 0 & \frac{K_{c,2}}{a_2} \end{bmatrix} \begin{bmatrix} \chi_1 \\ \chi_2 \\ y_2^* \end{bmatrix} + \begin{bmatrix} -\frac{K_{c,1}+K_{o,1}}{a_1} & 0 \\ 0 & -\frac{K_{c,2}}{a_2} \end{bmatrix} \begin{bmatrix} y_1 \\ y_2 \end{bmatrix}
$$

4.4.2 Anti-windup feature

When saturation occurs, the anti-windup action is ensured by the fact that the estimators (4.26) are driven by the real control action u_S, defined by

$$u_S = \mathrm{sat}(u, u_-, u_+) = u + \Delta u_S \tag{4.29}$$

while the secondary set-point generator (4.27b) is driven by the saturated primary control action u_S^* as follows:

$$u_S^* = \mathrm{sat}(u^*, u_-, u_+) = u^* + \Delta u_S^* \tag{4.30}$$

Remark 4.5 *The estimators dynamics and the secondary temperature set-point generator expressions must be manipulated as follows in order to obtain the state-space representation of the cascade controller when saturation is present:*

$$
\begin{aligned}
\dot{\chi}_1 &= -K_{o,1}\chi_1 - K_{o,1}(a_1u_S + K_{o,1}y_1) \\
&= -K_{o,1}\chi_1 - K_{o,1}(a_1u + K_{o,1}y_1) - K_{o,1}a_1\Delta u_S \\
&= -K_{c,2}K_{o,1}\frac{a_1}{a_2}y_2^* + K_{c,1}K_{o,1}y_1 + K_{c,2}K_{o,1}\frac{a_1}{a_2}y_2 - K_{o,1}a_1\Delta u_S \\
\dot{\chi}_2 &= -K_{o,2}\chi_2 - K_{o,2}(a_2u_S + K_{o,2}y_2)
\end{aligned}
$$

$$
\begin{aligned}
&= -K_{o,2}\chi_2 - K_{o,2}(a_2u + K_{o,2}y_2) - K_{o,2}a_2\Delta u_S \\
&= -K_{o,2}\frac{a_2}{a_1}\chi_1 - K_{o,2}\chi_2 - K_{c,2}K_{o,2}y_2^* + K_{o,2}(K_{c,1}+K_{o,1})\frac{a_2}{a_1}y_1 \\
&\quad + K_{o,2}(K_{c,2}-K_{o,2})y_2 - K_{o,2}a_2\Delta u_S \\
\dot{y}_2^* &= a_2u_S^* + \chi_2 + K_{o,2}y_2 = a_2(u^* + \Delta u_S^*) + \chi_2 + K_{o,2}y_2 \\
&= -\frac{a_2}{a_1}\left((K_{c,1}+K_{o,1})y_1 + \chi_1\right) + \chi_2 + K_{o,2}y_2 + a_2\Delta u_S^* \\
&= -\frac{a_2}{a_1}\chi_1 + \chi_2 - \frac{a_2}{a_1}(K_{c,1}+K_{o,1})y_1 + K_{o,2}y_2 + a_2\Delta u_S^*
\end{aligned}
$$

The resulting state-space form is here illustrated:

$$
\begin{bmatrix} \dot{\chi}_1 \\ \dot{\chi}_2 \\ \dot{y}_2^* \end{bmatrix} = \begin{bmatrix} 0 & 0 & -K_{c,2}K_{o,1}\frac{a_1}{a_2} \\ K_{o,2}\frac{a_1}{a_2} & -K_{o,2} & -K_{c,2}K_{o,2} \\ -\frac{a_1}{a_2} & 1 & 0 \end{bmatrix} \begin{bmatrix} \chi_1 \\ \chi_2 \\ y_2^* \end{bmatrix}
$$

$$
+ \begin{bmatrix} -K_{c,1}K_{o,1} & -K_{c,2}K_{o,1}\frac{a_1}{a_2} & -K_{o,1}a_1 & 0 \\ -K_{c,2}(K_{c,1}+K_{o,1})\frac{a_2}{a_1} & K_{o,2}(K_{c,2}+K_{o,2}) & -K_{o,2}a_2 & 0 \\ -\frac{a_2}{a_1}(K_{c,1}+K_{o,1}) & K_{o,2} & 0 & a_2 \end{bmatrix} \begin{bmatrix} y_1 \\ y_2 \\ \Delta u_S \\ \Delta u_S^* \end{bmatrix}
$$

$$
\begin{bmatrix} u^* \\ \tilde{u} \end{bmatrix} = \begin{bmatrix} -\frac{1}{a_1} & 0 & 0 \\ 0 & 0 & \frac{K_{c,2}}{a_2} \end{bmatrix} \begin{bmatrix} \chi_1 \\ \chi_2 \\ y_2^* \end{bmatrix} + \begin{bmatrix} -\frac{K_{c,1}+K_{o,1}}{a_1} & 0 & 0 & 0 \\ 0 & -\frac{K_{c,2}}{a_2} & 0 & 0 \end{bmatrix} \begin{bmatrix} y_1 \\ y_2 \\ \Delta u_S \\ \Delta u_S^* \end{bmatrix}
$$

4.4.3 Derivation of a cascade PI form

Recall the primary observer (4.26a)

$$
\dot{\chi}_1 = -K_{o,1}\chi_1 - K_{o,1}(a_1u + K_{o,1}y_1) \tag{4.31}
$$

and the following expression for a_1u which can be derived from the controller (4.27a):

$$
\begin{aligned}
a_1u &= a_1(u^* + \tilde{u}) \\
&= -(K_{c,1}+K_{o,1})y_1 - \chi_1 - K_{c,2}\frac{a_1}{a_2}e_2
\end{aligned} \tag{4.32}
$$

Substituting Eq. (4.32) into Eq. (4.31), an expression for χ_1 can be obtained as follows:

$$
\begin{aligned}
\dot{\chi}_1 &= -K_{o,1}\chi_1 - K_{o,1}(a_1u + K_{o,1}y_1) \\
&= -K_{o,1}\chi_1 - K_{o,1}\left(-(K_{c,1}+K_{o,1})y_1 - \chi_1 - K_{c,2}\frac{a_1}{a_2}e_2\right) \\
&= K_{c,1}K_{o,1}y_1 + K_{c,2}K_{o,1}\frac{a_1}{a_2}e_2
\end{aligned}
$$

$$\Downarrow$$

$$\chi_1 = K_{c,1}K_{o,1}\int y_1\,dt + K_{c,2}K_{o,1}\frac{a_1}{a_2}\int e_2\,dt \tag{4.33}$$

The combination of Eq. (4.27a) and Eq. (4.33) yields the following *cascade controller in IMC closed-loop form*:

$$u = u^* + \tilde{u} \tag{4.34a}$$

$$u^* = -\frac{K_{c,1}+K_{o,1}}{a_1}y_1 - \frac{K_{c,1}K_{o,1}}{a_1}\int y_1\,dt - \frac{K_{c,2}K_{o,1}}{a_2}\int e_2\,dt \tag{4.34b}$$

$$\tilde{u} = -\frac{K_{c,2}}{a_2}e_2 \tag{4.34c}$$

Since $e_2 = y_2 - y_2^*$, an IMC closed-loop expression for y_2^* has to be obtained in order to get a complete closed-loop controller expression. Such expression for y_2^* can be obtained starting from Eq. (4.27b), which is recalled below:

$$\dot{y}_2^* = a_2u^* + \chi_2 + K_{o,2}y_2 \tag{4.35}$$

Eq. (4.35) implies that

$$\chi_2 = \dot{y}_2^* - a_2u^* - K_{o,2}y_2 \tag{4.36}$$

Recall now the secondary observer (4.26b)

$$\dot{\chi}_2 = -K_{o,2}\chi_2 - K_{o,2}(a_2u + K_{o,2}y_2) \tag{4.37}$$

A closed-loop expression for χ_2 to be substituted into Eq. (4.35) can be derived by jointing (4.36) and (4.37) as follows:

$$\begin{aligned}
\dot{\chi}_2 &= -K_{o,2}\chi_2 - K_{o,2}(a_2u + K_{o,2}y_2)\\
&= -K_{o,2}(\dot{y}_2^* - a_2u^* - K_{o,2}y_2) - K_{o,2}(a_2u + K_{o,2}y_2)\\
&= -K_{o,2}\dot{y}_2^* - K_{o,2}a_2\tilde{u}\\
&= -K_{o,2}\dot{y}_2^* + K_{c,2}K_{o,2}e_2\\
&\Downarrow\\
\chi_2 &= -K_{o,2}y_2^* + K_{c,2}K_{o,2}\int e_2\,dt
\end{aligned} \tag{4.38}$$

On the other hand, an expression for a_2u^* to be substituted into Eq. (4.35) can be derived from the primary controller u^* in Eq. (4.34b) as

$$a_2u^* = -\frac{a_2}{a_1}\left((K_{c,1}+K_{o,1})y_1 + K_{c,1}K_{o,1}\int y_1\,dt + K_{c,2}K_{o,1}\frac{a_1}{a_2}\int e_2\,dt\right) \tag{4.39}$$

Combining Eq. (4.38), Eq. (4.39) and Eq. (4.35), the IMC closed-loop expression for y_2^* is obtained as:

$$\begin{aligned}
\dot{y}_2^* &= -\frac{a_2}{a_1}\left((K_{c,1}+K_{o,1})y_1 + K_{c,1}K_{o,1}\int y_1\,dt + K_{c,2}K_{o,1}\frac{a_1}{a_2}\int e_2\,dt\right) - K_{o,2}y_2^* \\
&\quad + K_{c,2}K_{o,2}\int e_2\,dt + K_{o,2}y_2 \\
&= -\frac{a_2}{a_1}(K_{c,1}+K_{o,1})y_1 - \frac{a_2}{a_1}K_{c,1}K_{o,1}\int y_1\,dt + K_{c,2}K_{o,1}\int e_2\,dt - K_{o,2}y_2^* \\
&\quad + K_{c,2}K_{o,2}\int e_2\,dt + K_{o,2}y_2 \\
&= \frac{a_2}{a_1}(K_{c,1}+K_{o,1})y_1 - \frac{a_2}{a_1}K_{c,1}K_{o,1}\int y_1\,dt + K_{o,2}e_2 + K_{c,2}(K_{o,1}+K_{o,2})\int e_2\,dt \\
&\Downarrow \\
y_2^* &= -\frac{a_2}{a_1}(K_{c,1}+K_{o,1})\int y_1\,dt - \frac{a_2}{a_1}K_{c,1}K_{o,1}\int\left(\int y_1\,dt\right)dt + K_{o,2}\int e_2\,dt \\
&\quad + K_{c,2}(K_{o,1}+K_{o,2})\int\left(\int e_2\,dt\right)dt
\end{aligned} \tag{4.40}$$

The combination of Eq. (4.34) and Eq. (4.40) can be rewritten in PI-like form as

$$\begin{aligned}
u &= -\frac{K_{c,1}+K_{o,1}}{a_1}y_1 - \frac{K_{c,1}K_{o,1}}{a_1}\int y_1\,dt - \frac{K_{c,2}}{a_2}e_2 - \frac{K_{c,2}K_{o,1}}{a_2}\int e_2\,dt \\
&= -\frac{K_{c,1}+K_{o,1}}{a_1}\left(y_1 + \frac{K_{c,1}K_{o,1}}{K_{c,1}+K_{o,1}}\int y_1\,dt\right) - \frac{K_{c,2}}{a_2}\left(e_2 + K_{o,1}\int e_2\,dt\right) \\
&= -K_{P,1}\left(y_1 + \frac{1}{\tau_{I,1}}\int y_1\,dt\right) - K_{P,2}\left(e_2 + \frac{1}{\tau_{I,2}}\int e_2\,dt\right)
\end{aligned} \tag{4.41a}$$

$$\begin{aligned}
y_2^* &= \frac{a_2}{a_1}(K_{c,1}+K_{o,1})\int y_1\,dt - \frac{a_2}{a_1}K_{c,1}K_{o,1}\int\left(\int y_1\,dt\right)dt + K_{o,2}\int e_2\,dt \\
&\quad + K_{c,2}(K_{o,1}+K_{o,2})\int\left(\int e_2\,dt\right)dt \\
&= \frac{a_2}{a_1}(K_{c,1}+K_{o,1})\left(\int y_1\,dt + \frac{K_{c,1}K_{o,1}}{K_{c,1}+K_{o,1}}\int\left(\int y_1\,dt\right)dt\right) \\
&\quad + K_{o,2}\left(\int e_2\,dt + \frac{K_{c,2}(K_{o,2}-K_{o,1})}{K_{o,2}}\int\left(\int e_2\,dt\right)dt\right) \\
&= K_{I,1}^*\left(\int y_1\,dt + \frac{1}{\tau_{II,1}^*}\int\left(\int y_1\,dt\right)dt\right) \\
&\quad + K_{I,2}^*\left(\int e_2\,dt + \frac{1}{\tau_{II,2}^*}\int\left(\int e_2\,dt\right)dt\right)
\end{aligned} \tag{4.41b}$$

The controller (4.41a) shows PI-like components (both proportional and inte-

gral terms) for both primary and secondary temperatures, while the set-point generator (4.41b) has I and II (double integrator) components for both temperatures. Differently from conventional case, the cascade controller obtained is not equivalent to the classical cascade PI form.

4.4.4 Dynamics in second order form

It is interesting to show how a second-order dynamic expression is obtained for the primary temperature closed-loop dynamics if jointing primary and secondary closed-loop expressions given in Eq. (4.28) and (4.23) respectively. Such expression is useful in order to determine and analyze the second-order response parameters (characteristic frequency and damping factor), by connecting them with the cascade ones. Recall first-order dynamic expressions for sakes of clarity:

$$\dot{y}_1 = -K_{c,1} y_1 - K_{c,2} \frac{a_1}{a_2} e_2 \tag{4.42a}$$

$$\dot{e}_2 = -K_{c,2} e_2 \tag{4.42b}$$

If Eq. (4.42a) is derived with respect to time, the following second order equation is obtained:

$$\ddot{y}_1 = -K_{c,1} \dot{y}_1 - K_{c,2} \frac{a_1}{a_2} \dot{e}_2 \tag{4.43}$$

Let substitute Eq. (4.42b) in Eq. (4.43):

$$\begin{aligned} \ddot{y}_1 &= -K_{c,1} \dot{y}_1 - K_{c,2} \frac{a_1}{a_2} \dot{e}_2 \\ &= -K_{c,1} \dot{y}_1 + {K_{c,2}}^2 \frac{a_1}{a_2} e_2 \end{aligned} \tag{4.44}$$

Finally, by inserting the expression for e_2 extracted from Eq. (4.42a), the primary temperature second order dynamics are obtained:

$$\begin{aligned} \ddot{y}_1 &= -K_{c,1} \dot{y}_1 + {K_{c,2}}^2 \frac{a_1}{a_2} e_2 = -K_{c,1} \dot{y}_1 + {K_{c,2}}^2 \frac{a_1}{a_2} \left(\frac{-K_{c,1} y_1 - \dot{y}_1}{K_{c,2} \frac{a_1}{a_2}} \right) \\ &= -K_{c,1} \dot{y}_1 - K_{c,1} K_{c,2} y_1 - K_{c,2} \dot{y}_1 \\ &= -(K_{c,1} + K_{c,2}) \dot{y}_1 - K_{c,1} K_{c,2} y_1 \end{aligned}$$

Since a standard second order equation is written as follows:

$$\ddot{y}_1 + 2\xi\omega \dot{y}_1 + \omega^2 y_1 = 0 \tag{4.45}$$

the characteristic frequency ω and the damping factor ξ are

$$\omega = \sqrt{K_{c,1} K_{c,2}}, \qquad \xi = \frac{K_{c,1} + K_{c,2}}{2\sqrt{K_{c,1} K_{c,2}}} \tag{4.46}$$

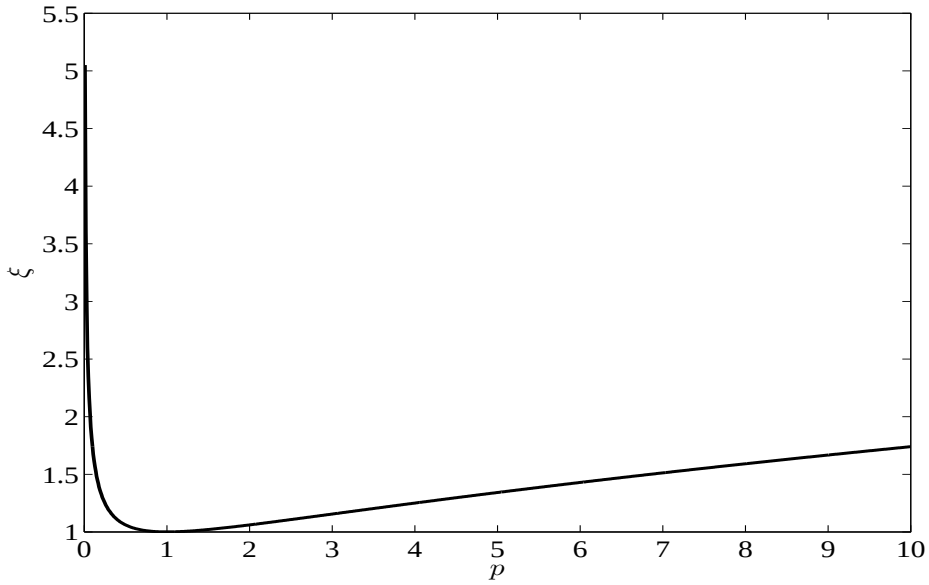

Figure 4.3: Damping factor ξ versus gain separation factor p for the second order response of a cascade controller

Note that the controller gains $K_{c,1}$ and $K_{c,2}$ are interchangeable, meaning that no difference in dynamics results from exchanging primary and secondary controller gains. If a gain separation factor p is defined such that

$$K_{c,2} = pK_{c,1}, \qquad p > 0$$

the following expressions for the characteristic frequency and the damping factor are obtained

$$\omega = \sqrt{p}K_{c,1}, \qquad \xi = \frac{1+p}{2\sqrt{p}} \tag{4.47}$$

meaning that the damping factor only depends on the separation factor p.

From an analysis of the damping factor ξ as a function of p, it follows that the second-order response (4.43) is always overdamped, given that the condition $\xi \geq 1$ is always verified. The plot in Figure 4.3 shows the damping factor ξ versus the gain separation factor p.

4.4.5 Tuning

The cascade controller can be easily tuned on the basis of the following rules based on Castellanos-Sahagún *et al.* (2005):

$$K_{c,1} \approx \text{1-2}\omega, \qquad K_{c,2} \approx \text{1-2}K_{c,1}, \qquad K_{o,1} = K_{o,2} \approx \text{5-10}K_{c,1} \tag{4.48}$$

The tuning rules given in Eq. (4.48) can be easily interpreted as follows: (i) the primary controller gain $K_{c,1}$ represents the characteristic frequency of the primary controller, which must be forced to be equal or at most twice larger of the characteristic frequency of the system ω; (ii) the secondary controller gain $K_{c,2}$ represents the characteristic frequency of the secondary controller, which must be forced to be equal or at most twice larger of the primary one $K_{c,1}$; the (iii) the estimator gains $K_{o,1}$ and $K_{o,2}$ represent the characteristic frequencies of primary and secondary estimators, and it is desired that the estimation errors decay much faster than the primary regulation one (from 5 to 10 times quicker).

As for conventional controller case, the observer frequencies $K_{o,1}$ and $K_{o,2}$ cannot exceed $\frac{1}{3}$ of holdup characteristic frequency ω_H, in order to avoid system destabilization. In addition, the controller (4.27) can be simply tuned once the characteristic frequency of the system is known. Characteristic frequency can be found as already explained in Section 4.3.4, and then the controller parameters can be easily computed.

4.5 CLF controller based on Control Lyapunov functions

In this Section, a parallel cascade-type controller is built on the basis of nonlinear constructive control theory according to the Lyapunov stability criteria. The goal here is to obtain a control function such that its application yields a stable system in the sense of Lyapunov: (i) firstly, a positive definite Lyapunov function which represents the energy of the system has to be found; (ii) then, a control function has to be forced in order to render the time-derivative of such Lyapunov function negative definite. Such control function is defined as Control Lyapunov Function (CLF). Like for the cascade controller proposed in previous Section, composition is indirectly controlled through a manipulated input which regulates a primary temperature through the assistance of a secondary temperature control loop. The role of the secondary temperature is again the fast rejection of feed disturbances. This controller was introduced in Castellanos-Sahagún *et al.* (2010) for a binary column, and is here extended for the multicomponent case. Being the CLF controller a cascade-type one, its scheme is the same of the cascade controller reported in Figure 4.2.

4.5.1 Derivation

As already done for the cascade case, consider again the dynamics of a primary temperature T_{k_1} and of a secondary temperature T_{k_2}, driven by a manipulated

input u_l (either Q or R):

$$\dot{y_1} = a_1 u + b_1 \tag{4.49a}$$

$$\dot{y_2} = a_2 u + b_2 \tag{4.49b}$$

where the deviated variables $y_1 = T_{k_1} - \bar{T}_{k_1}$, $y_2 = T_{k_2} - \bar{T}_{k_2}$ and $u = u_l - \bar{u}_l$ are used. Note that, as well as for cascade case, Eq. (4.49) has been already manipulated as in Eq. (4.4), meaning that the actual parameters $\overset{*}{a_1}$, and $\overset{*}{a_2}$ have already been substituted with suitable approximations with the same sign a_1 and a_2, and therefore the procedure is not reported again.

The first step when attempting to find a CLF for system (4.49), consists in obtaining a candidate Lyapunov function $\mathcal{V}$ which represents the energy of such system. $\mathcal{V}$ must be positive definite at nominal SS conditions, meaning that has to be always positive except at nominal SS where has to be equal to zero. A possible system Lyapunov function is the following:

$$\mathcal{V}(y_1, e_2) = \frac{1}{2}({y_1}^2 + {e_2}^2) \succ 0 \tag{4.50}$$

where $e_2 = y_2 - y_2^*$, y_2^* denotes the dynamic secondary set-point, which is generated from the primary controller u^* as

$$\dot{y_2^*} = a_2 u^* + b_2 \tag{4.51}$$

The primary controller u^* and the secondary controller $\tilde{u}$ form the entire control action u as

$$u = u^* + \tilde{u}$$

Note that Eq. (4.50) is positive definite at nominal SS conditions (i.e., in $(y_1, e_2) = (0, 0)$) since is always positive, except at SS, where is equal to zero ($\mathcal{V}(0, 0) = 0$).

Once the Lyapunov function has been chosen, the control action must be forced in such a way that the time derivative $\dot{\mathcal{V}}$ of Eq. (4.50) be negative definite at SS (in $(y_1, e_2) = (0, 0)$), meaning that $\dot{\mathcal{V}}$ has to be always negative, except at SS conditions, where has to be equal to zero. $\dot{\mathcal{V}}$ can be obtained as follows making use of the expressions for $\dot{y}_1$ and $\dot{y}_2$ given in Eq. (4.49).

$$\begin{aligned}
\dot{\mathcal{V}}(y_1, e_2) &= y_1 \dot{y}_1 + e_2 \dot{e}_2 = y_1(a_1 u + b_1) + e_2(a_2 u + b_2 - a_2 u^* - b_2) \\
&= y_1(a_1(u^* + \tilde{u}) + b_1) + a_2 e_2 \tilde{u} \\
&= y_1(a_1 u^* + b_1) + (a_1 y_1 + a_2 e_2)\tilde{u}
\end{aligned} \tag{4.52}$$

The last manipulation in Eq. (4.52) is denoted as backstepping procedure (Sepulchre *et al.*, 1997), and consists in splitting the function $\dot{y}$ in two parts in such a way that one part be only function of the primary controller u, and the other be only function of the secondary controller $\tilde{u}$. In order to render Eq. (4.52) negative definite, u^* and $\tilde{u}$ must be appropriately forced: here the idea is to determine u^* so that the term $y_1(a_1 u^* + b_1)$ be always negative, and $\tilde{u}$ for doing the same with

the term $(a_1 y_1 + a_2 e_2)\tilde{u}$. A possible selection of primary and secondary control actions to achieve the above mentioned aim is the following:

$$u^* = -\frac{K_{c,1} y_1 + b_1}{a_1} \tag{4.53a}$$

$$\tilde{u} = -K_{c,2}\left(\frac{a_1}{{a_2}^2} y_1 + \frac{1}{a_2} e_2\right) \tag{4.53b}$$

If Eq. (4.53a) and Eq. (4.53b) expressions are used in Eq. (4.52), the latter becomes negative definite at SS, as shown in the following:

$$\begin{aligned}
\dot{\mathcal{V}}(y_1, e_2) &= y_1(a_1 u^* + b_1) + (a_1 y_1 + a_2 e_2)\tilde{u} \\
&= y_1\left(a_1\left(-\frac{K_{c,1} y_1 + b_1}{a_1}\right) + b_1\right) \\
&\quad + (a_1 y_1 + a_2 e_2)\left(-K_{c,2}\left(\frac{a_1}{{a_2}^2} y_1 + \frac{1}{a_2} e_2\right)\right) \\
&= y_1(-K_{c,1} y_1 - b_1 + b_1) - K_{c,2}\frac{a_1 y_1 + a_2 e_2}{a_2}\left(\frac{a_1}{a_2} y_1 + e_2\right) \\
&= -K_{c,1}{y_1}^2 - K_{c,2}\left(\frac{a_1}{a_2} y_1 + e_2\right)^2
\end{aligned} \tag{4.54}$$

It is clear than Eq. (4.54) is equal to zero only if $(y_1, e_2) = (0, 0)$ and negative elsewhere, meaning that is negative definite in $(0, 0)$, as required. This condition can be rewritten in mathematical terms as

$$\dot{\mathcal{V}}(y_1, e_2) = -K_{c,1}{y_1}^2 - K_{c,2}\left(\frac{a_1}{a_2} y_1 + e_2\right)^2 \prec 0 \tag{4.55}$$

Conditions (4.50) and (4.55) mean that the controller

$$u = u^* + \tilde{u} = -\frac{K_{c,1} y_1 + b_1}{a_1} - K_{c,2}\left(\frac{a_1}{{a_2}^2} y_1 + \frac{1}{a_2} e_2\right) \tag{4.56}$$

is a CLF for the system (4.49).

The closed-loop dynamics forced by Eq. (4.56) are:

$$\begin{aligned}
\dot{y_1} &= a_1 u + b_1 = a_1\left(-\frac{K_{c,1} y_1 + b_1}{a_1} - K_{c,2}\left(\frac{a_1}{{a_2}^2} y_1 + \frac{1}{a_2} e_2\right)\right) + b_1 \\
&= -K_{c,1} y_1 - b_1 - K_{c,2}\left(\left(\frac{a_1}{a_2}\right)^2 y_1 + \frac{a_1}{a_2} e_2\right) + b_1 \\
&= -\left(K_{c,1} + K_{c,2}\left(\frac{a_1}{a_2}\right)^2\right) y_1 - K_{c,2}\frac{a_1}{a_2} e_2
\end{aligned} \tag{4.57a}$$

$$\dot{e_2} = \dot{y}_2 - \dot{y}_2^* = a_2 u + b_2 - a_2 u^* - b_2 = a_2\tilde{u} = -a_2 K_{c,2}\left(\frac{a_1}{{a_2}^2} y_1 + \frac{1}{a_2} e_2\right)$$

$$= -K_{c,2}\left(\frac{a_1}{a_2}y_1 + e_2\right) \tag{4.57b}$$

As well as for the cascade case, b_1 and b_2 can be indirectly estimated through the following first order estimators:

$$\dot{\chi}_1 = -K_{o,1}\chi_1 - K_{o,1}(a_1 u + K_{o,1}y_1), \qquad \hat{b}_1 = \chi_1 + K_{o,1}y_1 \tag{4.58a}$$

$$\dot{\chi}_2 = -K_{o,2}\chi_2 - K_{o,2}(a_2 u + K_{o,2}y_2), \qquad \hat{b}_2 = \chi_2 + K_{o,2}y_2 \tag{4.58b}$$

Finally, jointing Eq. (4.51), Eq. (4.56) and Eq. (4.58), the *Control Lyapunov function (CLF) in open-loop form* is derived as

$$u = u^* + \tilde{u} = -\frac{K_{c,1}y_1 + b_1}{a_1} - K_{c,2}\left(\frac{a_1}{{a_2}^2}y_1 + \frac{1}{a_2}e_2\right) \tag{4.59a}$$

$$\dot{y}_2^* = a_2 u^* + K_{o,2}y_2 + \chi_2 \tag{4.59b}$$

$$\dot{\chi}_1 = -K_{o,1}\chi_1 - K_{o,1}(a_1 u + K_{o,1}y_1) \tag{4.59c}$$

$$\dot{\chi}_2 = -K_{o,2}\chi_2 - K_{o,2}(a_2 u + K_{o,2}y_2) \tag{4.59d}$$

Remark 4.6 *The state variables for the controller based on CLF are the two estimated variables χ_1 and χ_2 and the secondary set-point y_2^*. The state-space representation is similar to the cascade case, and can be obtained manipulating time derivative variables as follows:*

$$\begin{aligned}
\dot{\chi}_1 &= -K_{o,1}\chi_1 - K_{o,1}(a_1 u + K_{o,1}y_1) \\
&= -K_{o,1}\chi_1 - K_{o,1}\left(-(K_{c,1} + K_{o,1})y_1 - \chi_1 - K_{c,2}\frac{a_1}{{a_2}^2}(a_1 y_1 + a_2(y_2 - y_2^*))\right) \\
&\quad - {K_{o,1}}^2 y_1 \\
&= -K_{c,2}K_{o,1}\frac{a_1}{a_2}y_2^* + \left(K_{c,2}K_{o,1}\left(\frac{a_1}{a_2}\right)^2 + K_{c,1}K_{o,1}\right)y_1 + K_{c,2}K_{o,1}\frac{a_1}{a_2}y_2 \\
\dot{\chi}_2 &= -K_{o,2}\chi_2 - K_{o,2}(a_2 u + K_{o,2}y_2) \\
&= -K_{o,2}\chi_2 - K_{o,2}\left(-\frac{a_2}{a_1}(K_{c,1}y_1 + b_1) - K_{c,2}\frac{1}{a_2}(a_1 y_1 - a_2 e_2) + K_{o,2}y_2\right) \\
&= -K_{o,2}\frac{a_2}{a_1}\chi_1 - K_{o,2}\chi_2 - K_{c,2}K_{o,2}y_2^* + K_{o,2}\left((K_{c,1} + K_{o,1})\frac{a_2}{a_1} + K_{c,2}\frac{a_1}{a_2}\right)y_1 \\
&\quad + K_{o,2}(K_{c,2} - K_{o,2})y_2 \\
\dot{y}_2^* &= a_2 u^* + \chi_2 + K_{o,2}y_2 = -\frac{a_2}{a_1}\left((K_{c,1} + K_{o,1})y_1 + \chi_1\right) + \chi_2 + K_{o,2}y_2 \\
&= -\frac{a_2}{a_1}\chi_1 + \chi_2 - \frac{a_2}{a_1}(K_{c,1} + K_{o,1})y_1 + K_{o,2}y_2
\end{aligned}$$

The controller (4.59) *can then be written in state-space form as:*

$$\begin{bmatrix} \dot{\chi}_1 \\ \dot{\chi}_2 \\ \dot{y}_2^* \end{bmatrix} = \begin{bmatrix} 0 & 0 & -K_{c,2}K_{o,1}\frac{a_1}{a_2} \\ K_{o,2}\frac{a_1}{a_2} & -K_{o,2} & -K_{c,2}K_{o,2} \\ -\frac{a_1}{a_2} & 1 & 0 \end{bmatrix} \begin{bmatrix} \chi_1 \\ \chi_2 \\ y_2^* \end{bmatrix}$$
$$+ \begin{bmatrix} K_{c,2}K_{o,1}\left(\frac{a_1}{a_2}\right)^2 + K_{c,1}K_{o,1} & -K_{c,2}K_{o,1}\frac{a_1}{a_2} \\ (K_{c,1}+K_{o,1})\frac{a_2}{a_1} + K_{c,2}\frac{a_1}{a_2} & K_{o,2}(K_{c,2}+K_{o,2}) \\ -\frac{a_2}{a_1}(K_{c,1}+K_{o,1}) & K_{o,2} \end{bmatrix} \begin{bmatrix} y_1 \\ y_2 \end{bmatrix}$$
$$\begin{bmatrix} u^* \\ \tilde{u} \end{bmatrix} = \begin{bmatrix} -\frac{1}{a_1} & 0 & 0 \\ 0 & 0 & \frac{K_{c,2}}{a_2} \end{bmatrix} \begin{bmatrix} \chi_1 \\ \chi_2 \\ y_2^* \end{bmatrix} + \begin{bmatrix} -\frac{K_{c,1}+K_{o,1}}{a_1} & 0 \\ -K_{c,2}\frac{a_1}{{a_2}^2} & -\frac{K_{c,2}}{a_2} \end{bmatrix} \begin{bmatrix} y_1 \\ y_2 \end{bmatrix}$$

4.5.2 Anti-windup feature

As well as for the cascade case, the anti-windup action is ensured when saturation occurs since the estimators in Eq. (4.58) are driven by the real control action u_S, defined as

$$u_S = \text{sat}(u, u_-, u_+) = u + \Delta u_S \tag{4.60}$$

and the secondary temperature set-point generator is driven by the saturated primary control action, defined as:

$$u_S^* = \text{sat}(u^*, u_-, u_+) = u^* + \Delta u_S^* \tag{4.61}$$

Remark 4.7 *The estimators dynamics and the secondary temperature set-point generator expressions must be manipulated as follows in order to obtain the state-space representation of the cascade controller when saturation is present:*

$$\begin{aligned}
\dot{\chi}_1 &= -K_{o,1}\chi_1 - K_{o,1}(a_1 u_S + K_{o,1}y_1) \\
&= -K_{o,1}\chi_1 - K_{o,1}(a_1 u + K_{o,1}y_1) - K_{o,1}a_1\Delta u_S \\
&= -K_{o,1}\chi_1 - K_{o,1}\left(-(K_{c,1}+K_{o,1})y_1 - \chi_1 - K_{c,2}\frac{a_1}{{a_2}^2}(a_1 y_1 + a_2(y_2 - y_2^*))\right) \\
&\quad - {K_{o,1}}^2 y_1 - K_{o,1}a_1\Delta u_S \\
&= -K_{c,2}K_{o,1}\frac{a_1}{a_2}y_2^* + \left(K_{c,2}K_{o,1}\left(\frac{a_1}{a_2}\right)^2 + K_{c,1}K_{o,1}\right)y_1 + K_{c,2}K_{o,1}\frac{a_1}{a_2}y_2 \\
&\quad - K_{o,1}a_1\Delta u_S \\
\dot{\chi}_2 &= -K_{o,2}\chi_2 - K_{o,2}(a_2 u_S + K_{o,2}y_2) \\
&= -K_{o,2}\chi_2 - K_{o,2}(a_2 u + K_{o,2}y_2) - K_{o,2}a_2\Delta u_S \\
&= -K_{o,2}\chi_2 + K_{o,2}\frac{a_2}{a_1}(K_{c,1}y_1 + \chi_1 + K_{o,1}y_1) + K_{c,2}K_{o,2}\frac{1}{a_2}(a_1 y_1 - a_2(y_2 - y_2^*)) \\
&\quad - K_{o,2}y_2 - K_{o,2}a_2\Delta u_S
\end{aligned}$$

$$
\begin{aligned}
&= -K_{o,2}\frac{a_2}{a_1}\chi_1 - K_{o,2}\chi_2 - K_{c,2}K_{o,2}y_2^* + K_{o,2}\left((K_{c,1}+K_{o,1})\frac{a_2}{a_1} + K_{c,2}\frac{a_1}{a_2}\right)y_1 \\
&\quad + K_{o,2}(K_{c,2}-K_{o,2})y_2 - K_{o,2}a_2\Delta u_S \\
\dot{y}_2^* &= a_2 u_S^* + \chi_2 + K_{o,2}y_2 = a_2(u^* + \Delta u_S^*) + \chi_2 + K_{o,2}y_2 \\
&= -\frac{a_2}{a_1}\left((K_{c,1}+K_{o,1})y_1 + \chi_1\right) + \chi_2 + K_{o,2}y_2 + a_2\Delta u_S^* \\
&= -\frac{a_2}{a_1}\chi_1 + \chi_2 - \frac{a_2}{a_1}(K_{c,1}+K_{o,1})y_1 + K_{o,2}y_2 + a_2\Delta u_S^*
\end{aligned}
$$

The state-space representation is the following:

$$
\begin{bmatrix} \dot{\chi}_1 \\ \dot{\chi}_2 \\ \dot{y}_2^* \end{bmatrix} = \begin{bmatrix} 0 & 0 & -K_{c,2}K_{o,1}\frac{a_1}{a_2} \\ K_{o,2}\frac{a_1}{a_2} & -K_{o,2} & -K_{c,2}K_{o,2} \\ -\frac{a_1}{a_2} & 1 & 0 \end{bmatrix} \begin{bmatrix} \chi_1 \\ \chi_2 \\ y_2^* \end{bmatrix}
$$

$$
+ \begin{bmatrix} K_{c,2}K_{o,1}\left(\frac{a_1}{a_2}\right)^2 + K_{c,1}K_{o,1} & -K_{c,2}K_{o,1}\frac{a_1}{a_2} & -K_{o,1}a_1 & 0 \\ (K_{c,1}+K_{o,1})\frac{a_2}{a_1} + K_{c,2}\frac{a_1}{a_2} & K_{o,2}(K_{c,2}+K_{o,2}) & -K_{o,2}a_2 & 0 \\ -\frac{a_2}{a_1}(K_{c,1}+K_{o,1}) & K_{o,2} & 0 & a_2 \end{bmatrix} \begin{bmatrix} y_1 \\ y_2 \\ \Delta u_S \\ \Delta u_S^* \end{bmatrix}
$$

$$
\begin{bmatrix} u^* \\ \tilde{u} \end{bmatrix} = \begin{bmatrix} -\frac{1}{a_1} & 0 & 0 \\ 0 & 0 & \frac{K_{c,2}}{a_2} \end{bmatrix} \begin{bmatrix} \chi_1 \\ \chi_2 \\ y_2^* \end{bmatrix} + \begin{bmatrix} -\frac{K_{c,1}+K_{o,1}}{a_1} & 0 & 0 & 0 \\ -K_{c,2}\frac{a_1}{{a_2}^2} & -\frac{K_{c,2}}{a_2} & 0 & 0 \end{bmatrix} \begin{bmatrix} y_1 \\ y_2 \\ \Delta u_S \\ \Delta u_S^* \end{bmatrix}
$$

4.5.3 Derivation of a conventional CLF PI form

The procedure shown in Section 4.4.3 can also be used in order to obtain a PI-like expression for the CLF controller (4.56). Since manipulations are substantially the same shown in Section 4.4.3, only the final expressions are here reported.

$$
\begin{aligned}
u &= -\left(\frac{K_{c,1}+K_{o,1}}{a_1} + K_{c,2}\frac{a_1}{{a_2}^2}\right)y_1 - \frac{K_{o,1}}{a_1}\left(K_{c,1} + K_{c,2}\left(\frac{a_1}{a_2}\right)^2\right)\int y_1\,dt \\
&\quad - \frac{K_{c,2}}{a_2}e_2 - \frac{K_{c,2}K_{o,1}}{a_2}\int e_2\,dt \\
&= -\frac{1}{a_1}\left(K_{c,1}+K_{o,1}+K_{c,2}\left(\frac{a_1}{a_2}\right)^2\right)\left(y_1 + K_{o,1}\frac{K_{c,1}+K_{c,2}\left(\frac{a_1}{a_2}\right)^2}{K_{c,1}+K_{o,1}+K_{c,2}\left(\frac{a_1}{a_2}\right)^2}\int y_1\,dt\right) \\
&\quad - \frac{K_{c,2}}{a_2}\left(e_2 + K_{o,1}\int e_2\,dt\right) \\
&= -K_{P,1}\left(y_1 + \frac{1}{\tau_{I,1}}\int y_1\,dt\right) - K_{P,2}\left(e_2 + \frac{1}{\tau_{I,2}}\int e_2\,dt\right) \qquad (4.62a) \\
y_2^* &= \frac{a_2}{a_1}(K_{c,1}+K_{o,1})\int y_1\,dt
\end{aligned}
$$

$$
\begin{aligned}
&- \left(K_{c,1} K_{o,1} \frac{a_2}{a_1} + K_{c,2}(K_{o,2} - K_{o,1}) \frac{a_1}{a_2} \right) \int \left(\int y_1 \, dt \right) dt \\
&+ K_{o,2} \int e_2 \, dt + K_{c,2}(K_{o,1} + K_{o,2}) \int \left(\int e_2 \, dt \right) dt \\
&= \frac{a_2}{a_1}(K_{c,1} + K_{o,1}) \left(\int y_1 \, dt + \frac{K_{c,1} K_{o,1} + K_{c,2}(K_{o,2} - K_{0,1}) \left(\frac{a_1}{a_2} \right)^2}{K_{c,1} + K_{o,1}} \int \left(\int y_1 \, dt \right) dt \right) \\
&+ K_{o,2} \left(\int e_2 \, dt + \frac{K_{c,2}(K_{o,2} - K_{o,1})}{K_{o,2}} \int \left(\int e_2 \, dt \right) dt \right) \\
&= K^*_{I,1} \left(\int y_1 \, dt + \frac{1}{\tau^*_{II,1}} \int \left(\int y_1 \, dt \right) dt \right) \\
&+ K^*_{I,2} \left(\int e_2 \, dt + \frac{1}{\tau^*_{II,2}} \int \left(\int e_2 \, dt \right) dt \right) \qquad (4.62b)
\end{aligned}
$$

4.5.4 Dynamics in second order form

As in cascade controller case, a second order expression for the dynamics of the primary temperature can be obtained when a CLF is used. Such expression is useful for analyzing second-order response parameters (characteristic frequency and damping factor) and connecting them with the controllers ones.

Recall the expressions for primary and secondary closed-loop dynamics given in Eq. (4.57):

$$\dot{y}_1 = - \left(K_{c,1} + K_{c,2} \left(\frac{a_1}{a_2} \right)^2 y_1 \right) - K_{c,2} \frac{a_1}{a_2} e_2 \qquad (4.63a)$$

$$\dot{e}_2 = -K_{c,2} \left(\frac{a_1}{a_2} y_1 + e_2 \right) \qquad (4.63b)$$

Deriving Eq. (4.63a) with respect to time, the following second order equation is obtained:

$$\ddot{y}_1 = - \left(K_{c,1} + K_{c,2} \left(\frac{a_1}{a_2} \right)^2 \right) \dot{y}_1 - K_{c,2} \frac{a_1}{a_2} \dot{e}_2 \qquad (4.64)$$

Eq. (4.64) can be rewritten as follows, by using expression (4.63b):

$$
\begin{aligned}
\ddot{y}_1 &= - \left(K_{c,1} + K_{c,2} \left(\frac{a_1}{a_2} \right)^2 \right) \dot{y}_1 - K_{c,2} \frac{a_1}{a_2} \left(-K_{c,2} \left(\frac{a_1}{a_2} y_1 + e_2 \right) \right) \\
&= - \left(K_{c,1} + K_{c,2} \left(\frac{a_1}{a_2} \right)^2 \right) \dot{y}_1 + \left(K_{c,2} \frac{a_1}{a_2} \right)^2 y_1 + {K_{c,2}}^2 \frac{a_1}{a_2} e_2 \qquad (4.65)
\end{aligned}
$$

An expression for e_2 can be extracted from Eq. (4.63b):

$$e_2 = -\frac{\left(K_{c,1} + K_{c,2}\left(\frac{a_1}{a_2}\right)^2\right) y_1 + \dot{y_1}}{K_{c,2}\frac{a_1}{a_2}} \tag{4.66}$$

On the basis of Eq. (4.63b), Eq. (4.65) can be manipulated as follows:

$$\begin{aligned}
\ddot{y_1} &= -\left(K_{c,1} + K_{c,2}\left(\frac{a_1}{a_2}\right)^2\right)\dot{y_1} + \left(K_{c,2}\frac{a_1}{a_2}\right)^2 y_1 + {K_{c,2}}^2\frac{a_1}{a_2}e_2 \\
&= -\left(K_{c,1} + K_{c,2}\left(\frac{a_1}{a_2}\right)^2\right)\dot{y_1} + \left(K_{c,2}\frac{a_1}{a_2}\right)^2 y_1 \\
&\quad - {K_{c,2}}^2\frac{a_1}{a_2}\frac{\left(K_{c,1} + K_{c,2}\left(\frac{a_1}{a_2}\right)^2\right) y_1 + \dot{y_1}}{K_{c,2}\frac{a_1}{a_2}} \\
&= -\left(K_{c,1} + K_{c,2}\left(\frac{a_1}{a_2}\right)^2\right)\dot{y_1} + \left(K_{c,2}\frac{a_1}{a_2}\right)^2 y_1 - K_{c,2}\left(K_{c,1} + K_{c,2}\left(\frac{a_1}{a_2}\right)^2\right) y_1 \\
&\quad - K_{c,2}\dot{y_1} \\
&= -\left(K_{c,1} + K_{c,2} + K_{c,2}\left(\frac{a_1}{a_2}\right)^2\right)\dot{y_1} + K_{c,1}K_{c,2}y_1
\end{aligned} \tag{4.67}$$

According to the standard second order equation

$$\ddot{y_1} + 2\xi\omega\dot{y_1} + \omega^2 y_1 = 0 \tag{4.68}$$

the characteristic frequency ω and the damping factor ξ are

$$\omega = \sqrt{K_{c,1}K_{c,2}}, \qquad \xi = \frac{K_{c,1} + K_{c,2} + K_{c,2}\left(\frac{a_1}{a_2}\right)^2}{2\sqrt{K_{c,1}K_{c,2}}} \tag{4.69}$$

Note that differently from the cascade case, the damping factor ξ depends on the ratio between a_1 and a_2, and $K_{c,1}$ and $K_{c,2}$ can not be interchanged in its expression.

If a gain separation factor p and a sensitivity ratio parameter q are defined such that

$$K_{c,2} = pK_{c,1}, \qquad a_2 = qa_1, \qquad p, q > 0$$

the following expressions for the characteristic frequency and the damping factor are obtained

$$\omega = \sqrt{p}K_{c,1}, \qquad \xi = \frac{1 + p + \frac{p}{q^2}}{2\sqrt{p}} \tag{4.70}$$

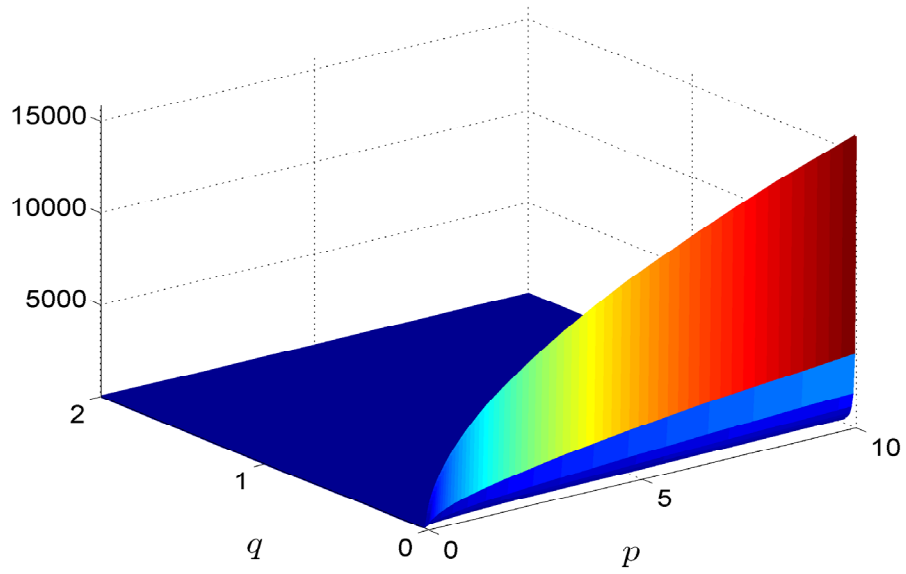

Figure 4.4: Damping factor ξ versus gain separation factor p and sensitivity ratio q for CLF second order dynamics

meaning that the damping factor only depends on the gain separation factor p and on the sensitivity ratio q.

From an analysis of the damping factor ξ as a function of p and q, it follows that the second-order response (4.68) is always overdamped, given that the condition $\xi \geq 1$ is always verified. The plot in Figure 4.4 shows the damping factor ξ versus the gain separation factor p and sensitivity ratio q.

4.5.5 Tuning

The CLF controller can be easily tuned on the basis of the following rules based on Castellanos-Sahagún *et al.* (2005):

$$K_{c,1} \approx 1\text{-}2\omega, \qquad K_{c,2} \approx 1\text{-}2K_{c,1}, \qquad K_{o,1} = K_{o,2} \approx 5\text{-}10K_{c,1} \tag{4.71}$$

The rules are the same of the cascade case, and therefore the explanation can be found in Section 4.4.5.

4.5.6 Differences with cascade controller

In this Subsection, the main differences between CLF and cascade controllers in IMC form are shown. Such controllers are recalled in the following:

Cascade controller

$$u = u^* + \tilde{u} \tag{4.72a}$$
$$u^* = -\frac{K_{c,1}y_1 + b_1}{a_1} \tag{4.72b}$$
$$\tilde{u} = -\frac{K_{c,2}}{a_2}e_2 \tag{4.72c}$$
$$\dot{y}_2^* = a_2u^* + K_{o,2}y_2 + \chi_2 \tag{4.72d}$$
$$\dot{\chi}_1 = -K_{o,1}\chi_1 - K_{o,1}(a_1u + K_{o,1}y_1) \tag{4.72e}$$
$$\dot{\chi}_2 = -K_{o,2}\chi_2 - K_{o,2}(a_2u + K_{o,2}y_2) \tag{4.72f}$$

CLF controller:

$$u = u^* + \tilde{u} \tag{4.73a}$$
$$u^* = -\frac{K_{c,1}y_1 + b_1}{a_1} \tag{4.73b}$$
$$\tilde{u} = -K_{c,2}\left(\frac{a_1}{{a_2}^2}y_1 + \frac{1}{a_2}e_2\right) \tag{4.73c}$$
$$\dot{y}_2^* = a_2u^* + K_{o,2}y_2 + \chi_2 \tag{4.73d}$$
$$\dot{\chi}_1 = -K_{o,1}\chi_1 - K_{o,1}(a_1u + K_{o,1}y_1) \tag{4.73e}$$
$$\dot{\chi}_2 = -K_{o,2}\chi_2 - K_{o,2}(a_2u + K_{o,2}y_2) \tag{4.73f}$$

As it can be seen from Eq. (4.72) and (4.73), the most important difference is in secondary control action: in cascade controller the control action only depends on secondary temperature error (see Eq. (4.72c)), whereas in CLF controller there is also a dependence on the primary temperature error (see Eq. (4.73c)) due to backstepping. This means that cascade secondary controller action acts as primary temperature error is never present, whereas this limitation is removed in CLF secondary controller, with the result that a better cooperation between primary and secondary control actions is present in CLF case. Such difference should lead to a better control performance with respect to the cascade controller. This will be assessed in next section, where controller performance will be tested.

4.6 Chapter summary

In this Section, the observer-based algorithms used in this Thesis for temperature control have been illustrated. Such algorithms are based on passivity con-

cepts and nonlinear constructive theory, and are the following: (i) a conventional controller; (ii) a parallel cascade controller; (iii) a CLF controller (cascade-type parallel controller based on Control Lyapunov Functions).

The conventional controller is equivalent to a classical PI with anti-windup action. On the other hand, cascade and CLF controller are cascade-type controllers that are also endowed with anti-windup action, but are not equivalent to classical cascade-type PI schemes.

The tuning procedure for this family of algorithms is simpler and more intuitive compared to other well-known algorithms.

Chapter 5

Control structure

In this Chapter, the control structural problem is addressed. The selection of the control structure consists in the choice of (i) temperature sensor locations, (ii) manipulated inputs, and (iii) their pairing (for dual-end controllers), according to the control objective to be achieved. In order to do part of this, a new criterion is adopted: the temperature gradient with per-component contribution diagram in conjunction with a systematic procedure. Such method has the advantage of being easy to understand and to apply, and of needing steady-state information only. Finally, the candidate structures are selected for each control algorithm, and are then assessed through dynamic simulations.

5.1 Introduction

As illustrated in Section 3.4, the control objectives (CO) of the present Thesis are the fulfillments of the separation between C3 and iC4 according to the following conditions:

Control Objective 1 (CO1). This objective is the regulation of iC4 in the distillate (heavy-key impurity) around the nominal value (0.02) within a certain range (0.005), and has to be achieved at the nominal conditions SS1 (stripping section working at high-purity conditions) listed in Table 3.1.

$$c_D^{iC4} \in \bar{c}_D^{iC4} \pm \Delta c = 0.02 \pm 0.005 \tag{5.1}$$

Control Objective 2 (CO2), related to SS2 (see Table 3.2)

$$c_D^{iC4} \in \bar{c}_D^{iC4} \pm \Delta c = 0.02 \pm 0.005 \tag{5.2a}$$

$$c_B^{C3} \in \bar{c}_B^{C3} \pm \Delta c = 0.02 \pm 0.005 \tag{5.2b}$$

Requirements (5.1) and (5.2) must be satisfied through a single-end temperature controller and a dual-end temperature controller, respectively. Whereas in previous Chapter the control algorithm problem has been illustrated and the development of the algorithms has been shown, in this Chapter the remaining part of the entire control problem is presented. At this point, the following control items still have to be discussed:

- which temperatures have to be controlled in order to obtain the smaller composition offsets?
- which temperatures have to be chosen as secondary ones for achieving the disturbance rejection task? (only for cascade-type controllers)
- which manipulated variable is better to use?
- how to pair manipulated inputs with controlled temperatures? (only for dual-end control)

The precedent points constitute the *control structure* problem, a fundamental piece of the whole control issue, which must be solved in conjunction with the control algorithm part. In this Thesis, the problem is firstly solved in conjunction with every single control algorithm: at first, several candidate structures are found on the basis of a structural analysis; then, such structures are assessed with respect to the given control objective. Part of the control structure, that is, the location of temperature measurements, is selected through the temperature gradient with per-component contribution diagram, in conjunction with a systematic procedure.

In what follows, the structural analysis is thoroughly depicted for the CO1, where a single controller (either conventional, cascade or CLF-based) is used for performing the determined separation. On the other hand, the same analysis is made with less details for the CO2, since in this case the problem can be split into a section-wise fashion, given that a single controller is used for each different section. This means that the structural analysis for the CO2 can be divided into two parts, since each of them can be considered as a single control structure issue and therefore be solved as in CO1 case.

5.2 Control structure for conventional controller

In this Section, the control structure problem is solved in conjunction with the conventional control algorithm, where one control input and one control output must be found. The task to be carried out is therefore the selection of one or two appropriate input-output pairs (i.e., one or more (u_l, T_k) pairs, according to notation in Section 4.3), in order to obtain the best controller behavior on the basis of the control objective to be reached. Conventional controller schemes are

reported in Figure 4.1. After the selection of candidate structures, structural results are assessed through dynamic simulations.

5.2.1 Structural analysis for conventional controller - CO1

In this Subsection, the input-output pair (u_l, T_k) is found in order to achieve objective CO1, that is, the regulation of distillate iC4 around the nominal value (see Eq. (5.1)). Only one pair has to be found since a single-end controller is used, given that only one impurity effluent composition, the iC4 in the distillate, has to be regulated.

Temperature sensor location

A fundamental part of the control structure is thus the search of the best temperature tray where the controller has to be placed, in order to ensure the smaller composition offset for the impurity to be regulated, together with a satisfying disturbance rejection.

The appropriate temperature to be regulated is here chosen on the basis of the temperature gradient with per-component contribution diagram, which has been introduced in Section 3.7. Such criterion consists in a plot where the temperature gradient profile at the nominal SS operating conditions is shown, together with the per-component contributions. Therefore, in order to find the candidate control structures for CO1 case, the gradient diagram for SS1 conditions (recalled in Table 5.1) reported again in Figure 5.1 for sakes of clarity, has to be analyzed.

F	$\bar{c}_F^{C2}$	$\bar{c}_F^{C3}$	$\bar{c}_F^{iC4}$	$\bar{c}_F^{nC4}$	$\bar{c}_F^{iC5}$	T_F
88.2 $\mathrm{m^3\,h^{-1}}$	0.0036	0.281	0.236	0.4746	0.0004	320 K
Q			R			
3876645 $\mathrm{kcal\,h^{-1}}$			61.62 $\mathrm{m^3\,h^{-1}}$			

Table 5.1: Operating conditions for SS 1

Such criteria for the selection of temperature sensor locations for control purposes is based on the temperature-slope (or largest tray-to-tray temperature gradient) method (Rademaker *et al.*, 1975), where control sensor is placed in the stage with the largest gradient. In Rademaker *et al.* (1975) is also stated, for a multicomponent column, that sensors should be located where non-key compositions are almost constant; according to such consideration, Luyben (2006) and Hori and Skogestad (2007) suggest that locations close to top, bottom and feed stages be avoided.

In addition to the tray-to-tray temperature gradient plot, the temperature gradient with per-component contribution diagram also consists of drawing a per-

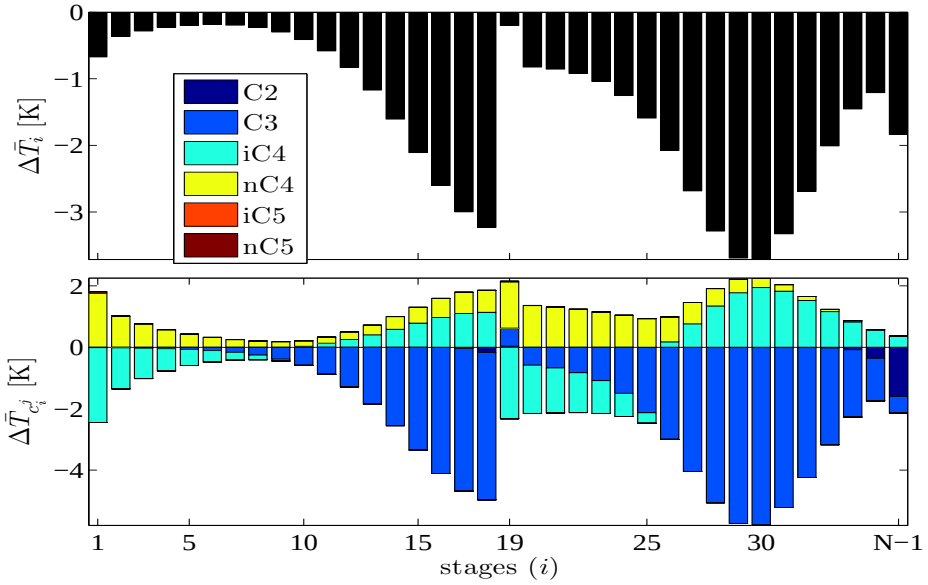

Figure 5.1: Steady-state temperature gradients with per-component contributions for case SS1

component contribution gradient profile which allows, in conjunction with the temperature gradient profile, the selection of locations where gradients are large and non-key contributions are negligible. The criteria for selecting temperature sensor locations can be therefore illustrated, on the basis of the contents of the diagram:

- temperature sensors have to be placed according to the control objective, that is, in the column region associated to it;
- an area with large temperature variations implies that compositions are changing, meaning that the most sensitive stages are there; however, the interest is in the separation between key components (C3 and iC4), and therefore it is suggested that temperature be regulated at a stage in which the gradient is mostly due to these components

On the basis of the preceding considerations in the light of Figure 5.1, the following structural analysis can be made:

- being the control objective the regulation of the iC4 in the distillate, it is clear that the section of interest is the enriching one, and thus a temperature has to be regulated in this section;

- largest temperature gradients can be found around 26-th and 33-th stage, but the 33-th stage seems to be the best choice since the gradient at this section is almost completely due to C3 and iC4.

From the analysis made according to the temperature gradient with per-component contributions criteria, it results that 33-th stage should be the best candidate stage for the location of the temperature sensor. However, other sensor locations will also be tested, even in the stripping section, in order to give a complete assessment of proposed methodology for sensor location.

Manipulated variable selection

Another important step in the design of the control structure is the choice of the manipulated variable to be used for regulating the selected control temperature.

In this Thesis, it has been assumed that pressure, and reboiler and condenser levels are tight controlled, leaving two inputs for the use as manipulated variables for controlling temperatures of interest. These two inputs are typically reflux flow rate and reboiler heat, even if other selections are possible (distillate and bottom flows).

A possible criteria for the selection of manipulated variable is the *Sensitivity criterion* (Rademaker *et al.*, 1975). The criteria was originally thought for the joint selection of temperatures to be controlled and manipulated variables, but is here used only for the latter choice. According to this standard procedure, a very small change ($\approx 0.1\%$) is made for each of the two manipulated variables (with the other one kept constant) in both directions. Then, the input which causes the largest and most simmetrical temperature variations in the region where sensors will be located is chosen.

Such criteria is shown in Figure 5.2 for CO1 case. It can be seen that temperature variations due to both reboiler heat Q and reflux rate R are enough large (> 1K) and symmetrical for the stages of interest (between 26-th and 33-th stage). However, the variation due to Q is slightly larger, and therefore Q is chosen as manipulated variable, even if the employment of R would also be possible.

5.2.2 Structural results for conventional controller - CO1

The candidate structures will be tested in the following, according to two different scenarios (SC). In both cases, a step-plus-sinusoidal change is induced, but the two scenarios differ between each other for the direction and for the magnitude of the change, in order to test the column to different conditions. A case with controller saturation is also presented, in order to test the effectiveness of the anti-windup action.

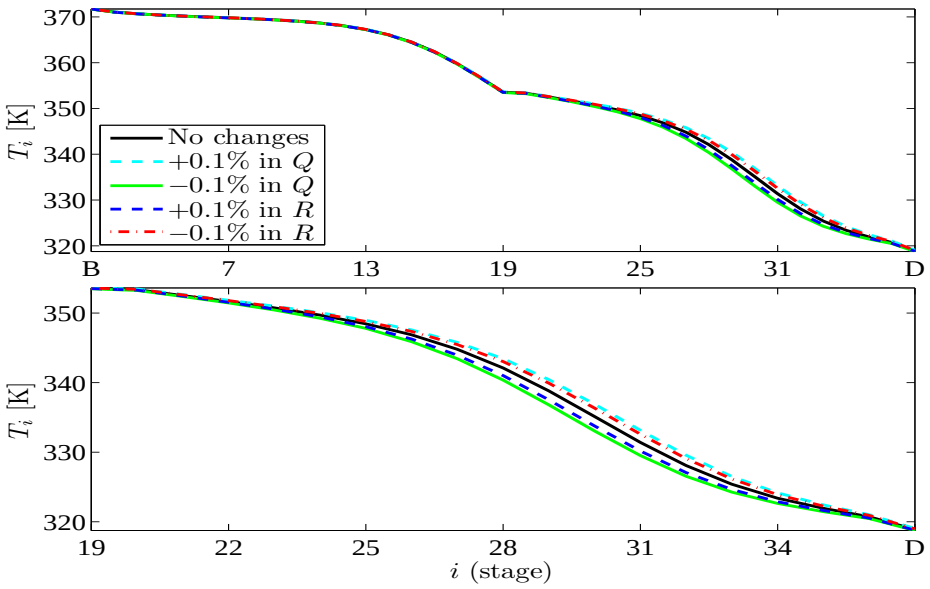

Figure 5.2: Sensitivity criterion for the selection of the manipulated variable: entire column (top) and enriching section (bottom).

At first, the tuning procedure used for both scenarios is described; then, the two scenarios are separately analyzed.

Tuning

Conventional controller tuning for CO1 case has been made as illustrated in Eq. (4.19). Dominant characteristic frequency ω has been computed on the basis of a standard model identification procedure where open-loop column responses to both negative and positive step changes ($\pm 0.1\%$) to both reboiler heat Q and reflux rate R are analyzed. Such responses are illustrated in Figure 5.3 for a stage of interest where sensor location is suggested (31-st stage), and show that a rough estimate of the time needed by the system step response to reach the 98% of its final value is $t_{98\%} \approx 4\text{h}$, and therefore

$$\omega = \frac{4}{t_{98\%}} \approx 1\text{h}^{-1}$$

Therefore, the following tuning parameters are chosen:

$$K_c = 2\omega = 2\text{h}^{-1}, \qquad K_o = 10K_c = 20\text{h}^{-1}$$

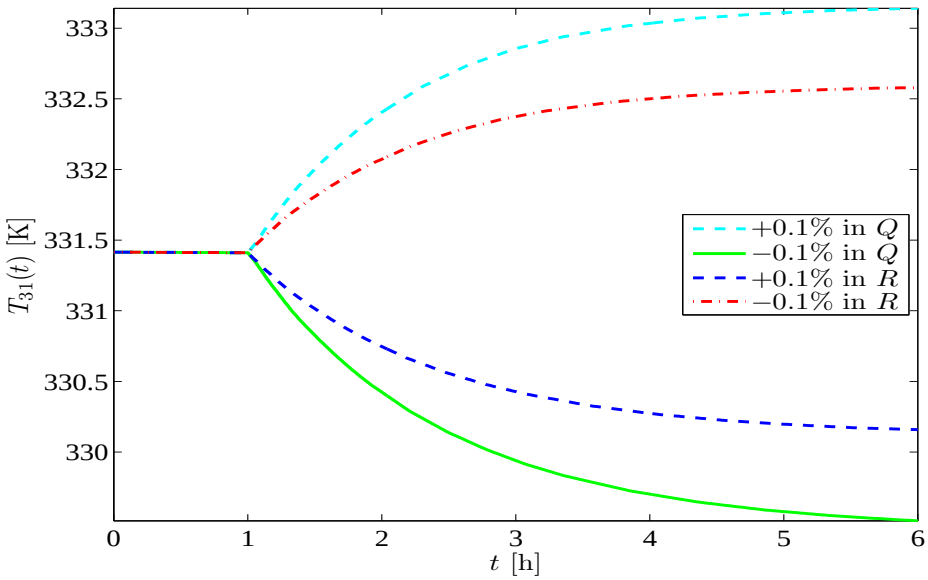

Figure 5.3: Open-loop system responses to ±0.1% changes in manipulated variables.

Remark 5.1 *Even if in this work the holdup dynamics have been neglected, it is worth recalling that the estimator frequency K_o should not exceed $\frac{1}{3}$ of the holdup characteristic frequency ω_H. Since a typical value for the latter is $\omega_H \approx 100\omega \approx 100h^{-1}$, the previous requirement is satisfied.*

Scenario 1 (SC1)

In Scenario 1 (SC1), a transient in the column is caused by a step-plus-sinusoidal change in the form

$$(B_D + A_D \sin(2\pi\omega_D t))\, H(t-1)$$

where $H(t-1)$ is an Heavside step applied at $t = 1$h (since disturbances enter the column after 1 hour), ω_D is the disturbance frequency, B_D and A_D are the magnitudes of the step and the sinusoidal disturbance respectively. The parameter values are reported in Table 5.2, and the disturbance changes are illustrated in Figure 5.4

From now on, the notation

$$\sigma_{C[j,i]}$$

will be used for denoting a single-end control structure, meaning that the manipulated variable j is used for controlling the temperature at i-th stage. If the

	0h$< t <$ 1h	B_D	A_D	ω_D
F	88.2 $m^3\,h^{-1}$	6.8 $m^3\,h^{-1}$	10 $m^3\,h^{-1}$	3 h^{-1}
c_F^{C2}	0.0036	−0.0016	0	3 h^{-1}
c_F^{C3}	0.281	−0.011	0.02	3 h^{-1}
c_F^{iC4}	0.236	−0.00128	0.02	3 h^{-1}
c_F^{nC4}	0.4746	0.0254	−0.04	3 h^{-1}
c_F^{iC5}	0.004	0	0	3 h^{-1}
c_F^{nC5}	0.0008	0	0	3 h^{-1}
T_F	320 K	−3 K	10 K	3 h^{-1}

Table 5.2: Disturbance parameters for scenario 1 (SC1)

notation

$$\sigma_{C[j,i]k}$$

is instead used, this means that in addition, the quantity k is kept fixed.

At first, a comparison between 3 structures where the temperature is controlled in different column regions, is made. In Figure 5.5 the dynamic behavior of distillate iC4 is compared for the control structures $\sigma_{C[Q,17]}$ (temperature controlled in a stripping section stage), $\sigma_{C[Q,23]}$ (temperature controlled in an enriching section stage with small gradient), $\sigma_{C[Q,31]}$ (temperature controlled in an enriching section stage with large gradient), and $\sigma_{C[Q,37]}$ (temperature controlled in the same stage of the impurity to be regulated). It can be noted that both steady-state and dynamic responses are better when the temperature is controlled at a stage with a large temperature gradient, since this implies a bigger sensitivity. Differently from the binary case (Castellanos-Sahagún *et al.*, 2005), the location of the temperature sensor in the same stage (37-th) of the impurity to be regulated does not ensure the best results in terms of offset-less regulation, but rather leads to the worst ones; this can be noted also from the absence of a control action, which stems from the small sensitivity.

Thus, a test where temperatures are controlled in a region of the enriching section with large gradients has been made. In Figure 5.6, the control structures $\sigma_{C[Q,27]}$, $\sigma_{C[Q,31]}$ and $\sigma_{C[Q,33]}$ are compared, showing that no particular differences are present in the dynamic behaviors of iC4 distillate. The structure $\sigma_{C[Q,27]}$ seems to behave slightly worse, maybe because of a larger influence of nC4 (non-key component) compared to the other structures.

Finally, the last comparison is made for different manipulated variables when controlling temperature at 33-th stage. The analyzed cases are: (i) temperature controlled by Q, with R fixed ($\sigma_{C[Q,33]}$); (ii) temperature controlled by R, with Q fixed ($\sigma_{C[R,33]}$); (iii) temperature controlled through Q, with $\frac{R}{F}$ fixed ($\sigma_{C[Q,33]\frac{R}{F}}$).

In Figure 5.7, the control structures $\sigma_{C[Q,33]}$, $\sigma_{C[R,33]}$ and $\sigma_{C[Q,33]\frac{R}{F}}$ are compared, showing almost the same results are obtained when using either Q or R as manipulated variable (with the other one kept fixed). On the other hand,

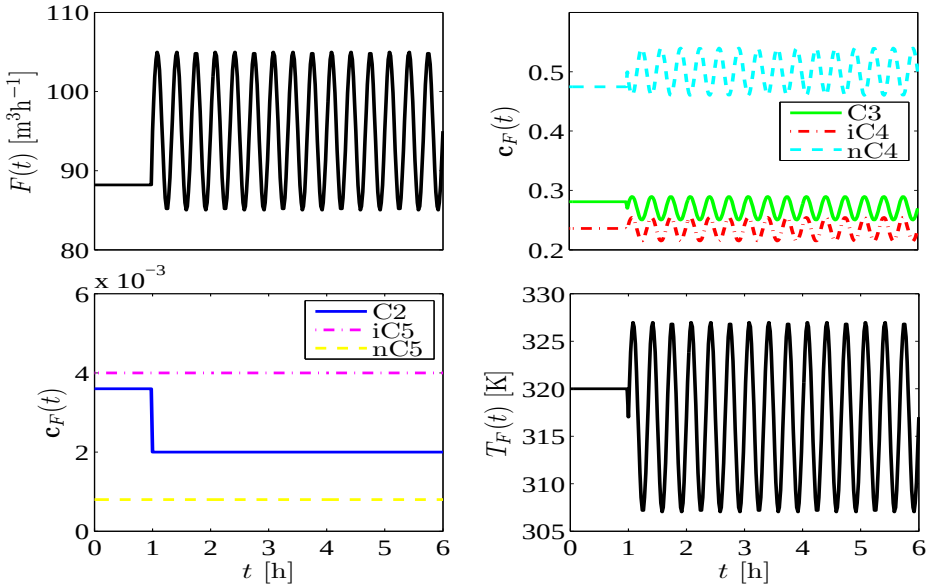

Figure 5.4: Disturbance changes for Scenario 1 (SC1)

performance gets worse when manipulating Q and fixing $\frac{R}{F}$.

Scenario 2 (SC2)

In Scenario 2 (SC2), a transient in the column is caused by a stronger and opposite step-plus-sinusoidal change, compared to the one of SC1. The parameter values are reported in Table 5.3, and the disturbance changes are illustrated in Figure 5.8.

	$0\text{h} < t < 1\text{h}$	B_D	A_D	ω_D
F	88.2 $\text{m}^3\,\text{h}^{-1}$	-22.2 $\text{m}^3\,\text{h}^{-1}$	10 $\text{m}^3\,\text{h}^{-1}$	3 h^{-1}
c_F^{C2}	0.0036	-0.0016	0	3 h^{-1}
c_F^{C3}	0.281	0.043	0.02	3 h^{-1}
c_F^{iC4}	0.236	0.021	0.02	3 h^{-1}
c_F^{nC4}	0.4746	-0.0704	-0.04	3 h^{-1}
c_F^{iC5}	0.004	0	0	3 h^{-1}
c_F^{nC5}	0.0008	0	0	3 h^{-1}
T_F	320 K	10 K	10 K	3 h^{-1}

Table 5.3: Disturbance parameters for scenario 2 SC2

Like for SC1, a comparison between 4 following structures with sensors in different column regions and Q as manipulated variable ($\sigma_{C[Q,17]}$, $\sigma_{C[Q,23]}$, $\sigma_{C[Q,31]}$ and $\sigma_{C[Q,37]}$) is made. Results are illustrated in Figure 5.9, and clearly show that

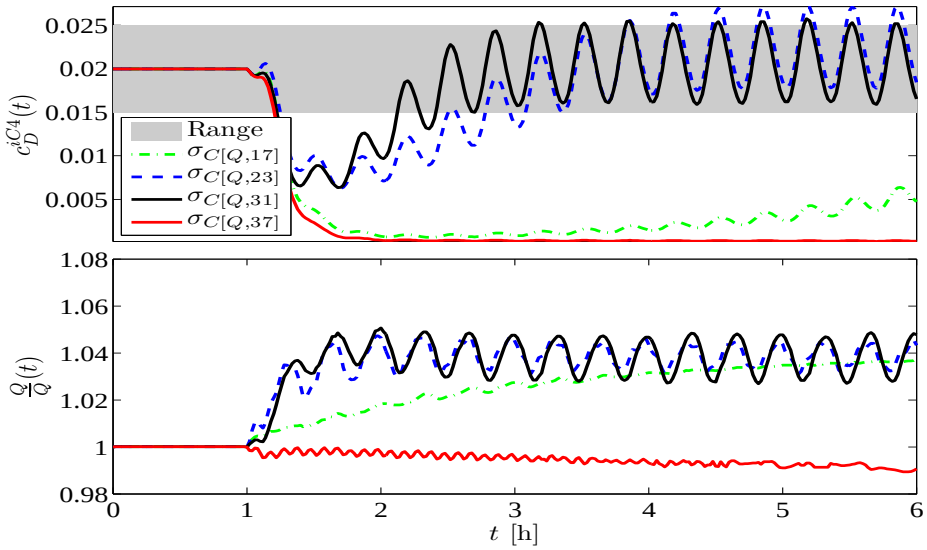

Figure 5.5: CO1, SC1, comparison between the control structures $\sigma_{C[Q,17]}$, $\sigma_{C[Q,23]}$, $\sigma_{C[Q,31]}$ and $\sigma_{C[Q,37]}$: distillate iC4 (top), and reboiler heat duty dynamics (bottom)

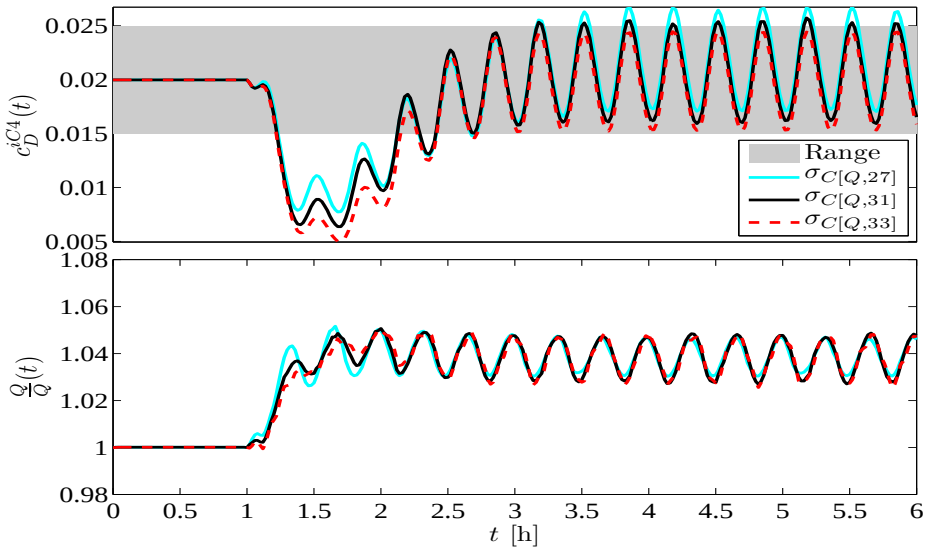

Figure 5.6: CO1, SC1, comparison between the control structures $\sigma_{C[Q,27]}$, $\sigma_{C[Q,31]}$ and $\sigma_{C[Q,33]}$: distillate iC4 (top), and reboiler heat duty dynamics (bottom)

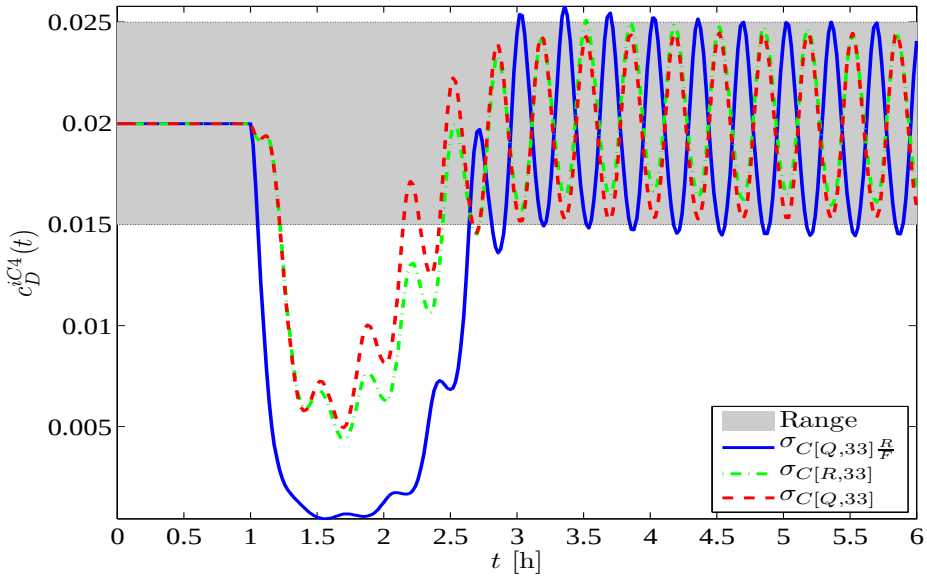

Figure 5.7: CO1, SC1: comparison between the control structures $\sigma_{C[Q,33]\frac{R}{F}}$, $\sigma_{C[R,33]}$ and $\sigma_{C[Q,33]}$

$\sigma_{C[Q,31]}$ is by far the best choice.

The comparison between control structures with sensors placed in the region with the largest gradients ($\sigma_{C[Q,27]}$, $\sigma_{C[Q,31]}$ and $\sigma_{C[Q,33]}$) is illustrated in Figure 5.10, showing that the best location for the temperature sensor is the 33-rd stage, as in SC1 case.

Finally, different selections of manipulated inputs for the best sensor locations have been tested ($\sigma_{C[Q,33]\frac{R}{F}}$, $\sigma_{C[R,33]}$ and $\sigma_{C[Q,33]}$). Comparison is shown in Figure 5.11, evidencing that the manipulated variable R is slightly better than Q for the dynamic behavior, while performance worsens if $\frac{R}{F}$ is kept constant, with Q manipulated.

Saturation

In order to assess the effectiveness of the anti-windup action, the column with control structure $\sigma_{C[Q,33]}$ is subjected to a test as in SC2, but in addition, feed conditions are brought back at the nominal values at $t = 6$h. Then, in order to force the saturation, it is assumed that the manipulated input Q lie between $0.9\bar{Q}$ and $1.1\bar{Q}$: as can be seen from Figure 5.10, the condition $Q < 0.9\bar{Q}$ is verified after the change at $t = 1$h, and therefore the saturation condition is met.

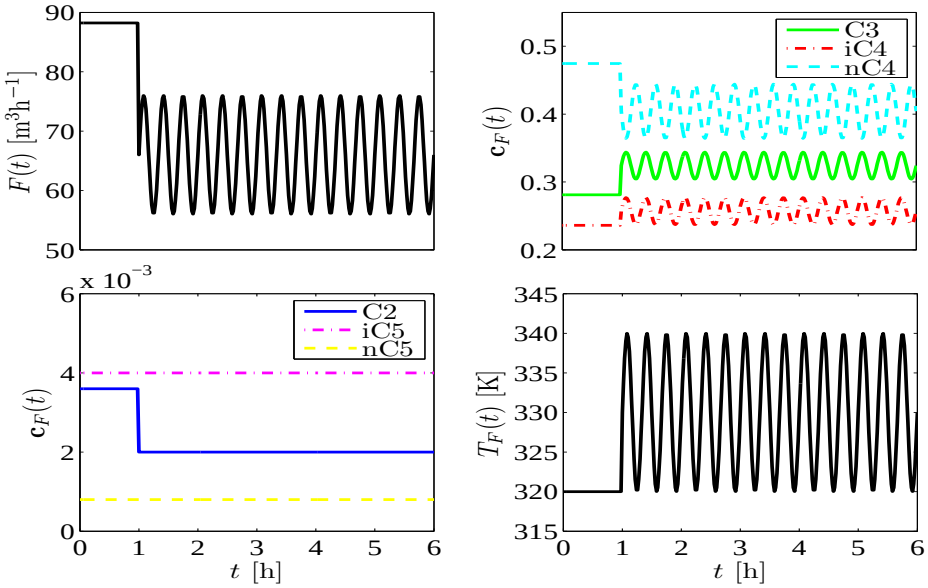

Figure 5.8: Disturbance changes for Scenario 2 (SC2)

The results are in Figure 5.12, and show that the control action Q quickly leaves the saturation condition after the change at $t = 6$h, as can also be seen from the good controller performance after that time.

Overall considerations

When considering the achievement of control objective CO1 (i.e., regulation of iC4 around the prescribed value, see Eq. (5.1)) with a conventional controller, both scenarios show that the best sensor location is the 33-rd stage. According to the structural analysis, this should be due to the fact that the contributions to the temperature gradient at 33-rd stage are mainly given by key components C3 and iC4. Such results confirm the considerations in Luyben (2006) and Hori and Skogestad (2007), which stated that temperature sensors not be located close to bottom, top, and feed stage. On the other hand, it can be seen that the choice of the manipulated variable (Q or R) does not significantly influence controller performance. Finally, the effectiveness of the anti-windup action has been successfully verified.

5.2.3 Structural analysis for conventional controller - CO2

In this Subsection, one (if single-end controllers are used) or two (if dual-end controllers are used) input-output pairs (u_l, T_k) have to be found in order to

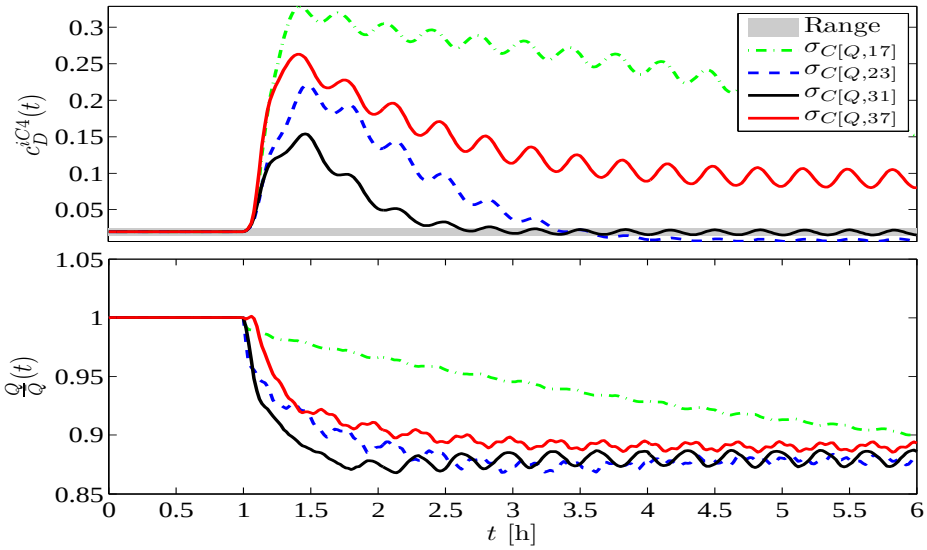

Figure 5.9: CO1, SC2, comparison between the control structures $\sigma_{C[Q,17]}$, $\sigma_{C[Q,23]}$, $\sigma_{C[Q,31]}$ and $\sigma_{C[Q,37]}$: distillate iC4 (top), and reboiler heat duty dynamics (bottom)

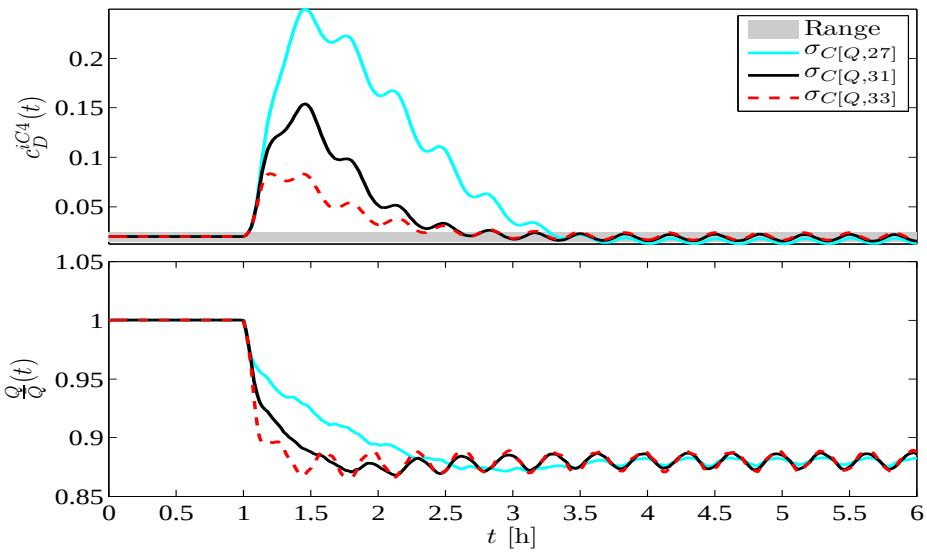

Figure 5.10: CO1, SC2, comparison between the control structures $\sigma_{C[Q,27]}$, $\sigma_{C[Q,31]}$ and $\sigma_{C[Q,33]}$: distillate iC4 (top), and reboiler heat duty dynamics (bottom)

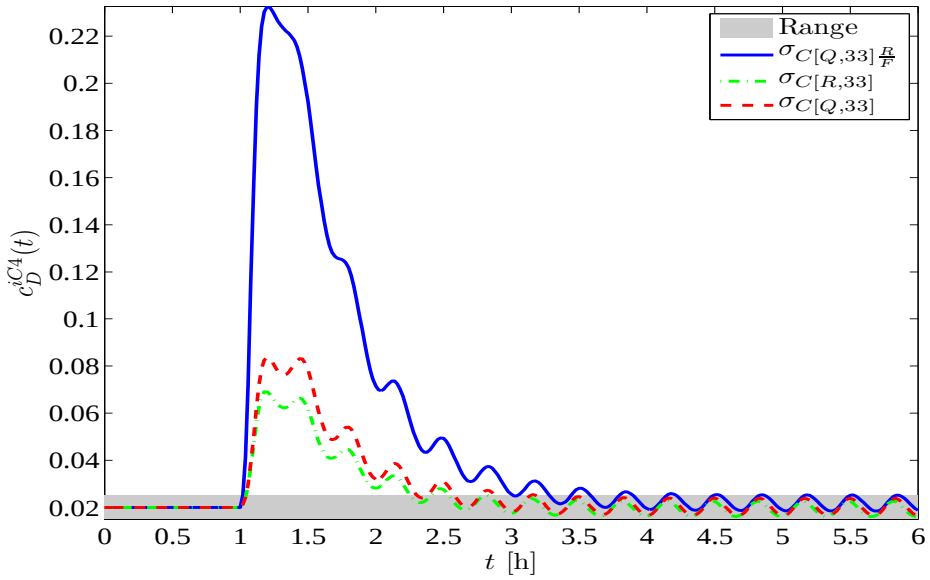

Figure 5.11: CO1, SC2: comparison between the control structures $\sigma_{C[Q,33]\frac{R}{F}}$, $\sigma_{C[R,33]}$ and $\sigma_{C[Q,33]}$

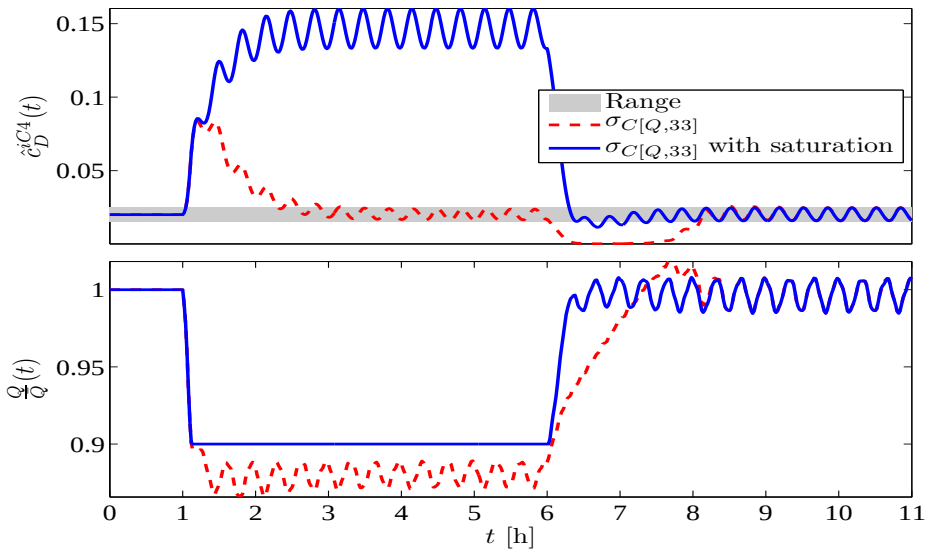

Figure 5.12: Performance of the conventional controller with structure $\sigma_{C[Q,33]}$ when saturation is present: composition (top) and manipulated variable dynamics (bottom).

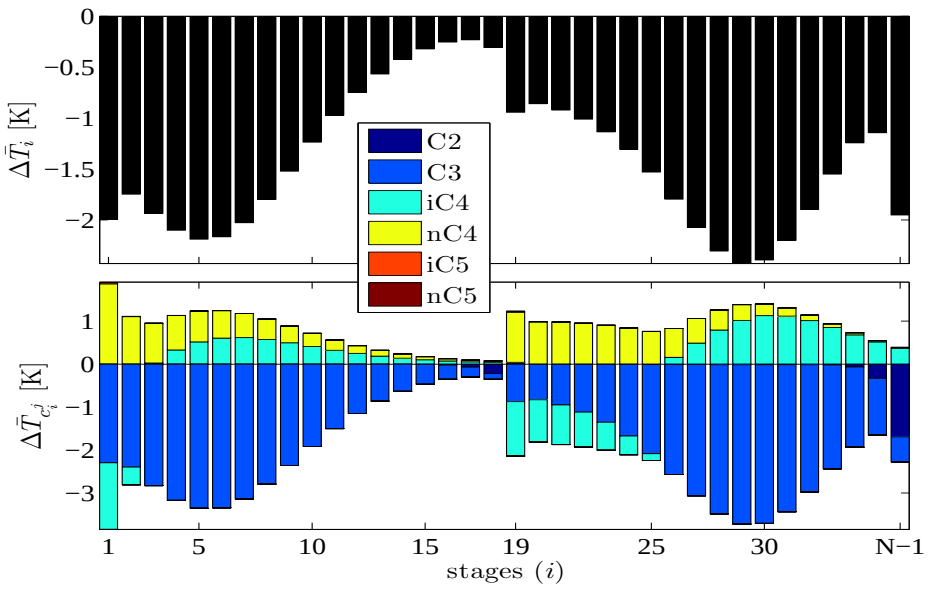

Figure 5.13: Steady-state temperature gradient with per-component contribution diagram for case SS2

achieve objective CO2, that is, the joint regulation of bottom C3 and distillate iC4 at their nominal values (see Eq. (5.2)).

Temperature sensor location

The criteria for selecting temperature sensor locations in CO2 is similar to the one depicted for the CO1 case, except that the procedure must be performed for each section if a dual-end controller is used.

CO2 is related to SS2 conditions (recalled in Table 5.4), and the related temperature gradient with per-component contribution diagram is reported again in Figure 5.13

$\bar{F}$	$\bar{c}_F^{C2}$	$\bar{c}_F^{C3}$	$\bar{c}_F^{iC4}$	$\bar{c}_F^{nC4}$	$\bar{c}_F^{iC5}$	$\bar{T}_F$
88.2 $m^3\,h^{-1}$	0.0036	0.281	0.236	0.4746	0.0004	320 K

$\bar{Q}$	$\bar{R}$
2665688 $kcal\,h^{-1}$	34.99 $m^3\,h^{-1}$

Table 5.4: Operating conditions for SS 2

On the basis of the analysis of Figure 5.13, the following considerations can be

made:

- the section of interest for the regulation of the iC4 in the distillate is the enriching one, while the stripping section is related to the regulation of the C3 in the bottom;
- in the enriching section the largest gradients are between 26-th and 33-rd stage, but stage 33 should be preferred because its gradient is mainly due to key components;
- in the stripping section the largest gradients lie between 1-st and 8-th stage, but the stages with the smallest influence of non key components are the 5-th and the 6-th.

Manipulated inputs and pairing

When a dual-end controlled is used, the best option is the pairing of each manipulated variable with a temperature in the corresponding section, meaning that a temperature in the enriching section should be controlled through the reflux rate R, while a temperature in the stripping section should be controlled through the reboiler heat Q. Otherwise, if a single-end controller is used, the manipulated variable to be used has to be chosen on the basis of the overall temperature profile after small step changes ($\pm 1\%$ in this specific case) in manipulated variables, as for CO1 case. Such test is shown in Figure 5.14, and shows that for single-end control the manipulated variable Q should be used since the overall temperature variations in the column are larger.

5.2.4 Structural results for conventional controller - CO2

Candidate structures found for CO2 objective are now tested, according to Scenarios 1 and 2. Firstly, tuning procedure is illustrated, and then the two scenarios are separately analyzed.

Tuning

As for CO1 case, the tuning procedure starts with the estimate of the characteristic frequency. For CO2 case, such procedure has to be carried out for each section, since temperature sensors can be placed in the stripping section.

Here, the tuning has been made on the basis of the open-loop dynamic responses of the column to both negative and positive step changes ($\pm 1\%$) to both reboiler heat Q and reflux rate R. The responses are illustrated in Figure 5.15, and show that a rough estimate of the time needed by the system step response to reach

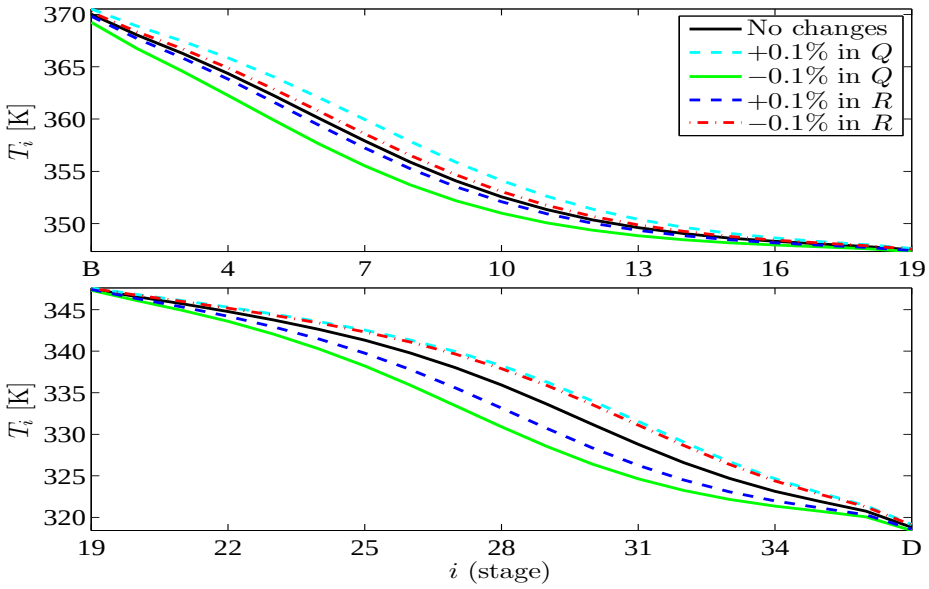

Figure 5.14: CO2: sensitivity criterion for the selection of the manipulated variable: stripping (top) and enriching section (bottom).

the 98% of its final value is $t_{98\%,S} \approx 2\text{h}$ for the stripping section, and $t_{98\%,E} \approx 4\text{h}$ for the enriching one, meaning that

$$\omega_S = \frac{4}{t_{98\%,S}} \approx 2\text{h}^{-1}, \qquad \omega_E = \frac{4}{t_{98\%,E}} \approx 1\text{h}^{-1}$$

Therefore, the following tuning parameters are chosen:

$$K_c^E = 2\omega_E = 2\text{h}^{-1}, \qquad K_o^E = 10K_c^E = 20\text{h}^{-1}$$
$$K_c^S = 2\omega_S = 4\text{h}^{-1}, \qquad K_o^S = 5K_c^S = 20\text{h}^{-1}$$

Note that observer frequency in the stripping section K_o^E has not been increased more than K_o^S in order not to exceed the threshold due to holdup dynamics, as explained in Remark 5.1.

The candidate structures for CO2 will be tested in the following, according to the scenarios SC1 (Table 5.2) and SC2 (Table 5.3) previously illustrated.

From now on, the notation

$$\sigma_{C[j_1,i_1][j_2,i_2]}$$

will be used for dual-end controllers meaning that the manipulated variable j_1 is used for controlling the i_1-th temperature and the manipulated variable j_2 is used for controlling the i_2-th temperature.

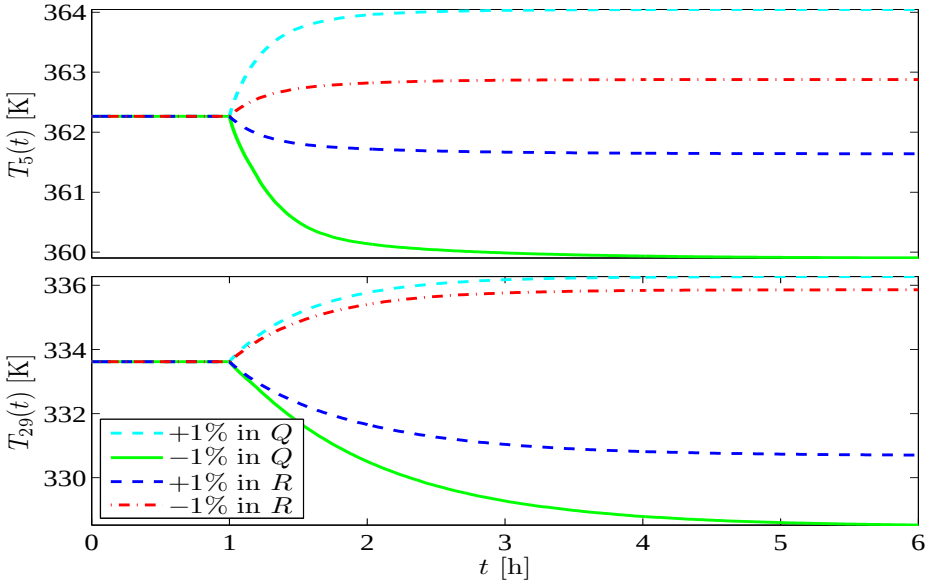

Figure 5.15: Open-loop system responses to ±1% changes in manipulated variables.

Scenario 1 (SC1)

According to SC1, a step-plus-sinusoidal change is made, with data given in Table 5.2. At first, only single-end structures are compared, with the reboiler heat duty Q used as manipulated variable (as suggested by the structural analysis), 3-rd and 5-th location tested for stripping section while only 33-rd one is tested for enriching section, due to its best performance for CO1.

In Figure 5.16, the control structures $\sigma_{C[Q,3]}$, $\sigma_{C[Q,5]}$, and $\sigma_{C[Q,33]}$ are compared, and it can be noted that single-end controllers are not able to achieve control objective CO2 (see Eq. (5.2)): (i) when a temperature is controlled in the enriching section (33-th stage), the condition (5.2b) is not verified since the concentration of C3 in the bottom is around 0.035; (ii) if the temperature is controlled in the stripping section (either 3-rd or 5-th stage), the condition (5.2a) is not verified since the concentration of iC4 in the distillate is around 0.045.

Since it is not possible to attain the objective CO2 with previous single-end controllers, other two structures are tested: (i) a single-end controller with temperature fixed at 33-rd stage through the reboiler heat duty Q, with the ratio $\frac{R}{F}$ kept fixed; (ii) a dual-end controller with temperature fixed at 5-th and 33-rd stages through the reboiler heat duty Q and the reflux rate R respectively. In Figure 5.17, it can be seen that (i) with the structure $\sigma_{C[Q,33]\frac{R}{F}}$, C3 concentra-

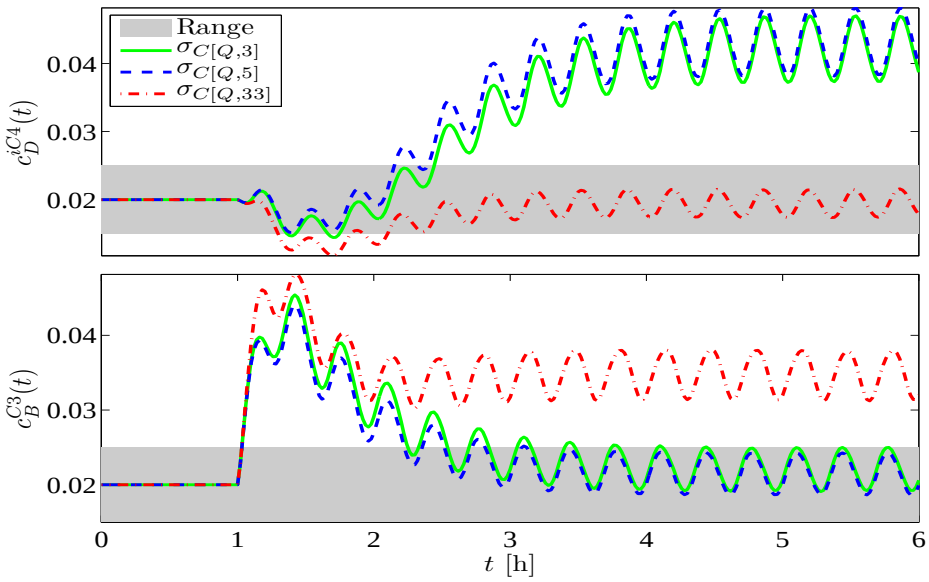

Figure 5.16: CO2, SC1: comparison between the control structures $\sigma_{C[Q,3]}$, $\sigma_{C[Q,5]}$ and $\sigma_{C[Q,33]}$.

tion in the bottom is equal to 0.013, meaning that performance is improved, but not enough, and that (ii) the dual-end controller with structure $\sigma_{C[Q,5][R,33]}$ is able to regulate the compositions of interest at the desired values (the conditions $c_B^{C3} \approx 0.02$ and $c_D^{iC4} \approx 0.02$ are met within the prescribed tolerances).

Scenario 2 (SC2)

The results obtained for the step-plus-sinusoidal change made according to SC2 (see Table 5.3) are illustrated in Figure 5.18. Only the control structure $\sigma_{C[Q,5][R,33]}$ is shown, since it gave the best performance for SC1 case. It can be seen again that requirements Eq. (5.2) are satisfied.

Overall considerations

When the control objective is CO2, that is, the joint regulation of bottom C3 and distillate iC4 around their nominal values (Eq. (5.2)), both scenarios show that a sensor location pair which allows the attainment of such objective is given by the 5-th and the 33-rd stage, with the former temperature controlled by reboiler duty and the latter controlled by reflux rate. According to the structural analysis, this should be due to the fact that the contributions to the tempera-

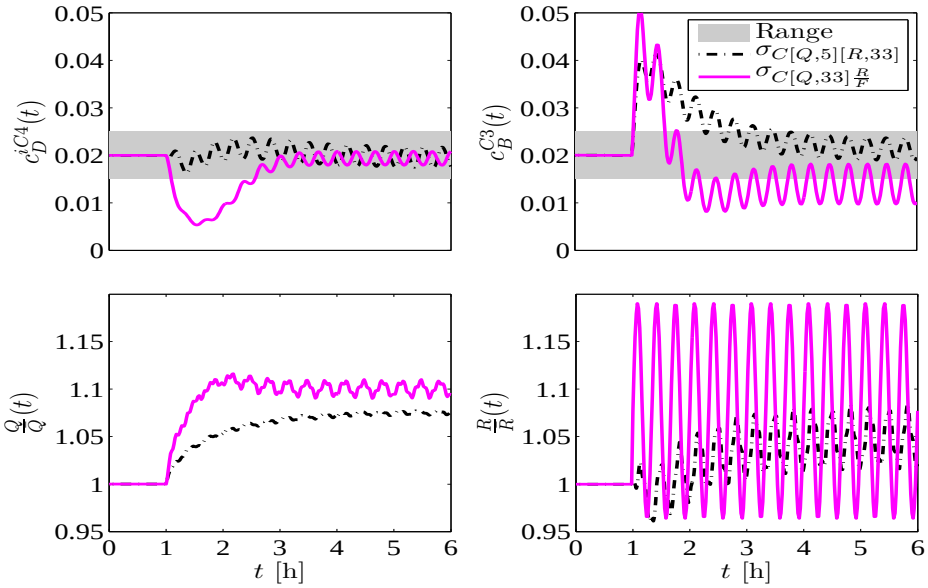

Figure 5.17: CO2, SC1: comparison between the control structures $\sigma_{C[Q,33]\frac{R}{F}}$ and $\sigma_{C[Q,5][R,33]}$.

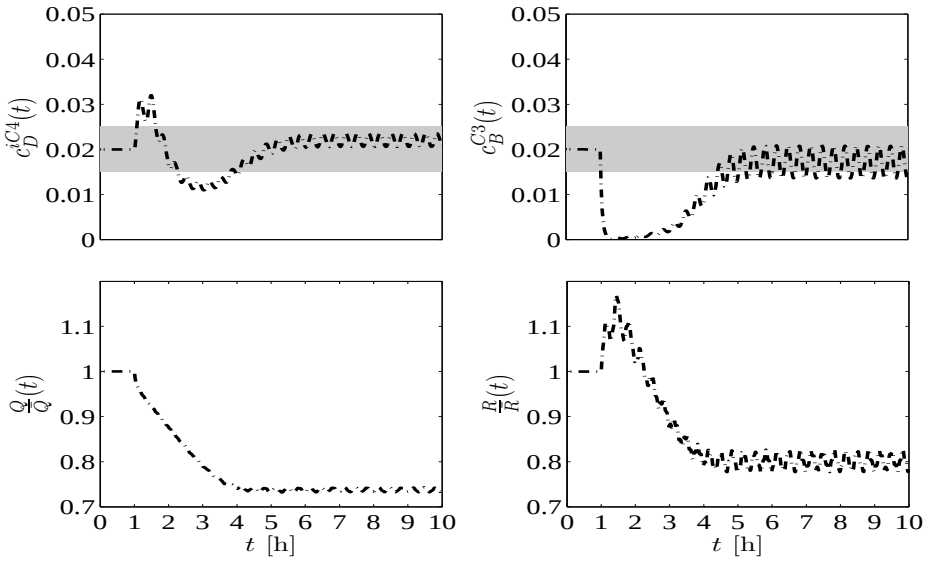

Figure 5.18: CO2, SC2, performance of the control structure $\sigma_{C[Q,5][R,33]}$: composition (top) and manipulated variable dynamics (bottom).

ture gradient at these stages are mainly given by key components C3 and iC4. Once again, temperature sensors are not placed closed to bottom, top, and feed stages, meaning that considerations of Luyben (2006) and Hori and Skogestad (2007) are confirmed. On the other hand, single-end structures does not allow the achievement of the control objective; however, this is not a general result for columns where both key-impurities are controlled, and a criterion to be used in order to decide between a single-end and a dual-end structure still has to be found (Luyben, 2006; Hori and Skogestad, 2007).

5.3 Control structure for cascade-type controllers

In this Section, the control problem is solved for a cascade-type controller (cascade or CLF), where one or two combinations of one manipulated variable and a primary-secondary temperature pair have to be found (u_l and a pair (T_{k_1}, T_{k_2})), according to notation in Sections 4.4 and 4.5) in order to achieve the given control objective. The problem is substantially the same of the conventional case, but in addition, the selection of secondary temperature locations must be addressed. On the other hand, the selection of both manipulated inputs and temperature sensor locations has to be dealt with as illustrated for conventional case. Cascade-type controller schemes are reported in Figure 4.2. After the selection of candidate structures, structural results are assessed through dynamic simulations.

5.3.1 Structural analysis for cascade-type controllers - CO1

In this Subsection, the control problem is solved in order to achieve objective CO1 (i.e., regulation of distillate iC4 around its nominal value, see Eq. (5.1)): since a single-end controller is sufficient, as seen from conventional case, this means that only an input u_l and a primary-secondary temperature pair (T_{k_1}, T_{k_2}) have to be found.

Primary temperature locations

Primary temperature locations have to be chosen as done for conventional case; indeed, the addition of a secondary temperature loop does not modify the primary temperature offset if primary location remains the same, meaning that the same primary location of conventional controller case can be used for cascade-type controllers. This means that 33-rd tray has been chosen as the primary temperature location, since it is the sensor placement which guarantees the minimum composition offset.

Secondary temperature sensor location

Secondary temperature location should be selected in such a way that a fast rejection of disturbances be obtained, according to the control objective. Two possibilities are therefore the following ones:

- location of secondary sensor in the section of interest (i.e. where the composition must be regulated) and in the most sensitive area (i.e. in the region with the largest gradients);
- placement of the secondary sensor in the region of interest and close to the disturbance source, that is, close to feed stage.

The previous considerations in conjunction with the diagram in Figure 3.6 lead to the choice of the following secondary temperature sensor locations: (i) the 30-th stage since it is the one with the largest gradient in the enriching section; (ii) the 23-rd stage, because it is close to feed stage (19-th one).

Manipulated inputs

The selection of manipulated inputs is the same of conventional case, and therefore the reboiler heat duty Q has been chosen as manipulated variable. Recall that no large difference in performance is expected if using the reflux flow rate R instead of Q.

5.3.2 Structural results for Cascade controller - CO1

After having described the structural problem for a cascade-type controller when the control objective is CO1 (i.e., regulation of distillate iC4), the candidate structure are now tested, according to the two scenarios SC1 (see Table 5.2) and SC2 (see Table 5.3) previously described. Firstly, the tuning procedure is shown, and then the scenarios are separately analyzed. Finally, a test with controller saturation is made.

Tuning

As in previous case, the controller has been tuned on the basis of the open-loop responses (see Figure 5.3) of the column to both negative and positive step changes ($\pm 0.1\%$) at both reboiler heat Q and reflux rate R. The characteristic frequency is $\omega \approx 1\text{h}^{-1}$, and therefore the following tuning parameters are chosen as follows, on the basis of cascade tuning rules given in Eq. (4.48).

$$K_{c,1} = 2\omega = 2\text{h}^{-1}, \qquad K_{c,2} = 2K_{c,1} = 4\text{h}^{-1}, \qquad K_{o,1} = K_{o,2} = 10K_{c,1} = 20\text{h}^{-1}$$

Scenario 1 (SC1)

Cascade controllers developed in order to reach the objective CO1 are now tested through Scenario 1 (SC1, see Table 5.2). The following notation is used in order to define a single-end cascade control structure where the manipulated variable j is used for regulating primary temperature T_{i_P} with the assistance of secondary temperature T_{i_S}

$$\sigma_{C[j,i_P,i_S]}$$

Primary temperature T_{33} and Q as manipulated variable have been chosen as this input-output control pair yielded the best result for single-end conventional control case.

At first, different secondary temperature sensor locations have been tested: the ones suggested by structural considerations ($\sigma_{C[Q,33,23]}$ and $\sigma_{C[Q,33,31]}$) have been compared with the conventional counterpart structure $\sigma_{C[Q,33]}$ and with the cascade structure $\sigma_{C[Q,33,17]}$ where the secondary sensor has been located in the stripping section, differently from the other cascade structures.

Test results are illustrated in Figure 5.19, and show that a slightly better performance is obtained when using a cascade structure. However, no particular difference is present among the several proposed cascade structures.

Another test has been made with several secondary locations around the most sensitive area of the enriching section (around 31-st stage): the comparison of structures $\sigma_{C[Q,33,27]}$, $\sigma_{C[Q,33,31]}$ and $\sigma_{C[Q,33,34]}$ is illustrated in Figure 5.20, showing that the different locations of secondary temperature sensors does not lead to different performance.

Scenario 2 (SC2)

When the column is subjected to a test according to Scenario 2 (SC2, see Table 5.3) is considered, a comparison among $\sigma_{C[Q,33,17]}$, $\sigma_{C[Q,33,23]}$, $\sigma_{C[Q,33,31]}$, $\sigma_{C[Q,33,34]}$ is illustrated in Figure 5.21. It is shown that the selection of a particular secondary sensor location does not influence performance, but every cascade structure analyzed performs better than the conventional counterpart, meaning that a cascade solution has to be preferred.

Saturation

As well as for conventional controller case, the effectiveness of the anti-windup action is tested for the cascade case. The column with control structure $\sigma_{C[Q,33,34]}$ is subjected to a test as in SC2, but in addition, feed conditions are brought back

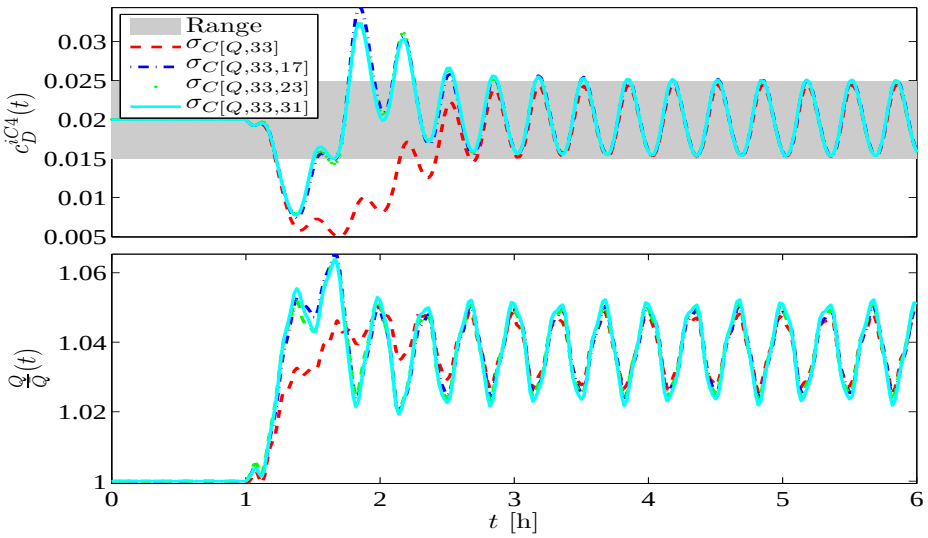

Figure 5.19: CO1, SC1, performance of cascade structures $\sigma_{C[Q,33,17]}$, $\sigma_{C[Q,33,23]}$, $\sigma_{C[Q,33,31]}$ and comparison with conventional counterpart $\sigma_{C[Q,33]}$: composition (top) and manipulated variable (bottom) dynamics.

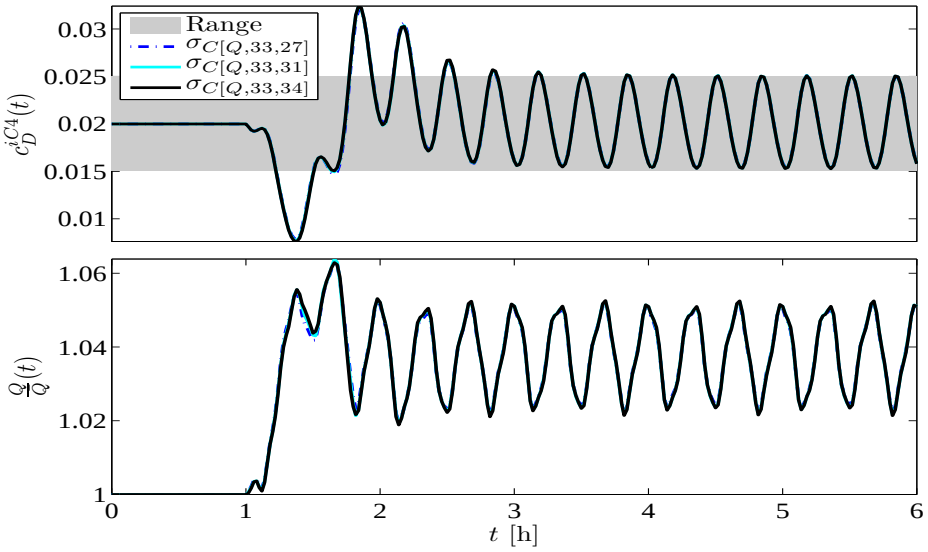

Figure 5.20: CO1, SC1, comparison of cascade structures $\sigma_{C[Q,33,27]}$, $\sigma_{C[Q,33,31]}$, $\sigma_{C[Q,33,34]}$: composition (top) and manipulated variable (bottom) dynamics.

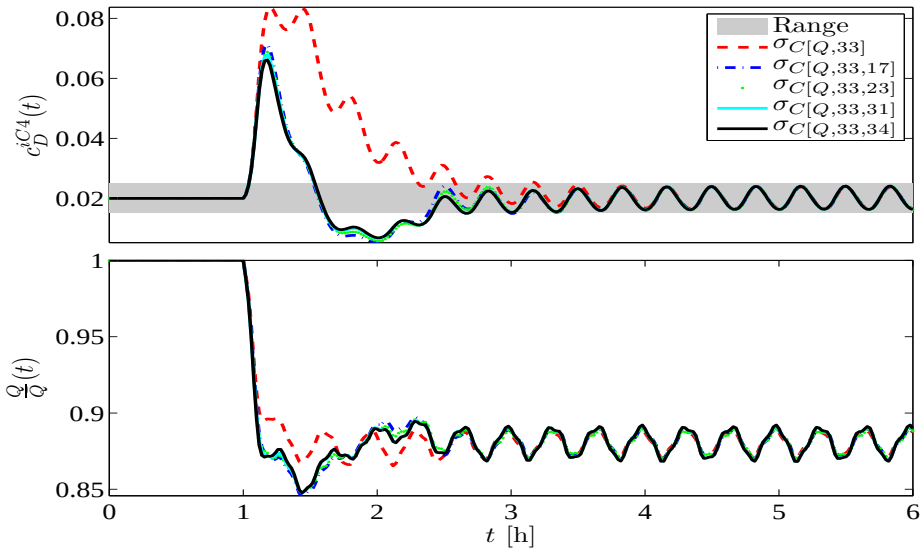

Figure 5.21: CO1, SC2, comparison between cascade structures $\sigma_{C[Q,33,17]}$, $\sigma_{C[Q,33,23]}$, $\sigma_{C[Q,33,31]}$, $\sigma_{C[Q,33,34]}$: composition (top) and manipulated variable (bottom) dynamics

at the nominal values at $t = 6$h. In order to force the saturation, it is assumed that the manipulated input Q lie between $0.9\bar{Q}$ and $1.1\bar{Q}$.

The results are in Figure 5.22, and show that the control action Q quickly leaves the saturation condition after the change at $t = 6$, as can also be seen from the good controller performance after that time.

Overall considerations

The results in this Subsection show that a cascade solution usually performs better than the conventional counterpart when the goal is the achievement of CO1 (i.e., regulation of distillate iC4 around its nominal value). This improvement does not seem to depend on the choice of a particular secondary sensor location. Anyway, note that the improvement with respect to the equivalent conventional case is stronger when considering SC2. This implies that a cascade solution is effective especially when strong disturbances are present. Finally, the effectiveness of the anti-windup action has been successfully verified.

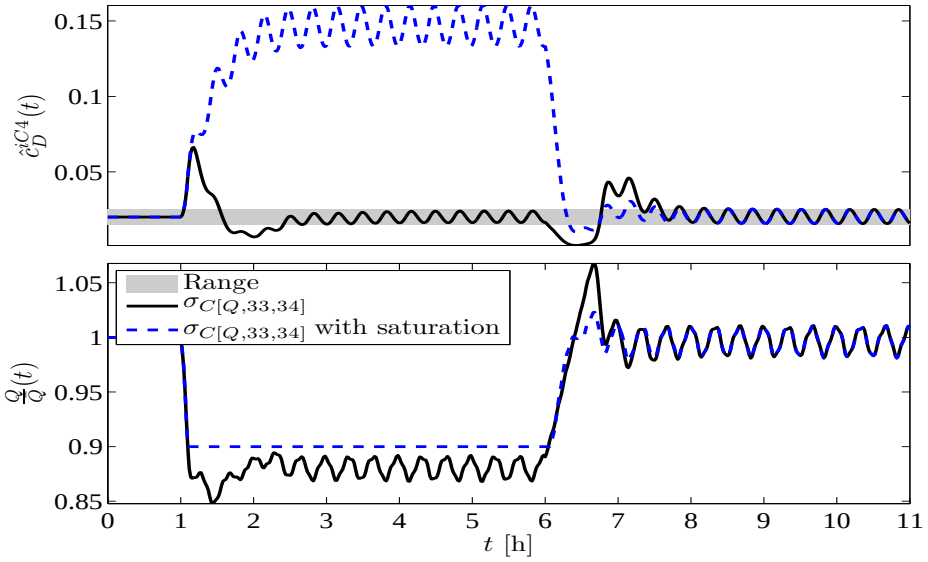

Figure 5.22: Performance of the cascade controller with structure $\sigma_{C[Q,33,34]}$ when saturation is present: composition (top) and manipulated variable dynamics (bottom).

5.3.3 Structural analysis for cascade-type controllers - CO2

After having described how a cascade controller performs when the control objective is CO1, performance for CO2 case (i.e., joint regulation of bottom C3 and distillate iC4 around their nominal values) is now shown.

Tuning

Equivalently to conventional case, the tuning procedure starts with the estimate of the characteristic frequency for each section. On the basis of the open-loop dynamic responses of the column to both negative and positive step changes ($\pm 1\%$) to both reboiler heat Q and reflux rate R shown in Figure 5.15, the resulting caracteristic frequencies are $\omega_S \approx 2\text{h}^{-1}$ and $\omega_E \approx 1\text{h}^{-1}$.

Therefore, the following tuning parameters are chosen:

$$K_{c,1}^S = 2\omega_S = 4\text{h}^{-1}, \qquad K_{c,2}^S = 2K_{c,1}^S = 8\text{h}^{-1}, \qquad K_{o,1}^S = K_{o,2}^S = 5K_{c,1}^S = 20\text{h}^{-1}$$

$$K_{c,1}^E = 2\omega_E = 2\text{h}^{-1}, \qquad K_{c,2}^E = 2K_{c,1}^E = 4\text{h}^{-1}, \qquad K_{o,1}^E = K_{o,2}^E = 10K_{c,1}^E = 20\text{h}^{-1}$$

Note that observer frequency in the stripping section (K_o^E) has not been increased

compared to the enriching one in order to not exceed the threshold due to holdup dynamics, as explained in Remark 4.3.

Primary temperature locations

As well as for CO1 case, primary temperature locations have to be chosen as done for conventional case, and therefore 5-th and 33-rd stages have been chosen, since these sensor locations guarantee control of both product compositions within a small range.

Secondary temperature locations

Since secondary temperature location seems not to influence performance of cascade controller in CO1 case, only one secondary sensor for each section has been tested. T_{34}, already tested in CO1 case, has been chosen for the enriching section; on the other hand, T_7 has been chosen for stripping section but even other locations would be possible.

Manipulated inputs and pairing

Like for conventional cases in which a dual-end controlled is used, the best option is to pair each manipulated variable with a temperature in the corresponding section, meaning that a temperature in the enriching section should be controlled through the reflux rate R, while a temperature in the stripping section should be controlled through the reboiler heat Q.

5.3.4 Structural results for Cascade controller - CO2

The following notation is used for dual-end cascade structures

$$\sigma_{C[j_1,i_{P_1},i_{S_1}][j_2,i_{P_2},i_{S_2}]}$$

meaning that the input j_i $(i = 1, 2)$ is used for controlling primary temperature T_{P_i} through the secondary temperature T_{S_i}.

Scenario 1 (SC1)

Since results for CO1 have shown that cascade controller performance does not depend on secondary sensor location, only the structure $\sigma_{C[Q,5,7][R,33,34]}$ has been tested and compared with the conventional counterpart. Results are illustrated in Figure 5.23, and show that a better bottom C3 regulation is obtained at the expense of a small worsening in distillation iC4 control.

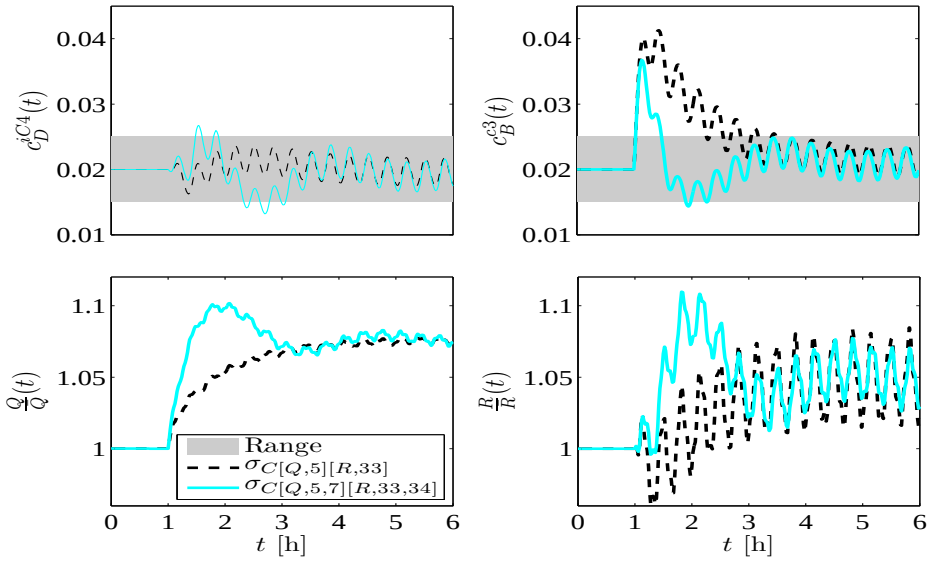

Figure 5.23: CO2, SC1, comparison of cascade structure $\sigma_{C[R,5,7][Q,33,34]}$ with the conventional structure $\sigma_{C[R,5][Q,33]}$: composition (top) and manipulated variable (bottom) dynamics.

Scenario 2 (SC2)

The structure $\sigma_{C[Q,5,7][R,33,34]}$ is the only one tested for SC2, according to the considerations given for SC1. Results are illustrated in Figure 5.24, and show that the use of a cascade controller improves bottom C3 regulation at the expenses of a worsening in distillate iC4 control.

Overall considerations

Figure 5.23 and Figure 5.24 show that a dual-end cascade structure is not better than its conventional counterpart when the objective to be achieved is CO2 (i.e., joint regulation of distillate iC4 and bottom C3). Therefore, it is suggested that a cascade controller not be used in order to achieve objective CO2, because of the higher complexity of a cascade structure with respect to a conventional one.

5.3.5 Structural results for CLF controller - CO1

After having illustrated cascade controller performance, CLF structural results are now shown, in the understanding that the structural analysis is the same for

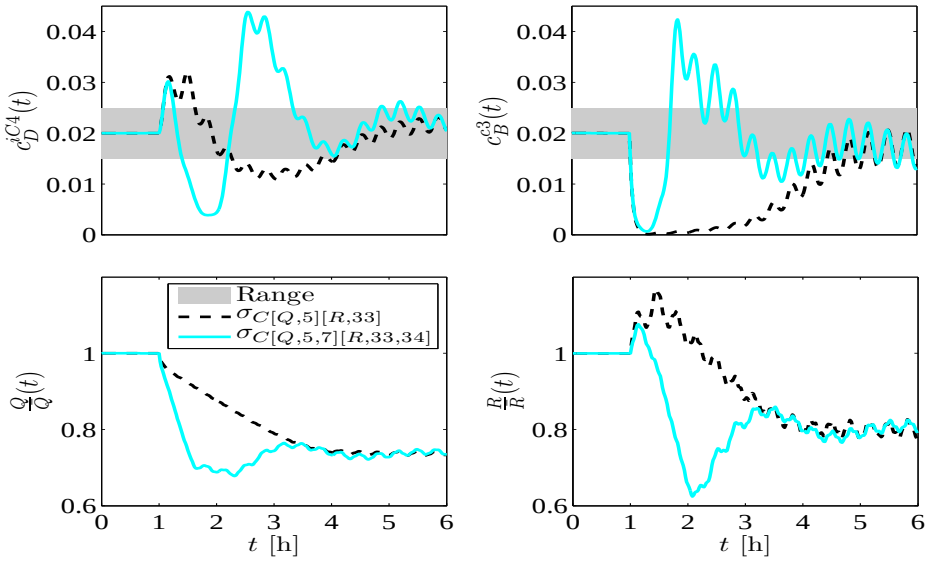

Figure 5.24: CO2, SC2, comparison of cascade structure $\sigma_{C[R,5,7][Q,33,34]}$ with the conventional structure $\sigma_{C[R,5][Q,33]}$: composition (top) and manipulated variable (bottom) dynamics.

both cascade-type controllers. In this subsection, performance of CLF controllers is assessed and compared with both conventional and cascade counterparts when the objective to be achieved is CO1 (i.e, regulation of distillate iC4 around its nominal value). Results obtained for CO2 objective will be shown in a subsequent Subsection.

Tuning

Tuning procedure is exactly the same of cascade case and therefore the following parameters are used:

$$K_{c,1} = 2\omega = 2\text{h}^{-1}, \qquad K_{c,2} = 2K_{c,1} = 4\text{h}^{-1}, \qquad K_{o,1} = K_{o,2} = 10K_{c,1} = 20\text{h}^{-1}$$

Scenario 1 (SC1)

As well as the cascade controller, the CLF one is assessed through different simulations with a variable location of secondary temperature sensor.

Firstly, the column is subjected to a test according to Scenario 1 (SC1, see Table 5.2). A comparison among structures with secondary sensors in different regions of the column is made, by analyzing performance of $\sigma_{C[Q,33,17]}$, $\sigma_{C[Q,33,23]}$,

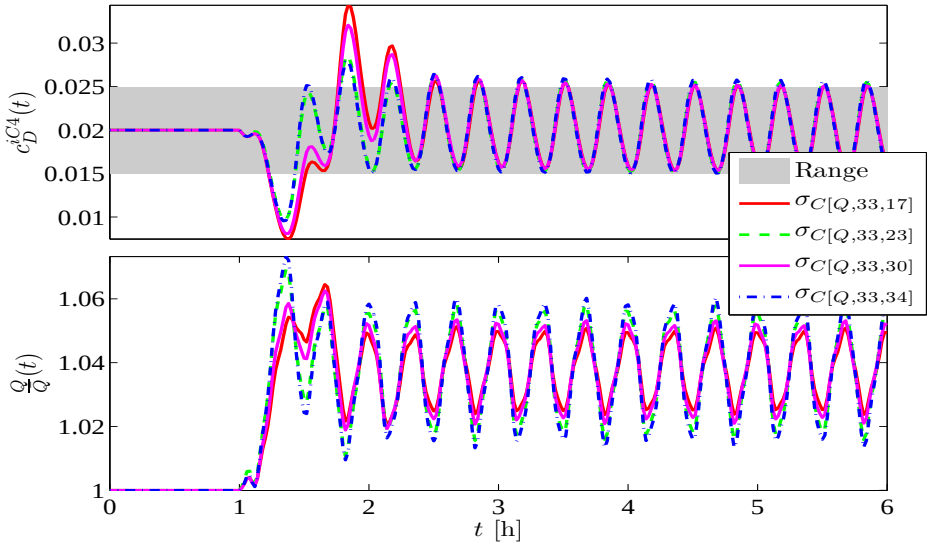

Figure 5.25: CO1, SC1, comparison of CLF structures $\sigma_{C[Q,33,17]}$, $\sigma_{C[Q,33,23]}$, $\sigma_{C[Q,33,30]}$, $\sigma_{C[Q,33,34]}$ with the conventional counterpart $\sigma_{C[Q,33]}$: composition (top) and manipulated variable (bottom) dynamics.

$\sigma_{C[Q,33,30]}$, and $\sigma_{C[Q,33,34]}$ structures: corresponding results are illustrated in Figure 5.25, and show that differently from the cascade case, the selection of an appropriate secondary sensor location is essential for obtaining good performance.

Finally, a comparison between one of the best CLF structures (with secondary sensor at 34-th stage) and its conventional and cascade counterparts is made. The results are shown in Figure 5.26, and clearly show as CLF algorithm is much better than its conventional counterparts.

Scenario 2 (SC2)

The same comparisons of SC1 case has been made in Scenario 2 (SC2, see Table 5.3). At first, a comparison between $\sigma_{C[Q,33,17]}$, $\sigma_{C[Q,33,23]}$, $\sigma_{C[Q,33,30]}$, and $\sigma_{C[Q,33,34]}$ structures is made. The results are illustrated in Figure 5.27, and show that the best results are obtained with either 23-rd or 34-th secondary temperatures, as well as SC1 case. Finally, a comparison between the best CLF (structure with secondary sensor at 34-th stage) and its conventional and cascade counterparts is made. The results are shown in Figure 5.28, and clearly show as the CLF algorithm is much better than its conventional counterparts. It is important to note that the improvement due to a CLF controller with respect to a conventional one is larger for SC2 than for SC1, as for cascade case. This means

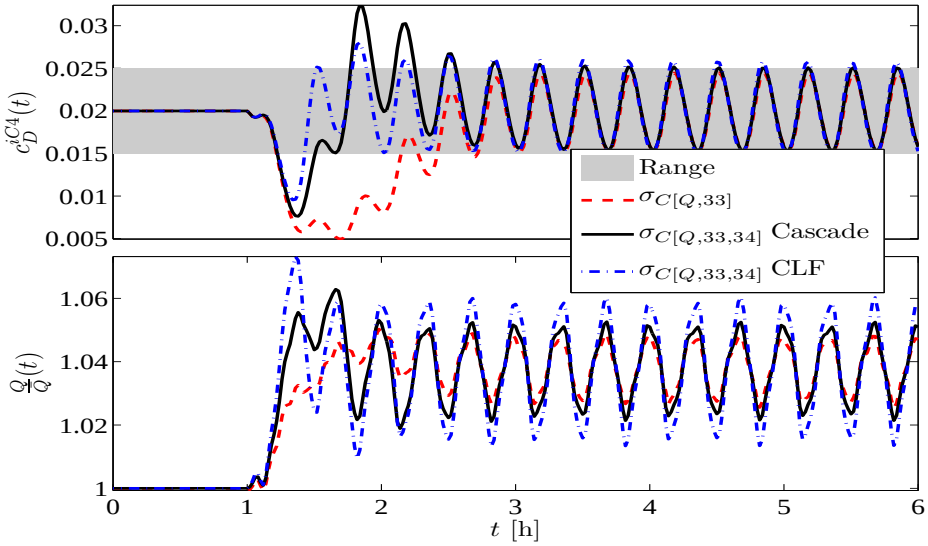

Figure 5.26: CO1, SC1, comparison of CLF with structure $\sigma_{C[Q,33,34]}$ with the conventional and cascade counterparts: composition (top) and manipulated variable (bottom) dynamics.

that a CLF controller is especially suitable for a strong disturbance entering the column.

Saturation

The effectiveness of the anti-windup action is now tested for the CLF case. The column with control structure $\sigma_{C[Q,33,34]}$ is subjected to a test as in SC2, but in addition, feed conditions are brought back at the nominal values at $t = 6$h. In order to force the saturation, it is assumed that the manipulated input Q lie between $0.9\bar{Q}$ and $1.1\bar{Q}$.

The results are in Figure 5.29, and show that the control action Q quickly leaves the saturation condition after the change at $t = 6$, as can also be seen from the good controller performance after that time.

Overall considerations

The CLF controller represents an effective solution for the rejection of disturbances in CO1 case, and produces better results than a cascade controller with the same temperature sensor locations, especially with strong disturbances (SC2

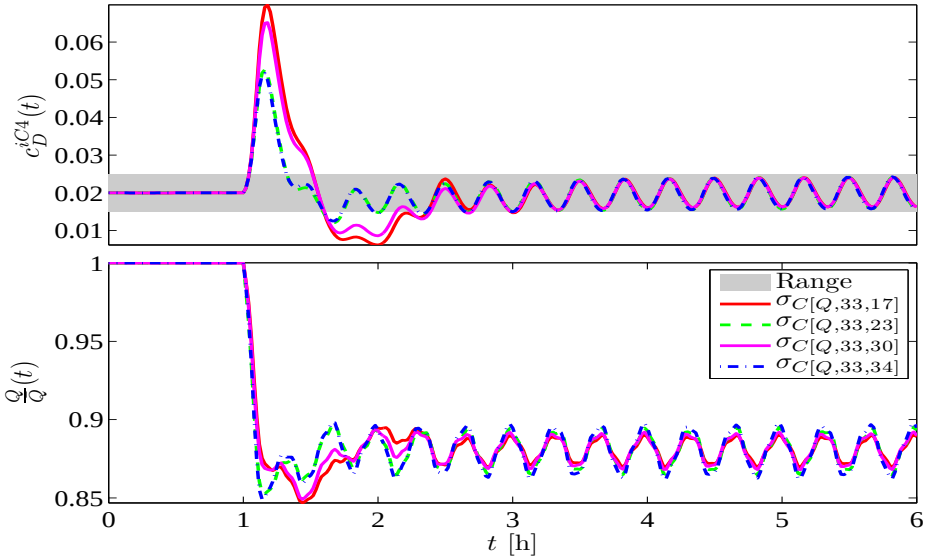

Figure 5.27: CO1, SC2, comparison of CLF structures $\sigma_{C[Q,33,17]}$, $\sigma_{C[Q,33,23]}$, $\sigma_{C[Q,33,30]}$, $\sigma_{C[Q,33,34]}$: composition (top) and manipulated variable (bottom) dynamics

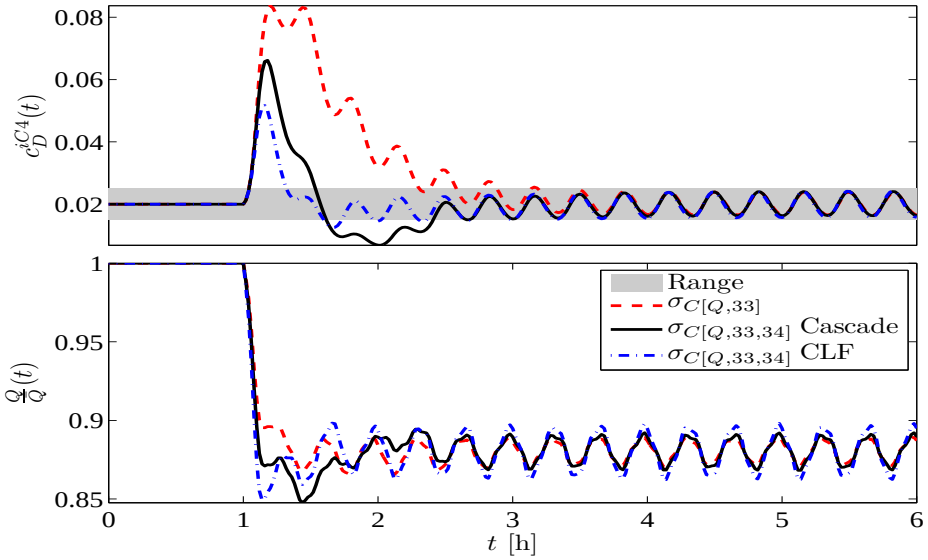

Figure 5.28: CO1, SC2, comparison of CLF structure $\sigma_{C[Q,33,34]}$ with its conventional and cascade counterparts: composition (top) and manipulated variable (bottom) dynamics.

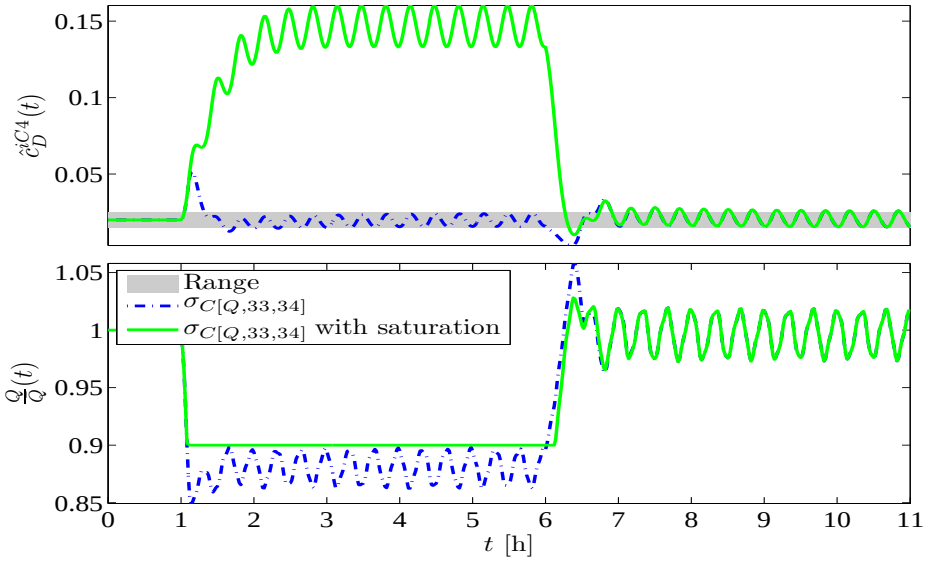

Figure 5.29: Performance of the CLF controller with structure $\sigma_{C[Q,33,34]}$ when saturation is present: composition (top) and manipulated variable dynamics (bottom).

case). Unlike the cascade case, the location of the secondary sensor has an influence in controller behavior, and the locations 23-rd and 34-th perform considerably better than others: (i) structure with 23-rd stage as secondary sensor location works since it is quite close to feed stage (remember this is a bad choice for a primary sensor location); on the other hand, (ii) we conjecture that 34-th works since the gradient at such stage is mainly due to key components, even if this has been stated as a criterion for primary sensor locations.. Finally, it has been demonstrated that the anti-windup action is effective.

5.3.6 Structural results for CLF controller - CO2

In this Subsection, CLF performance is assessed when the objective to be achieved is CO2 (i.e., joint regulation of bottom C3 and distillate iC4).

Tuning

Tuning procedure is exactly the same of cascade case and therefore the following parameters are used:

$$K_{c,1}^S = 2\omega_S = 4\text{h}^{-1}, \qquad K_{c,2}^S = 2K_{c,1}^S = 8\text{h}^{-1}, \qquad K_{o,1}^S = K_{o,2}^S = 5K_{c,1}^S = 20\text{h}^{-1}$$

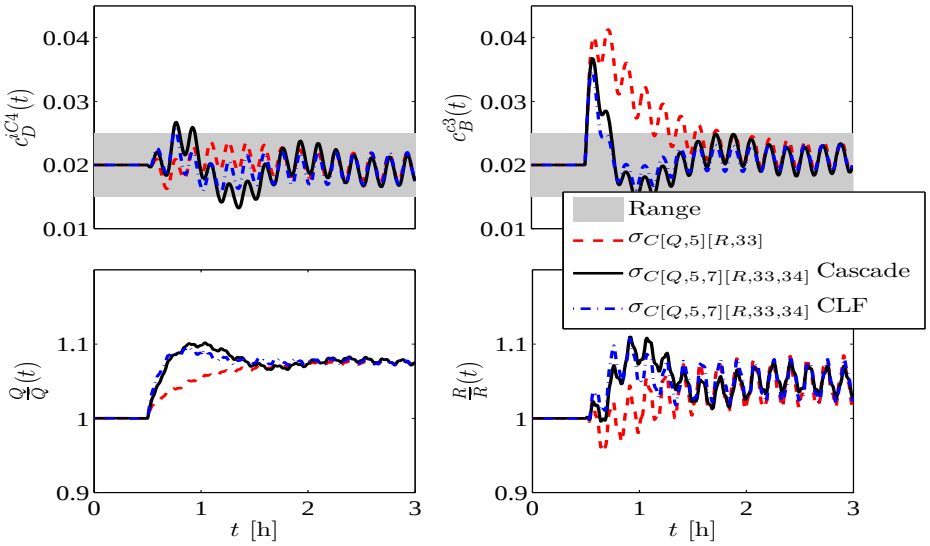

Figure 5.30: CO2, SC1, comparison of CLF controller with structure $\sigma_{C[Q,5,7][R,33,34]}$ with its conventional and cascade counterparts: composition (top) and manipulated variable (bottom) dynamics.

$$K_{c,1}^E = 2\omega_E = 2\text{h}^{-1}, \qquad K_{c,2}^E = 2K_{c,1}^E = 4\text{h}^{-1}, \qquad K_{o,1}^E = K_{o,2}^E = 10K_{c,1}^E = 20\text{h}^{-1}$$

Scenario 1 (SC1)

According to previous considerations, only the control structure $\sigma_{C[Q,5,7][R,33,34]}$ is tested here, and compared with its conventional and cascade counterparts. Results are depicted in Figure 5.30, where it can be seen as the CLF controller outperforms the corresponding conventional and cascade ones.

Scenario 2 (SC2)

In Figure 5.31, performance of CLF controller is analyzed when using the same control structure of SC1. Results are shown in Figure 5.31, where it can be seen as the CLF controller outperforms the corresponding conventional and cascade ones when regulating distillate iC4, while performance is substantially the same of cascade for the regulation of bottom C3.

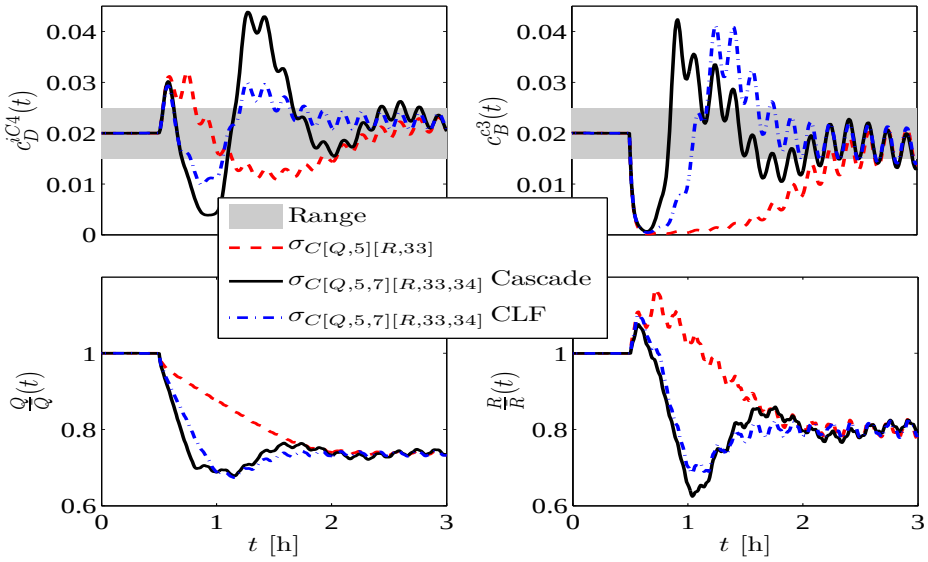

Figure 5.31: CO2, SC2, comparison of CLF structure $\sigma_{C[Q,5,7][R,33,34]}$ with its conventional and cascade counterparts: composition (top) and manipulated variable (bottom) dynamics.

Overall considerations

As in CO1 case, CLF controllers represent an effective alternative to conventional and cascade controllers when the objective to be achieved is CO2, since it often allows a faster disturbance rejection. The superior performance of the CLF controller compared to its cascade counterpart should be due to the better cooperation between primary and secondary action, as explained in Section 4.5.6.

5.4 Chapter summary

In this Chapter, the control structural analysis has been performed, and results have subsequently been assessed.

A new methodology based on the temperature gradient with per-component contribution diagram has been proposed and used for the selection of temperature sensor locations. Our methodology has been validated by structural results: primary temperature sensors have to be placed (i) in the section with the impurity to be regulated, (ii) in an area where the gradients are large, and (iii) where the gradient is mostly due to key components. In addition, for cascade-type controllers, secondary temperature sensor location should be either a stage selected

on the basis of the criterion used for primary location, or a stage close to feed one. On the other hand, manipulated variable and pairing with temperature (for dual-end controllers) have been chosen on the basis of well-known sensitivity criteria.

The best performance for a conventional controller is obtained regulating temperature at 33-rd stage through the reboiler heat duty Q for the objective CO1 (regulation of distillate iC4 around its nominal value), and regulating the temperature at 5-th stage through Q and the temperature at 33-rd stage through the reflux rate R for the objective CO2 (joint regulation of bottom C3 and distillate iC4 around their nominal values). Then, it has been shown that an improvement in disturbance rejection can be obtained through a cascade controller for CO1, but not for CO2; moreover, cascade performance does not depend on the secondary sensor location. Best results for both objectives have been obtained with a CLF controller, with secondary sensor located at 23-rd or 34-th sensor for enriching section, and at 7-th stage for stripping section; differently from cascade controller, the location of secondary stage has an influence on controller performance. Finally, the effectiveness of anti-windup action has been demonstrated for each controller.

Part II

Distillation column estimation

Estimation part overview

The estimation problem task has been introduced in Section 3.6: here it is only sufficient to recall that the objectives consist in inferring one or two key impurities of the multicomponent C3-C4 splitter described in Section 3.3, that is, the iC4 in the distillate and the C3 in the bottom, in order to monitor the separation. Like the control problem, also the estimation one is solved by partitioning it into a structural and an algorithmic part.

This estimation Part is organized as follows:

Chapter 6. In this Chapter, the estimation structural analysis problem is presented and assessed. By estimation structure, it is meant the selection of (i) components to be retained in the reduced model, (ii) number and location of temperature sensors, (iii) composition states to be innovated, and (iv) regions in which temperature has to be assumed constant. Candidate structures are selected through the temperature gradient with per-component contribution diagram in conjunction with a systematic procedure.

Chapter 7. In this Chapter, the control algorithms, that is, the dynamic processors that perform the estimation task, are illustrated. In this Thesis, the Geometric Estimator (GE) with partial innovation and the Extended Kalman Filter (EKF) with partial or complete innovation are employed.

Chapter 8. In this Chapter, estimation structural results are presented and assessed.

Chapter 6

Estimation structural analysis

In this Chapter, the estimation structural analysis problem is addressed. The selection of the estimation structure consists in the choice of (i) components to be retained in the reduced estimation model, (ii) number and location of temperature sensors, (iii) composition states to be innovated, and (iv) regions where the temperature is assumed constant. The candidate structures are selected according to the estimation objective to be achieved. The methodology is entirely based on the temperature gradient with per-component contribution diagram in conjunction with a systematic procedure. Such diagram has already been used in this Thesis for selecting part of the control structure. As well as for estimation case, this method has the advantage to be easy to understand and to apply.

6.1 Introduction

As introduced in Section 3.6, the estimation problem consists in separately achieving estimation objectives EO1 and EO2, which are here recalled:

Estimation Objective 1 (EO1). This objective is the estimation of distillate iC4 dynamics within the prescribed range when the control objective is CO1 (i.e., regulation of distillate iC4), and has to be attained with nominal conditions SS1 (stripping section working at high-purity conditions), listed in Table 3.1

$$\hat{c}_D^{iC4}(t) \in c_D^{iC4}(t) \pm \Delta\hat{c} = c_D^{iC4}(t) \pm 0.015 \tag{6.1}$$

Estimation Objective 2 (EO2). This objective is the joint estimation of distillate iC4 and bottom C3 dynamics within the prescribed range when the control objective is CO2 (i.e., regulation of distillate iC4 and bottom C3), and has to be attained with nominal conditions SS2 (no section working at high-purity

conditions), listed in Table 3.2

$$\hat{c}_D^{iC4}(t) \in c_D^{iC4}(t) \pm \Delta\hat{c} = c_D^{iC4}(t) \pm 0.015 \tag{6.2a}$$

$$\hat{c}_B^{C3}(t) \in c_B^{C3}(t) \pm \Delta\hat{c} = c_B^{C3}(t) \pm 0.015 \tag{6.2b}$$

As it can be seen from Eq. (6.1) and (6.2), the impurities to be estimated are the ones to be controlled. Indeed, such compositions have to be estimated in order to monitor the desired separation. The estimator that is going to be developed, can be run in parallel with the controller in order to allow such monitoring.

The estimation structure consists in the selection of (i) components to be retained in the reduced estimation model, (ii) number and location of temperature sensors, (iii) composition states to be innovated, and (iv) regions where the temperature is assumed constant. From now on, the points (ii) and (iii) will be jointly referred to as *measurement structure*. In addition to the binary case, in the multicomponent case here addressed the estimation structure contains the selection of the components to be retained in the estimation model as a design degree of freedom. Differently from the binary case in Fernandéz (2007) and Álvarez and Fernandéz (2009), where detectability measures were used, the structural analysis is here made through the temperature gradient with per-component contribution diagram in conjunction with a systematic procedure. Such method is considerably simpler and more intuitive, and only requires steady-state information at the nominal operating conditions.

6.2 Structural analysis

In this Section, the estimation structural analysis problem is presented and separately solved for both objectives EO1 and EO2. The criteria for selecting the estimation structure is thoroughly illustrated for EO1; since the extension for EO2 case is straightforward, only a resume is given for such case.

6.2.1 Structural analysis - EO1

In this Subsection, the structural analysis is thoroughly illustrated for EO1 objective (i.e., estimation of distillate iC4 dynamics).

Reduction of model components

The estimation structural problem starts with the design of a model with a reduced number of components that, driven by appropriate temperature measurements, will be used for inferring the impurity compositions of interest. The reduction in the number of components is performed on the basis of the temperature

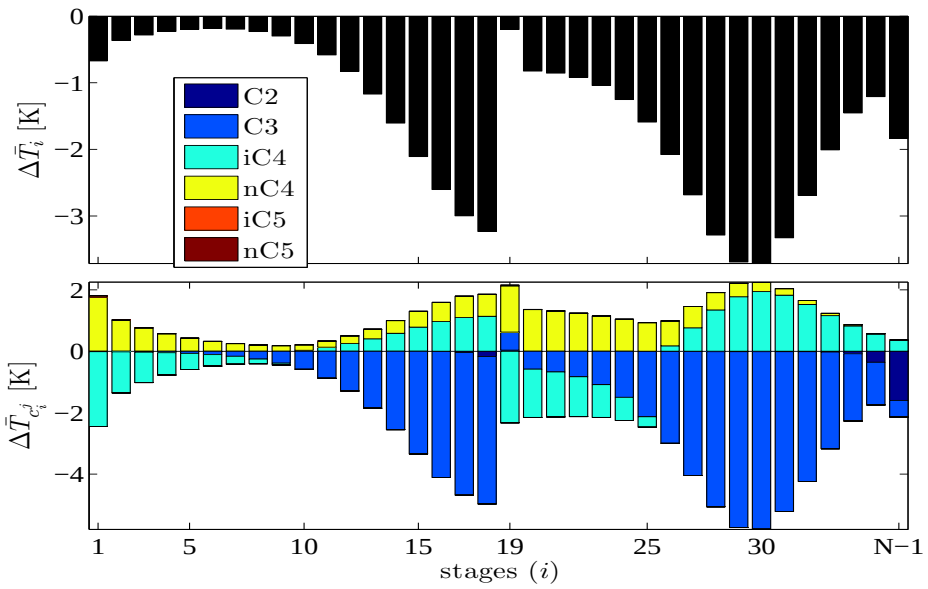

Figure 6.1: Steady-state temperature gradients with per-component contributions for case SS1

gradient with per-component contribution diagram. The operating conditions of interest for EO1 case are the ones of SS1 case given in Table 6.1. The estimation objective has to be achieved when the column is controlled in order to attain control objective CO1 (regulation of distillate iC4 around its nominal value, see Eq. (5.1)); the related gradient diagram for SS1 case is reported again in Figure 6.1 for sakes of convenience.

F	$\bar{c}_F^{C2}$	$\bar{c}_F^{C3}$	$\bar{c}_F^{iC4}$	$\bar{c}_F^{nC4}$	$\bar{c}_F^{iC5}$	T_F
88.2 $m^3\,h^{-1}$	0.0036	0.281	0.236	0.4746	0.0004	320 K

Q	R
3876645 $kcal\,h^{-1}$	61.62 $m^3\,h^{-1}$

Table 6.1: Operating conditions for SS 1

The criteria for selecting components to be kept in the reduced model consists in retaining the ones that mostly contribute to overall temperature gradient profile along the column. It can be seen from Figure 6.1 that these components are the C3, the iC4 and the nC4. On the contrary, C2, iC5 and nC5 are discarded since they have comparatively small manifestations. Thus, the set of modeled components is

$$\{\phi_1\ \phi_2\} = \{\text{C3 iC4}\}$$

since nC4 does not need to be directly modeled because of the mass conservation condition illustrated in Section 3.2.

Note that C2 strongly influences top temperature gradients, but nevertheless, it has been decided not to model it; the C2 removal must be taken into account in next steps of estimation structure selection.

Measurement structure

Measurement structure consists in the joint selection of temperature sensor locations and states to be innovated on the basis of the temperature gradient with per-component contribution diagram.

Let see now how to choose the sensor locations and the innovated components, starting by looking at which information is contained in the gradient diagram:

- temperature sensors have to be placed according to the estimation objective, that is, in the column section with the key impurity to be estimated;
- an area with large temperature variations implies that important compositions are changing, meaning that the most sensitive stages are there; it signifies that measurement sensors have to be placed there;
- a large contribution of a component to the overall gradient signifies that the information contained in the temperature measurement mostly reflects the variation of that component, implying that: (i) the stages whose temperature gradient is due to an unmodeled component must not be taken into account as sensor locations for avoiding error propagation; (ii) the component which mostly contributes to a gradient related to a sensor location has to be chosen as innovated component, in such a way to have the largest amount of useful information.

The interest in EO1 case is in estimating distillate iC4 dynamics, and thus, one or more sensors have to be placed in the enriching section, which is the region of interest. On the basis of the preceding considerations in the light of Figure 6.1, it can be stated that: (i) largest temperature gradients in the enriching section lie between 26-th and 33-rd stages; (ii) the removed component C2 has a not negligible contribution in the top of the column, and therefore no sensors have to be placed between 35-th and 37-th stage; (iii) the C3 mostly contributes to the temperature gradients along these stages, meaning that the variation in temperature is mainly due to its gradient, and therefore such component has to be innovated where temperature sensors are placed.

Therefore, the candidate measurement structures include one or more temperature sensors along the most sensitive area, with the C3 as innovated component

for each temperature measurement, that is, in mathematical notation,

$$s_k \in \{26, \dots, 33\}, \qquad \mu_k = \text{C3}, \qquad \text{for} \quad k = 1, \dots, m$$

meaning that the component μ_k is innovated at s_k-th stage.

These structures will be subsequently tested and compared with each other, in order to select the best structure according to the given estimation objective.

Note that the criterion for the selection of temperature sensor locations is similar to the one of control case: however, in the control case it is important to place sensors where large gradients mainly due to key components are present, whereas in the estimation case sensors have to be placed where large gradients are not due to unmodeled components.

Temperature approximation

A further estimation model reduction is suggested by the temperature gradient profile in Figure 6.1: it can be noted, indeed, that temperature gradients are quite small in the stripping section, between 1-st and 17-th stages, meaning that temperature can be assumed constant in such region; moreover, being the distillate iC4 the only impurity effluent to be estimated, such approximation should not influence very much the estimate of interest.

In this Thesis, temperatures are approximated as explained in the following. Consider q regions where temperature has to be assumed constant: in the k-th region, where I_K and F_K are the initial and the final stage respectively, temperature is approximated as

$$T_{A,k} = \frac{\hat{T}_{I_k} + \hat{T}_{F_k}}{2} \qquad \text{for } k = 1, \dots, q \tag{6.3a}$$

$$\hat{T}_i = T_{A,k} \qquad \text{for } k = 1, \dots, q, \quad i = I_k + 1, \dots, F_k - 1 \tag{6.3b}$$

where $T_{A,k}$ is the average temperature in the k-th region. Note that the temperature approximation illustrated in Eq. (6.3) implies that temperature is kept constant as the average one only in the internal stages of every region k.

An important consequence of approximation (6.3), is that a composition, for instance the one of the $(C_M - 1)$-th component retained in the estimation model, can be modeled through the following algebraic equation derived from Eq. (3.2g), in stages where temperature is approximated:

$$\hat{c}_i^{\phi_{C_M-1}} = \frac{P_i - \sum_{j=1}^{C_M-2} \hat{c}_i^{\phi_j} \hat{P}_i^{\phi_j} - (1 - \sum_{j=1}^{C_M-2} \hat{c}_i^{\phi_j}) \hat{P}_i^{\phi_j}}{\hat{P}_i^{\phi_{C_M-1}} - \hat{P}_i^{\phi_{C_M}}}$$
$$\text{for} \quad k = 1, \dots, q \quad i = I_k + 1, \dots, F_k - 1 \tag{6.4}$$

Note that because of the temperature approximation (6.3), also the partial pressure for each component becomes constant, that is:

$$\hat{P}_i^{\phi_j} := P_{A,k}^{\phi_j}(T_{A,k}) \qquad \text{for} \quad k = 1, \ldots, q \quad i = I_k + 1, \ldots, F_k - 1$$

This means that if n_k is the number of internal stages in the k-th region, $\sum_{k=1}^{q} n_k$ ODEs are not needed anymore.

6.2.2 Structural analysis - EO2

After having thoroughly discussed the estimation problem for EO1 case, the equivalent one has to be discussed in order to achieve EO2 (i.e., joint estimation of bottom C3 and distillate iC4 dynamics). The structural problem is substantially the same of EO1 case, and therefore only a brief explanation is given.

Reduced model

Model reduction procedure is the same of EO1 case, and therefore the analysis must be made on the basis of the gradient diagram. Such diagram for EO2 case is the one related to SS2 operating conditions (recalled in Table 6.2), and is reported again for sakes of clarity in Figure 6.2.

F	$\bar{c}_F^{C2}$	$\bar{c}_F^{C3}$	$\bar{c}_F^{iC4}$	$\bar{c}_F^{nC4}$	$\bar{c}_F^{iC5}$	T_F
88.2 $\mathrm{m^3\,h^{-1}}$	0.0036	0.281	0.236	0.4746	0.0004	320 K
Q			R			
2665688 $\mathrm{kcal\,h^{-1}}$			34.99 $\mathrm{m^3\,h^{-1}}$			

Table 6.2: Operating conditions for SS 2

On the basis of same considerations given for EO1 case, it can be stated that only C3, iC4 and nC4 gradients significantly contribute to the temperature gradient profile along the column, and therefore these components are modeled in the reduced estimation model. This means that the set of modeled components is:

$$\{\phi_1 \ \phi_2\} = \{\text{C3 iC4}\}$$

since nC4 does not need to be directly modeled because of the mass conservation condition illustrated in Section 3.2.

Note that, as well as for the EO1 case, C2 has a remarkable influence on top stages, but nevertheless, it has been decided not to model it.

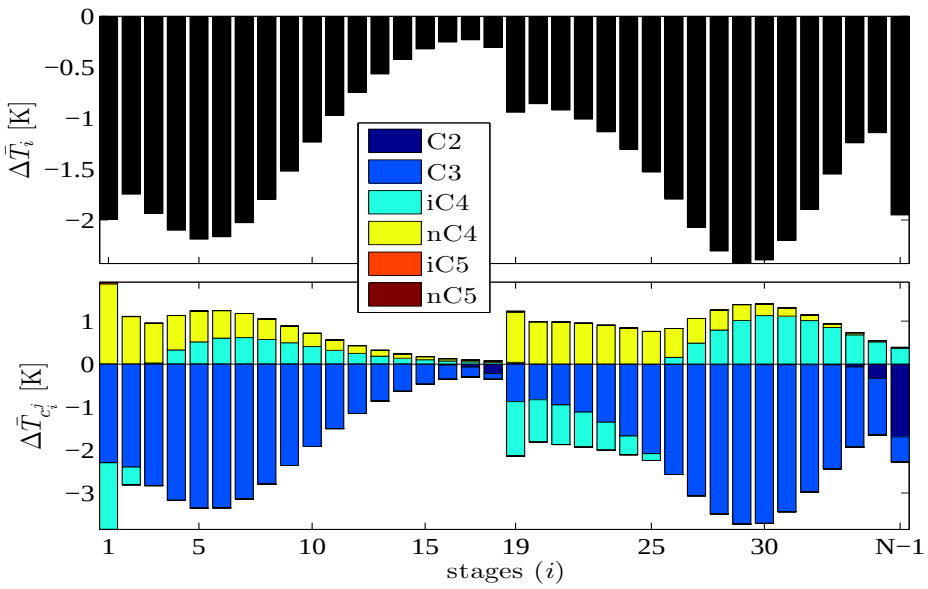

Figure 6.2: Steady-state temperature gradients with per-component contributions for case SS2

Measurement structure

In order to design the measurement structure for EO2 case, the same analysis made for EO1 must be repeated for each section since the objective is the joint estimation of both key impurities. The task can be solved section-wise: firstly, temperature sensor locations and states to be innovated are chosen for the enriching section; then, the same is made for the stripping section.

On the basis of the diagram in Figure 6.2, it can be seen that the same conclusions of EO1 case (one or more sensors between 26-th and 33-th stages) hold for the enriching section in EO2 case. As regards the stripping section, one or more sensors have to be placed between 3-rd and 7-th stages, where the gradients are the largest. In spite of large gradients, 1-st and 2-nd stages should be avoided, because a small contribution of iC5 and nC5 is present. The component to be innovated is the C3 in both stripping and enriching sections, since it is the one which mainly contributes to the large temperature gradients selected for sensor locations. Mathematically speaking, we have

$$s_k \in \{3, \dots, 7\} \cup \{26, \dots, 33\}, \qquad \mu_k = \text{C3}, \qquad \text{for} \quad k = 1, \dots, m$$

meaning that the component μ_k is innovated at s_k-th stage.

Temperature approximation

For EO2 case, the temperature approximation substantially works as for EO1 case. Figure 6.2 suggests that temperature can be approximated in the stripping section between 10-th and 17-th stages, and in the enriching section between 21-st and 23-rd stages. However, note that in this case, being the estimation objective the joint inferring of bottom C3 and distillate iC4, such temperature approximation will have an influence in the estimates of interest.

6.3 Chapter summary

In this Chapter, the estimation structural analysis problem has been addressed. A new methodology based on the temperature gradient with per-component contribution diagram has been proposed and used for the selection of entire structure: (i) the components to be retained in the estimation model are the ones that mostly contribute to the overall temperature gradient profile along the column; (ii) one or more temperature sensors have to be placed in an area with large temperature gradients (most sensitive area) not due to unmodeled components; (iii) the component that mostly contributes to a gradient in a stage chosen as sensor location has to be chosen as innovated component in that stage; (iv) temperature can be approximated as the average one in regions where gradients are small.

In the light of previous considerations, C3, iC4 and nC4 have been selected as the components to be retained in the estimation model since they mostly contribute to the overall gradients, for both estimation objectives. Moreover, (i) for EO1 objective, one or more sensors have to be placed between 26-th and 33-th stage, with C3 as innovated components and a possible temperature approximation in the region from 1-st to 16-th stage, and (ii) for EO2 objective, in addition to EO1 case, one or more sensors have to be placed between 3-rd and 7-th stage, with C3 as innovated component, while temperature approximation can be done from 10-th to 17-th stage and from 21-st to 23-rd.

Chapter 7

Estimation algorithm

Once a reduced model, temperature sensor locations and composition states to be innovated for estimation purposes have been selected, a method to connect them has to be found. This means that an appropriate *estimation algorithm*, that is, a dynamic data processor that performs the estimation task, has to be chosen.

In this Chapter two kinds of estimation algorithm are considered: (i) the Geometric Estimator (GE), which will be used as a reduced order observer (i.e., with partial innovation); (ii) the Extended Kalman Filter (EKF), which will be used in both complete and reduced form (i.e., with both complete and partial innovation).

7.1 Geometric Estimator (GE)

In this Section, the Geometric Estimator (GE) in its form with partial innovation is described.

7.1.1 Definition

The Geometric Estimator (GE) (Álvarez, 2000) is an extension of the Luenberger observer (LO) for nonlinear systems, and provides a systematic tuning construction over all admissible structures, coupled with a convergence criteria; therefore it has been chosen as the principal estimation algorithm of the present Thesis. Its full implementation would require computation of Lie derivatives, becoming intractable with large orders, typical of staged processes as multicomponent distillation columns. Therefore, in order to avoid such problems, only the

GE with adjustable structure and partial innovation (Tronci *et al.*, 2005; Fernandéz, 2007; Pulis, 2007; Álvarez and Fernandéz, 2009) is considered in this Thesis, meaning that it is used in conjunction with the chosen candidate structures designed on the basis of considerations given in Chapter 6.

The reduced order form of the GE is the following:

Innovated states (for any innovated stage $\hat{c}_{s_k}^{\mu_k}$, with $k = 1, \ldots, m$)

$$\dot{\hat{c}}_{s_k}^{\mu_k} = \hat{f}_{s_k}^{\mu_k}(\hat{\mathbf{x}}_{i-1}, \hat{\mathbf{x}}_{s_k}, \hat{\mathbf{x}}_{s_k+1}) + \frac{1}{\hat{\beta}'_{s_k,\mu_k}} \left(K_{P,s_k}(T_{s_k} - \hat{T}_{s_k}) + K_{I,s_k} z_{s_k} \right) \tag{7.1a}$$

Noninnovated states (for any noninnovated stage $\hat{c}_i^j$, with $(i,j) \neq (s_k, \mu_k)$)

$$\dot{\hat{c}}_i^j = \hat{f}_i^j(\hat{\mathbf{x}}_{i-1}, \hat{\mathbf{x}}_i, \hat{\mathbf{x}}_{i+1}) \tag{7.1b}$$

Integral actions ($k = 1, \ldots, m$)

$$\dot{z}_{s_k} = T_{s_k} - \hat{T}_{s_k} \tag{7.1c}$$

Temperatures ($k = 1, \ldots, m$)

$$\hat{T}_{s_k} = \hat{\beta}(\hat{\mathbf{x}}_{s_k}) \tag{7.1d}$$

where

$$\hat{\beta}'_{s_k,\mu_k} = \left. \frac{\partial \hat{T}_{s_k}}{\partial \hat{c}_{s_k}^{\mu_k}} \right|_{\hat{\mathbf{x}}_{s_k}}$$

In Eq. (7.1), the GE is illustrated in its form with partial innovation, meaning that only some of the states (i.e., the component μ_k at s_k-th stage, for $k = 1, \ldots, m$) are innovated, on the basis of the chosen measurement structure. According to the notation in Section 3.6, $\hat{x}_I = [\hat{c}_{s_1}^{\mu_1} \ldots \hat{c}_{s_m}^{\mu_m}]$ is the innovated stage vector, whereas $\hat{x}_{II} = \hat{x} - \hat{x}_I$ is the noninnovated one. Such kind of GE is therefore a reduced order observer. It contains a proportional-integral (PI) action, with $K_{P,i}$ and $K_{I,i}$ being the the proportional and the integral gain at i-th stage respectively. The integral action ensures the offset-free temperature estimation, meaning that a better composition estimation is expected compared to the case of the only proportional (P) action. As stated before, only one composition state per temperature measurement is innovated here. Such GE requires $n_M + m$ ODEs to be integrated. This means that for the candidate estimator structures taken into account, $74 + m$ ODEs need to be integrated. Note that a complete model with all components modeled would require the integration of $n = 185 + m$ ODEs.

7.1.2 Asymptotic error propagation measure in a GE for a given estimation structure

The asymptotic error propagation measure for a given estimation structure can be formally connected with the temperature gradient with per-component contribution diagram when using the GE as estimation algorithm. Indeed, for each innovated state in Eq. (7.1a), the corresponding error dynamics are given by:

$$\begin{aligned}\dot{\tilde{c}}^{\mu_k}_{s_k} &= \tilde{f}^{\mu_k}_{s_k} + \frac{1}{\hat{\beta}'_{s_k,\mu_k}}\left(K_{P,s_k}(\tilde{T}_{s_k} + T^E_{s_k}) + K_{I,s_k} z_{s_k}\right) \\ &\approx \tilde{f}^{\mu_k}_{s_k} + K_{P,s_k}\tilde{c}^{\mu_k}_{s_k} + K_{I,s_k}\int \tilde{c}^{\mu_k}_{s_k} + \frac{1}{\hat{\beta}'_{s_k,\mu_k}}\left(K_{P,s_k} T^E_{s_k} + K_{I,s_k}\int T^E_{s_k}\right)\end{aligned} \tag{7.2}$$

where

$$\tilde{T}_{s_k} = T_{s_k} - \hat{T}_{s_k}, \qquad \tilde{f}^{\mu_k}_{s_k} = f^{\mu_k}_{s_k} - \hat{f}^{\mu_k}_{s_k}, \qquad \tilde{c}^{\mu_k}_{s_k} \approx \frac{\hat{T}_{s_k}}{\hat{\beta}'_{s_k,\mu_k}}$$

and $T^E_{s_k}$ represents the temperature measurement error at s_k-th stage. A consequent measure of the error contribution due to $T^E_{s_k}$ at steady state (i.e. when $\dot{\tilde{c}}^{\mu_k}_{s_k} = 0$) is

$$K_{P,s_k}\tilde{c}^{\mu_k}_{s_k} + K_{I,s_k}\int \tilde{c}^{\mu_k}_{s_k} = -\tilde{f}^{\mu_k}_{s_k} - \frac{1}{\hat{\beta}'_{s_k,\mu_k}}\left(K_{P,s_k} T^E_{s_k} + K_{I,s_k}\int T^E_{s_k}\right) \tag{7.3}$$

This means that a large sensitivity term $\hat{\beta}'_{s_k,\mu_k}$ implies small contribution of $T^E_{s_k}$ in $\tilde{c}^{\mu_k}_{s_k}$. Since the component contribution depends on the sensitivity term, this consideration further motivates the use of the temperature gradient with per-component contribution diagram as a mean for the selection of the measurement structure.

7.1.3 Tuning

The simple and systematic tuning construction for every given estimation structure is one of the aspects which motivates the use of the GE Eq. (7.1), since this gives the certainty that the estimator functioning results are due to the structure and not to the tuning scheme. The guidelines are given by the following rules (Álvarez, 2000):

$$K_{P,i} = 2\xi_i\lambda_i, \qquad K_{I,i} = {\lambda_i}^2, \qquad \lambda_i = 5 \div 10\omega_i, \qquad \xi_i = 1 \div 3 \tag{7.4}$$

In Eq. (7.4), ω_i and λ_i are the characteristic system and estimator frequencies, and ξ_i is the damping factor at i-th stage.

The characteristic frequency ω_i and the damping factor ξ_i are the only parameters needed for the tuning. It must be taken into account that the estimator speed must be greater than the system one, but cannot exceed a certain limit given by the fast unmodeled holdup dynamics, as already said in Remark 4.3.

7.2 Extended Kalman Filter

The Extended Kalman Filter (EKF) (Jazwinsky, 1970) is a well-known nonlinear estimation algorithm, derived by a linearization procedure from the Kalman Filter. The EKF is by far the most used estimation algorithm for inferring compositions in a distillation column, once an estimation model and some temperature measurements are present. Given the availability of adequate models (Skogestad, 1997; Baratti *et al.*, 1998), the EKF has been successfully implemented in binary (Baratti *et al.*, 1995; Yang and Lee, 1997), ternary (Baratti *et al.*, 1998), and four-component systems (Venkateswarlu and Kumar, 2006). The advantages of the EKF are: (i) the accumulated experience to set diagonal measurement and block diagonal modeling error covariance matrices (Baratti *et al.*, 1998; Fernandéz and Álvarez, 2007), (ii) the straightforward construction once the structure of the error covariances is known, and (iii) the robust functioning in the sense of functioning over an ample set of column types, conditions and separation mixtures.

7.2.1 Extended Kalman Filter with complete innovation

The standard implementation of the EKF is in its complete form, that is, with complete innovation, and is reported below in its continuous-discrete form:

State estimation

$$\dot{\hat{x}} = \hat{f}(\hat{x}, \hat{F}, \hat{x}_F, \hat{T}_F, \hat{Q}, \hat{R}) \tag{7.5a}$$

Error covariance propagation

$$\dot{\hat{P}_E} = F_E P_E {F_E}^T + Q_E \tag{7.5b}$$

Kalman gain matrix

$$K_E = P_E H_E (H_E P_E {H_E}^T + R_E)^{-1} \tag{7.5c}$$

State estimate update

$$\hat{x}^+ = \hat{x} + K_E(T - \hat{T}) \tag{7.5d}$$

Error covariance update

$${P_E}^+ = (I - K_E H_E) P_E \tag{7.5e}$$

Temperature

$$\hat{T} = \hat{\beta}(\hat{x}) \tag{7.5f}$$

Eq. (7.5) is written in matricial form, meaning that x is the composition vector, $T = [T_{s_1} \dots T_{s_m}]$ is the temperature vector, F_E and H_E are the jacobian and measurement matrices, Q_E and R_E are the model and measurement error covariances, P_E is the system covariance and K_E is the gain matrix.

A little modification in the definition of measurement structure given in Chapter 6 is needed when considering the EKF in the complete form (7.5): all composition states are innovated in the stages where sensors are placed, meaning that the measurement structure only consists in selecting appropriate temperature sensor locations.

Compared to the GE case, the EKF has a difficult tuning, since Q_E and R_E must be adequately chosen on the basis of the expected model and measurement errors, resulting in an expensive trial and error procedure. Furthermore, the EKF with total innovation (7.5) presents the drawback of the huge number of ODEs to be integrated (the resulting model order is $\frac{n_M(n_M+1)}{2} + n_M$), due to the computation of the high-dimensional gain matrix P_E through the Riccati equation (7.5b). Indeed, in the present case, 2849 ODEs need to be integrated.

The last considerations, together with the structural considerations given in Chapter 6 (i.e., only some composition states need to be innovated through temperature measurements), suggest that a version of the EKF with partial innovation (a reduced order observer) be considered; this results in the Extended Kalman Filter (REKF) with partial innovation, whose formulation is given in next subsection.

7.2.2 Extended Kalman Filter with partial innovation (REKF)

In this subsection the EKF with partial innovation (REKF) is presented. The idea is that the measurement injection in all composition states does not significantly contribute to the effluent estimation task. Compared to the EKF, the REKF presents a partial innovation scheme: only some of the composition states are innovated, according to the selected measurement structure. The REKF is written as follows:

Innovated states (for any innovated stage $\hat{c}_{s_k}^{\mu_k}$, with $k = 1, \dots, m$)

$$\dot{\hat{c}}_{s_k}^{\mu_k} = \hat{f}_{s_k}^{\mu_k}(\hat{\mathbf{x}}_{s_k-1}, \hat{\mathbf{x}}_{s_k}, \hat{\mathbf{x}}_{s_k+1}) \tag{7.6a}$$

Noninnovated states (for any noninnovated stage $\hat{c}_i^j$, with $(i,j) \neq (s_k, \mu_k)$)

$$\dot{\hat{c}}_i^j = \hat{f}_i^j(\hat{\mathbf{x}}_{i-1}, \hat{\mathbf{x}}_i, \hat{\mathbf{x}}_{i+1}) \tag{7.6b}$$

Error covariance propagation (for $k = 1, \ldots, m$)

$$\dot{\hat{P}}^{\mu_k}_{E,s_k} = F^{\mu_k}_{E,s_k} P^{\mu_k}_{E,s_k} F^{\mu_k}_{E,s_k} + Q^{\mu_k}_{E,s_k} \tag{7.6c}$$

Kalman gain matrix (for $k = 1, \ldots, m$)

$$K^{\mu_k}_{E,s_k} = \frac{P^{\mu_k}_{E,s_k} H^{\mu_k}_{E,s_k}}{H^{\mu_k}_{E,s_k} P^{\mu_k}_{E,s_k} H^{\mu_k}_{E,s_k} + R^{\mu_k}_{E,s_k}} \tag{7.6d}$$

State estimate update (for $k = 1, \ldots, m$)

$$\hat{c}^{\mu_k +}_{s_k} = \hat{c}^{\mu_k}_{s_k} + K^{\mu_k}_{E,s_k} (T_{s_k} - \hat{T}_{s_k}) \tag{7.6e}$$

Error covariance update (for $k = 1, \ldots, m$)

$$P^{\mu_k +}_{E,s_k} = (I - K^{\mu_k}_{E,s_k} H^{\mu_k}_{E,s_k}) P^{\mu_k}_{E,s_k} \tag{7.6f}$$

Temperatures ($k = 1, \ldots, m$)

$$\hat{T}_{s_k} = \hat{\beta}(\hat{\mathbf{x}}_{s_k}) \tag{7.6g}$$

Equations for covariance propagation, gain computation, covariance and composition updates are the same of the EKF case, except for the fact that only the covariance terms related to innovated states are propagated. The propagation of each covariance term is decoupled, resulting in a model with lower dimension. In fact, compared to the EKF, the number of ODEs to be integrated in the REKF is considerably smaller: $n_M + m$ ODEs have to be integrated, meaning that the GE and the REKF here considered have the same dimensionality.

7.3 Chapter summary

In this Section, the two estimation algorithms employed in this Thesis have been described: the Geometric Observer (GE) with partial innovation and the Extended Kalman Filter (EKF) with both partial and complete innovation. Regardless of the algorithm, the partial innovation permits a considerable reduction of the number of ODEs to be integrated: if the order of the estimation model is n_M and m temperature sensors are used for innovation, the order of the partial estimator is $n_M + m$, while the order is $\frac{n_M(n_M+1)}{2} + n_M$ if complete innovation is used. As regards the algorithm, the main advantage of the GE compared to EKF is its systematic tuning procedure for every admissible structure, while the EKF has to been tuned with a time expensive trial and error technique.

Chapter 8

Estimation structural results

In this Chapter, the estimation structural results are assessed. The candidate structures selected through the analysis of the temperature gradient with per-component contribution diagram are here assessed through dynamic simulations, as the best compromise among speed, simplicity and robustness. The Geometric Estimator (GE) is considered as the main estimation algorithm and is used in order to compare the different structures, while the EKF with partial or complete innovation is used for sakes of comparison between algorithms, considering only the best estimation structures.

8.1 Introduction

The candidate estimation structures obtained through the temperature gradient with per-component contribution diagram are assessed for both estimation objectives EO1 and EO2, which are here recalled for sakes of clarity:

Estimation Objective 1 (EO1). This objective is the estimation of distillate iC4 dynamics within the prescribed range when the control objective is CO1 (i.e., regulation of distillate iC4), and has to be attained with nominal conditions SS1 (stripping section working at high-purity conditions), listed in Table 3.1

$$\hat{c}_D^{iC4}(t) \in c_D^{iC4}(t) \pm \Delta\hat{c} = c_D^{iC4}(t) \pm 0.015 \tag{8.1}$$

Estimation Objective 2 (EO2). This objective is the joint estimation of distillate iC4 and bottom C3 dynamics within the prescribed range when the control objective is CO2 (i.e., regulation of distillate iC4 and bottom C3), and has to be attained with nominal conditions SS2 (no section working at high-purity

conditions), listed in Table 3.2

$$\hat{c}_D^{iC4}(t) \in c_D^{iC4}(t) \pm \Delta\hat{c} = c_D^{iC4}(t) \pm 0.015 \tag{8.2a}$$

$$\hat{c}_B^{C3}(t) \in c_B^{C3}(t) \pm \Delta\hat{c} = c_B^{C3}(t) \pm 0.015 \tag{8.2b}$$

In order to test the structures, the column is subjected to a changes in operating conditions as in Scenario 1 (SC1, see Table 5.2) and Scenario 2 (SC2, Table 5.3), the same considered in control case. For both Scenarios, it is assumed that *feed flow and temperature are measured*, while *feed composition is not*, since online composition analyzers are not available. The estimator (3.10) is always set with: (i) initial conditions equal to estimator steady-state; (ii) feed composition at its nominal value; (iii) temperature measurement noise approximated with a sinusoidal wave of amplitude 0.2 K and frequency 60h^{-1}; (iv) thermodynamics given by the standard 3-constant Antoine Equation (Reid *et al.*, 1998), and therefore approximated with respect to the extended 7-constant equation used for the full model in Eq. (3.9).

Each estimation structure here considered is based on the reduced model (3.10) with only C3, iC4 and nC4 as modeled components. Such model is used in conjunction with different measurement structures, which from now on will be denoted as

$$\sigma_{E[\mu,s_1,\ldots,s_m]}$$

meaning that the component μ is innovated in the stages $s_1, \ldots, s_m$. The best estimation structures are then compared with different temperature approximations made as illustrated in Eq. (6.3). A structure with temperature approximation will be denoted as

$$\sigma_{E[\mu,s_1,\ldots,s_m]T[I_1,F_1,\ldots,I_q.F_q]}$$

if temperatures are approximated from I_k-th to F_k-th stage, for $k = 1, \ldots, q$.

8.2 Estimation Objective 1 (EO1)

According to the estimation objective EO1, the goal is to infer distillate iC4 composition, that is, the key distillate impurity. EO1 objective is related to control objective CO1, since the impurity to be regulated in CO1 case is the one to be estimated in EO1 case: it is assumed here that the column is working in closed-loop, with the temperature at 33-rd stage controlled through the reboiler heat duty Q with a conventional single-end controller (i.e., with a control structure $\sigma_{C[Q,33]}$, see Chapter 5). Both Scenario 1 (SC1) and Scenario 2 (SC2) conditions are considered: at first, the Geometric Estimator (GE) is tested as estimation algorithm, in conjunction with several candidate estimation structures determined in Section 6.2.1, which are compared in order to find the best structure; then, the best estimation structure is tested with Extended Kalman Filters (with partial or reduced innovation), and compared to the GE case.

8.2.1 GE structural results - EO1

Geometric Estimator (GE) structural results are now assessed for EO1 case, with respect to SC1 and SC2.

Tuning

Tuning parameters are chosen according to guidelines given in Section 7.1.3. Estimator frequency λ is chosen 10 times larger than the characteristic frequency $\omega = 1\text{h}^{-1}$ in the enriching section (already computed in Section 5.2.2), meaning that $\lambda = 10\text{h}^{-1}$ while damping factor ξ is chosen equal to 3. The resulting tuning parameters are therefore the following:

$$K_P = 60 \qquad K_I = 100$$

Scenario 1 (SC1)

According to SC1, the column is tested to a step-plus-sinusoidal change in the form:

$$(B_D + A_D \sin(2\pi\omega_D t))\, H(t-1)$$

where H is an Heaviside step (at $t = 1\text{h}$ since the disturbance is applied at this time), ω_D is the disturbance frequency, B_D and A_D are the magnitudes of the step and of the sinusoidal disturbances respectively. The disturbance parameter values are reported again in Table 8.1. Recall that feed flow rate and temperature are measured, whereas feed composition is not, meaning that the estimator does not have information about its change and therefore is always set with feed composition at its nominal value, as shown in Figure 8.1.

	0h$< t <$ 1h	B_D	A_D	ω_D
F	$88.2\,\text{m}^3\,\text{h}^{-1}$	$6.8\,\text{m}^3\,\text{h}^{-1}$	$10\,\text{m}^3\,\text{h}^{-1}$	$3\,\text{h}^{-1}$
c_F^{C2}	0.0036	−0.0016	0	$3\,\text{h}^{-1}$
c_F^{C3}	0.281	−0.011	0.02	$3\,\text{h}^{-1}$
c_F^{iC4}	0.236	−0.00128	0.02	$3\,\text{h}^{-1}$
c_F^{nC4}	0.4746	0.0254	−0.04	$3\,\text{h}^{-1}$
c_F^{iC5}	0.004	0	0	$3\,\text{h}^{-1}$
c_F^{nC5}	0.0008	0	0	$3\,\text{h}^{-1}$
T_F	320 K	−3 K	10 K	$3\,\text{h}^{-1}$

Table 8.1: Disturbance parameters for Scenario 1 (SC1)

Firstly, several structures with one temperature sensor, with such sensor located at different column regions in either stripping or enriching section, are tested in order to find out whether the structural considerations made in Chapter 6 are

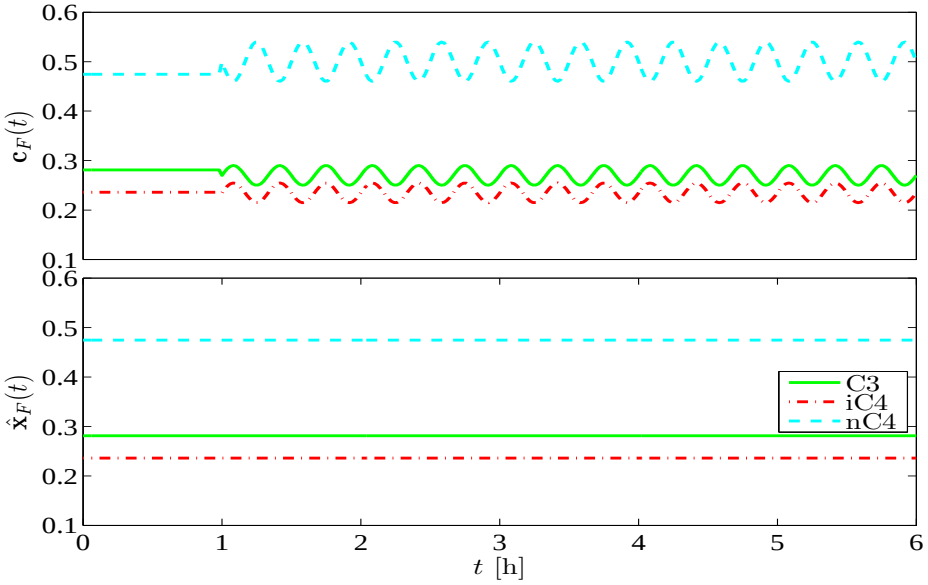

Figure 8.1: Actual (top) and modeled (bottom) composition feed behavior for Scenario 1 (SC1).

valid. Only C3 is innovated, since it is the component which mostly contributes to the temperature gradient and therefore can provide the largest amount of information. In Figure 8.2, measurement structures $\sigma_{E[C3,17]}$, $\sigma_{E[C3,23]}$, $\sigma_{E[C3,30]}$ and $\sigma_{E[C3,37]}$ have been tested and compared, showing that: (i) as expected the location of sensor at either 17-th or 37-th stage does not yield an acceptable estimate, given that no good estimate is obtained at both transient and steady-state; (ii) the structure with sensor at 30-th is by far the best one among the structures compared since both transient and steady-state tracking are obtained. As expected from the structural analysis, the estimator works better if the sensor is located in the area with the largest gradients in the section of interest (the enriching one in this case). Moreover, structure with sensor at 37-th stage does not permit the achievement of objectives because of the ethane influence, since it is a removed component in reduced estimator model (3.10).

A further test is made considering the location of the temperature sensor in the area with largest gradients (around 30-th stage), at different locations (30-th, 31-st and 33-rd stages). The comparison between $\sigma_{E[C3,30]}$, $\sigma_{E[C3,31]}$ and $\sigma_{E[C3,33]}$ structures in Figure 8.3 shows that no significant differences are present in the estimator performance.

In order to see whether the addition of more sensors improves performance, measurement structures with a variable number of sensors (from 1 to 4) in the area

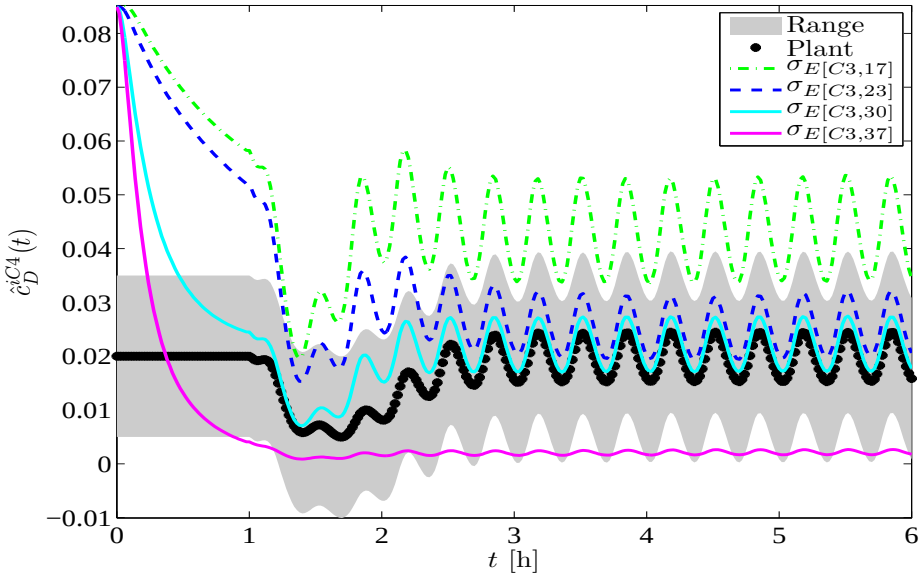

Figure 8.2: EO1, SC1: comparison between the measurement structures $\sigma_{E[C3,17]}$, $\sigma_{E[C3,23]}$, $\sigma_{E[C3,30]}$ and $\sigma_{E[C3,37]}$

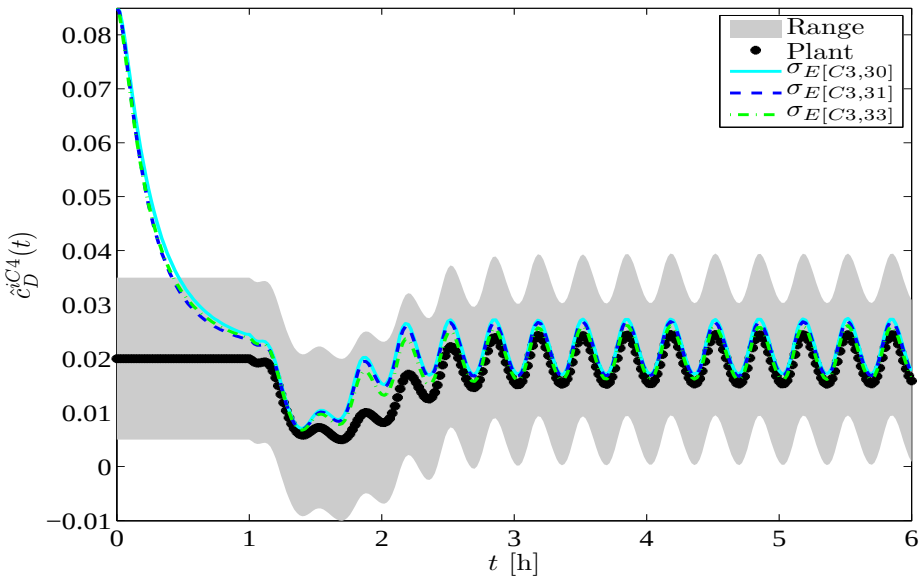

Figure 8.3: EO1, SC1: comparison between the measurement structures $\sigma_{E[C3,30]}$, $\sigma_{E[C3,31]}$ and $\sigma_{E[C3,33]}$

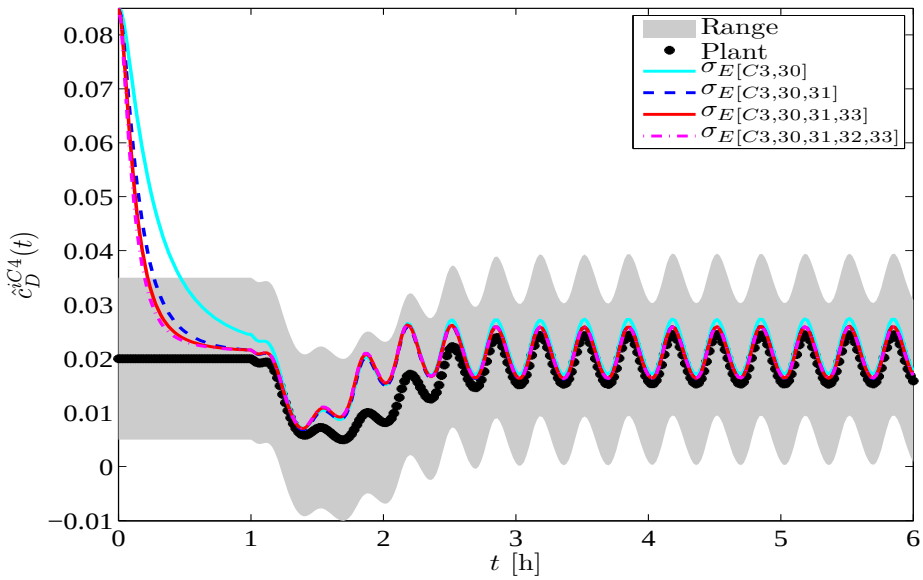

Figure 8.4: EO1, SC1: comparison between the measurement structures $\sigma_{E[C3,30]}$, $\sigma_{E[C3,30,31]}$, $\sigma_{E[C3,30,31,33]}$ and $\sigma_{E[C3,30,31,32,33]}$

of the enriching section with the largest gradients are tested and compared. In Figure 8.4, the comparison among $\sigma_{E[C3,30]}$, $\sigma_{E[C3,30,31]}$, $\sigma_{E[C3,30,31,33]}$ and $\sigma_{E[C3,30,31,32,33]}$ is shown. It can be seen that there is an improvement in estimating the initial steady-state when using more sensors if 2 or 3 sensors are used (while the 4-th sensor is almost useless). On the other hand, results do not change for transient and final steady-state estimation.

The 3-sensor structure $\sigma_{E[C3,30,31,33]}$ has also been tested with an estimation model with different temperature approximations as in Eq. (6.3). Temperature gradients in Figure 6.1 would suggest that temperature be approximated from 1-st to 16-th stages; however, for sakes of comparison, also the approximation from 1-st to 12-nd and 23-rd stages respectively have been tested, with results shown in Figure 8.5. It can be noted as the temperature approximation in the stripping section only does not yield a different behavior; on the other hand, the approximation from 1-st to 23-rd stage produces a much larger error, that could be explained by the inclusion of feed stage in the region where temperatures have been approximated.

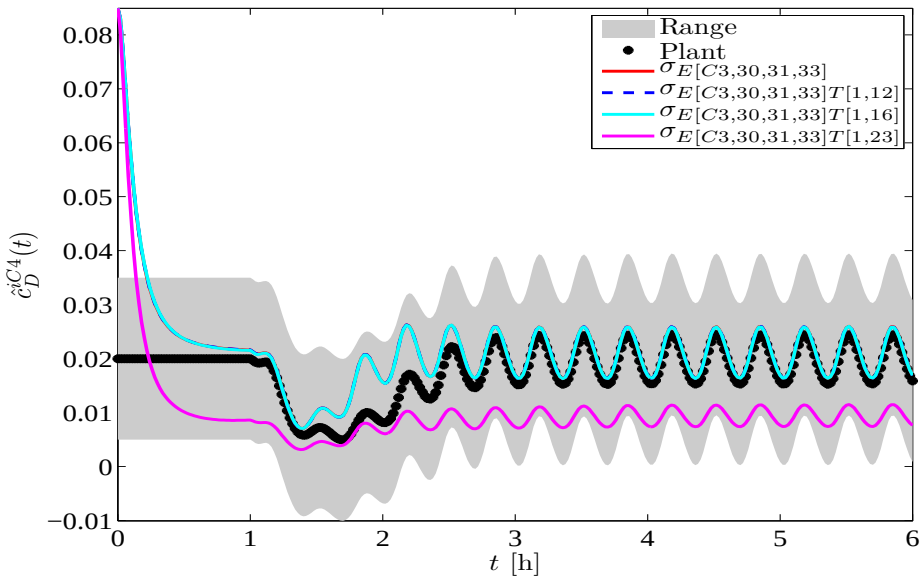

Figure 8.5: EO1, SC1: comparison between the measurement structures $\sigma_{E[C3,30,31,33]T[1,12]}$, $\sigma_{E[C3,30,31,33]T[1,16]}$ and $\sigma_{E[C3,30,31,33]T[1,23]}$

.

Scenario 2 (SC2)

Recall SC2, which consists in testing the column to a step-plus-sinusoidal change in the form

$$(B_D + A_D \sin(2\pi\omega_D t))\, H(t-1)$$

where H is an Heaviside step (at $t = 1$h since the disturbance is applied at this time), ω_D is the disturbance frequency, B_D and A_D are the magnitudes of the step and of the sinusoidal disturbances respectively. The change in SC2 is stronger and has opposite direction with respect to SC1 case, and the disturbance parameter values are reported again in Table 8.2. Recall again that feed flow rate and temperature are measured, whereas feed composition is not, meaning that the estimator does not have information about its change and therefore is always set with feed composition at its nominal value, as shown in Figure 8.6.

In Figure 8.7 the comparison among measurement structures $\sigma_{E[C3,30]}$, $\sigma_{E[C3,30,31]}$, $\sigma_{E[C3,30,31,33]}$ and $\sigma_{E[C3,30,31,32,33]}$: differently from SC1 case, at least 2 sensors are needed for obtaining an acceptable initial and final steady-state performance; furthermore 2 sensors ensure a good transient tracking. Note that as in SC1 case, the addition of the 4-th sensor does not produce any difference compared to the 3-sensor performance.

Subsequently, structure $\sigma_{E[C3,30,31,33]}$ has been tested with an estimation model

	0h$< t <$ 1h	B_D	A_D	ω_D
F	88.2 $m^3\,h^{-1}$	-22.2 $m^3\,h^{-1}$	10 $m^3\,h^{-1}$	3 h^{-1}
c_F^{C2}	0.0036	-0.0016	0	3 h^{-1}
c_F^{C3}	0.281	0.043	0.02	3 h^{-1}
c_F^{iC4}	0.236	0.021	0.02	3 h^{-1}
c_F^{nC4}	0.4746	-0.0704	-0.04	3 h^{-1}
c_F^{iC5}	0.004	0	0	3 h^{-1}
c_F^{nC5}	0.0008	0	0	3 h^{-1}
T_F	320 K	10 K	10 K	3 h^{-1}

Table 8.2: Disturbance parameters for Scenario 2 (SC2)

with different levels of temperature approximations, from 1-st to 12-nd, 16-th and 23-rd respectively, as in SC1 case. Results are depicted in Figure 8.8 showing that, as in SC1 case, only the approximation from 1-st to 23-rd stage yields a different behavior compared to the one without temperature approximation. Note that in this case, differently from SC1 case, the temperature approximation induces a compensation of the final steady-state estimation error; however, it is important to highlight that this is not a general case, as can be deduced form SC1 case.

Comparison between GE and EKF - EO1

A comparison between estimation algorithms is now made when considering the estimation measurement structure with 3 sensors located at 30-th, 31-st and 33-rd stage, and C3 as innovated component. Results are reported in Figure 8.9 for Scenario 2, showing that a partial innovation is sufficient in order to achieve the estimation objective. This can also be deduced form an analysis of the Kalman Gain Matrix in the EKF with complete innovation, which shows that the innovation mainly acts for the C3 in the area where temperature sensors are located.

Overall Considerations

In this Section, it has been shown how a GE based on a reduced model with 3 modeled components (C3, iC4 and nC4) in conjunction with temperature sensors is able to infer the composition of iC4 in the distillate, according to objective EO1. A structure with 2 sensors at 30-th and 31-st stage permits the achievement of the objective in both SC1 and SC2 case, while the addition of more sensors after the 3-rd one does not result in any improvement. Moreover, temperature can be assumed constant in a region from 1-st to 16-th stages (with small gradients and little information contribution for the estimation objective of interest), without altering estimator performance. Moreover, the comparison with EKF algorithms shows as partial innovation suffices in order to adequately perform

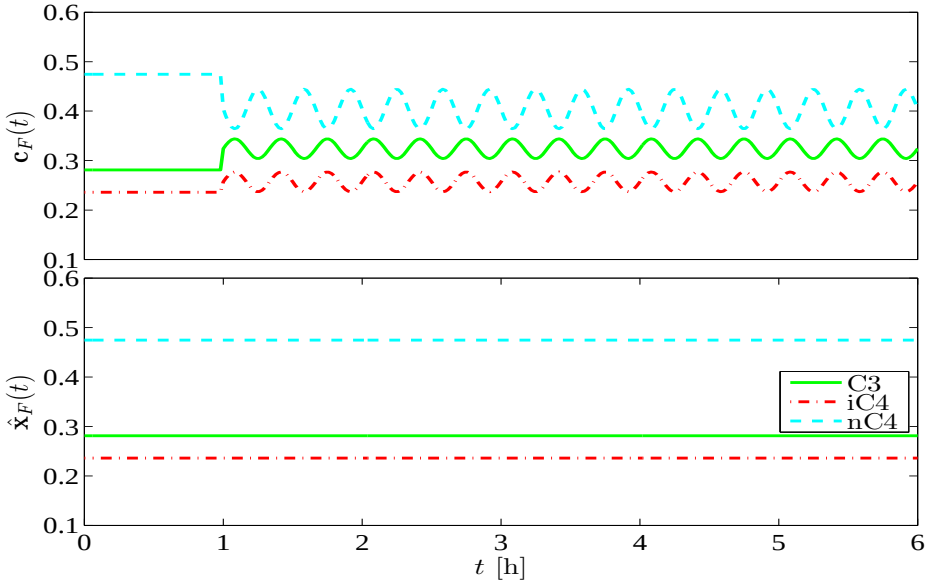

Figure 8.6: Actual (top) and modeled (bottom) composition feed behavior for Scenario 2 (SC2).

the estimation task.

8.3 Estimation Objective 2 (EO2)

The estimation objective 2 (EO2) consists in the joint inferring of both key impurity effluent compositions, that is, C3 in the bottom and iC4 in the distillate. The column works in closed-loop, since the temperatures at 5-th and 33-rd stages are controlled through the reboiler heat duty Q and the reflux rate R respectively with a conventional single-end controller, that is, the control structure $\sigma_{C[Q,5][R,33]}$ (see Chapter 5) is used. As for EO1 case, both Scenario 1 (SC1) and Scenario 2 (SC2) conditions are considered, and firstly, the Geometric Estimator (GE) is tested as estimation algorithm, in conjunction with the candidate estimation structures determined in Section 6.2.2; then, the best estimation structure is assessed with Extended Kalman Filters with partial or complete innovation, and compared to the GE case.

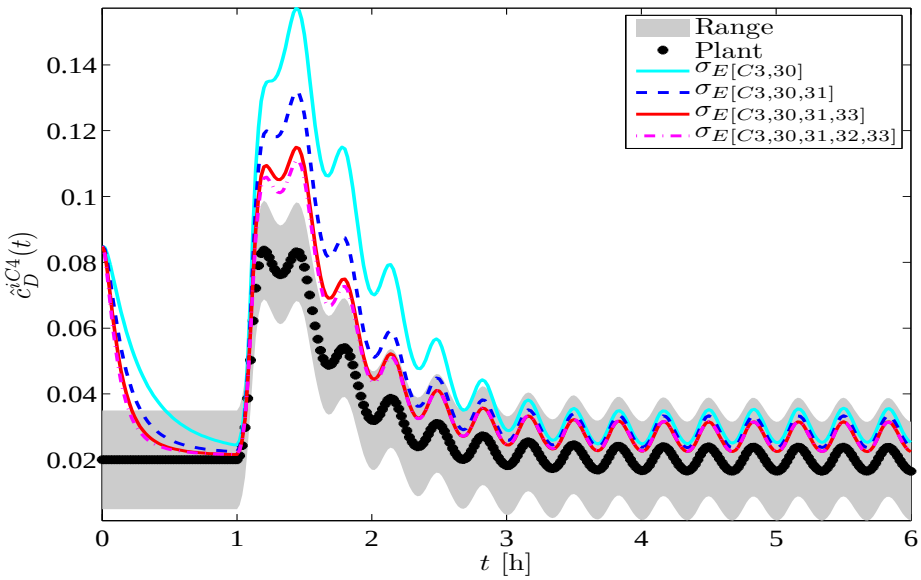

Figure 8.7: EO1, SC2: comparison among the measurement structures $\sigma_{E[C3,30]}$, $\sigma_{E[C3,30,31]}$, $\sigma_{E[C3,30,31,33]}$ and $\sigma_{E[C3,30,31,32,33]}$

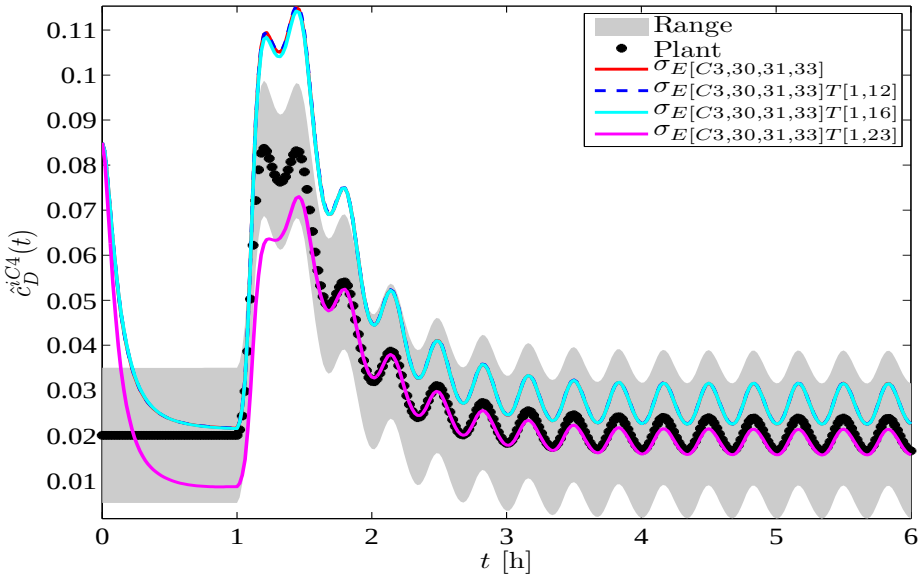

Figure 8.8: EO1, SC2: comparison between the measurement structures $\sigma_{E[C3,30,31,33]T[1,12]}$, $\sigma_{E[C3,30,31,33]T[1,16]}$ and $\sigma_{E[C3,30,31,33]T[1,23]}$

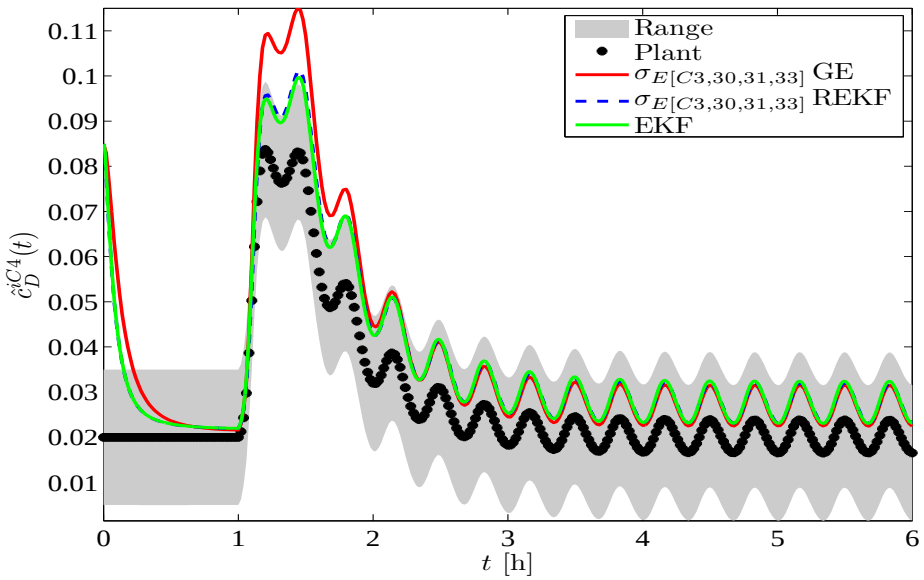

Figure 8.9: EO1, SC2, structure $\sigma_{E[C3,30,31,33]}$: comparison among GE, EKF and REKF

.

8.3.1 GE structural results - EO2

Geometric Estimator (GE) structural results are now assessed for EO2 case, with respect to SC1 and SC2.

Tuning

Tuning parameters are chosen according to guidelines given in Section 7.1.3. Estimator frequencies λ_S (stripping section) and λ_E (enriching section) are chosen 10 times larger than the characteristic frequencies $\omega_S = 2\text{h}^{-1}$ and $\omega_E = 1\text{h}^{-1}$ (already computed in Section 5.2.2 and 5.2.4 respectively) in the same sections, while damping factor is assumed to be $\xi_i = 3$.

The resulting tuning parameters are therefore the following:

$$K_P^S = 60 \qquad K_I^S = 100$$
$$K_P^E = 120 \qquad K_I^E = 400$$

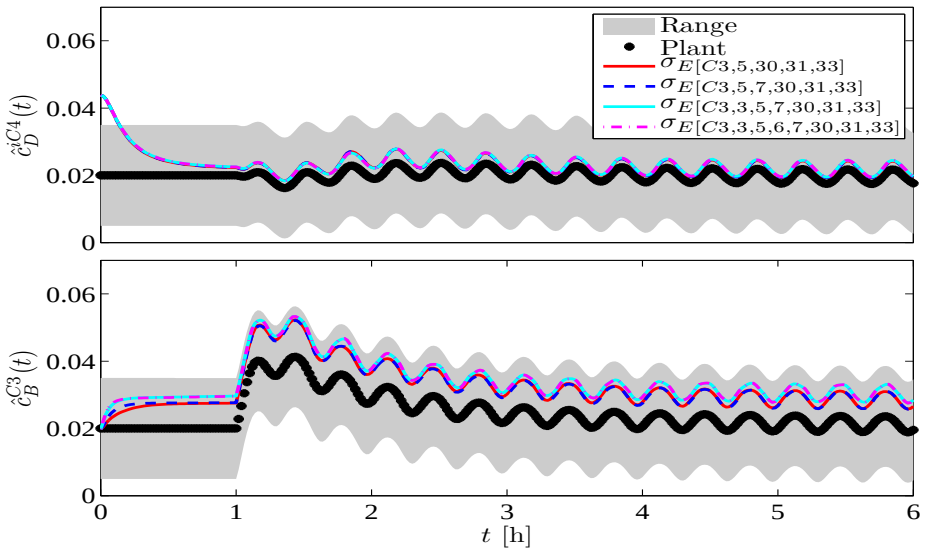

Figure 8.10: EO2, SC1: comparison among the measurement structures $\sigma_{E[C3,5,30,31,33]}$, $\sigma_{E[C3,5,7,30,31,33]}$, $\sigma_{E[C3,3,5,7,30,31,33]}$ and $\sigma_{E[C3,3,5,6,7,30,31,33]}$

Scenario 1 (SC1)

Being the goal the joint estimation of both bottom C3 and distillate iC4 compositions, temperature sensors need to be placed in both stripping and enriching section. Given that for EO1 case the 3-sensor structure with 30, 31 and 33 yields the best performance according to the objectives, these locations have been chosen also for EO2 case. In addition to this, one or more sensors (from 1 to 4) have been added in the stripping section, in the area with the largest gradients (around the 5-th stage), in order to find the best estimation structure. Structures $\sigma_{E[C3,5,30,31,33]}$, $\sigma_{E[C3,5,7,30,31,33]}$, $\sigma_{E[C3,3,5,7,30,31,33]}$ and $\sigma_{E[C3,3,5,6,7,30,31,33]}$ have been tested and compared in Figure 8.10. It can be noted as 1 sensor in the stripping section suffices to obtain good transient and steady-state dynamics for both impurities to be estimated.

Then, the structure $\sigma_{E[C3,5,30,31,33]}$, is tested with two different temperature approximations: (i) from 10-th to 17-th stage and from 21-st to 23-rd stage (approximation in 2 regions), and (ii) form 10-th to 23-rd stage (approximation in 1 region which includes the 2 regions of the approximation at point (i)). Results are shown in Figure 8.11, and shows as the first approximation ($\sigma_{E[C3,5,30,31,33]T[10,17,21,23]}$ structure) produces the same performance of the estimator without temperature approximation; on the other hand, the second approximation ($\sigma_{E[C3,5,30,31,33]T[10,17,21,23]}$ structure) results in a performance wors-

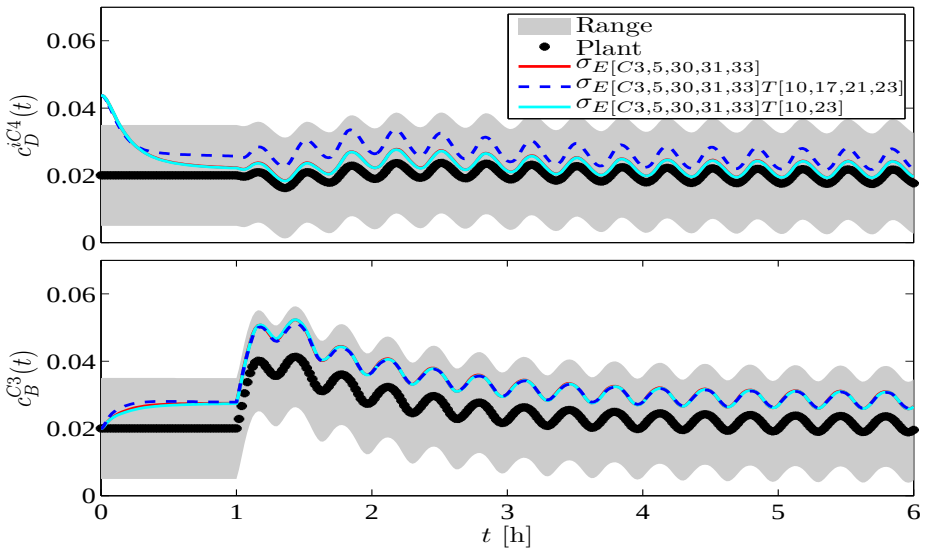

Figure 8.11: EO2, SC1: comparison among the measurement structures $\sigma_{E[C3,5,30,31,33]}$, $\sigma_{E[C3,5,30,31,33]T[10,17,21,23]}$ and $\sigma_{E[C3,5,30,31,33]T[10,23]}$

ening, probably due to the fact that the region in which temperature is approximated includes the feed stage.

Scenario 2 (SC2)

In SC2 case, the same tests as in SC1 one are made. Firstly, the structures with a variable number of sensors (from 1 to 4) in the stripping section around 5-th stage and 3 sensors in the enriching section (in 30-th, 31-st and 33-rd stages) have been tested and compared. Results are given in Figure 8.12, and shows as only 1 sensor in the stripping section is sufficient for obtaining good performance; rather, performance gets worse when either 3 or 4 sensors are placed in the enriching sensors.

Consider now $\sigma_{E[C3,5,30,31,33]}$ structure: if temperature approximation is used as in SC1 case, estimators perform as shown in Figure 8.13. Same considerations of SC1 case hold, meaning that estimator performance degrades if feed stage is included in the region of approximation.

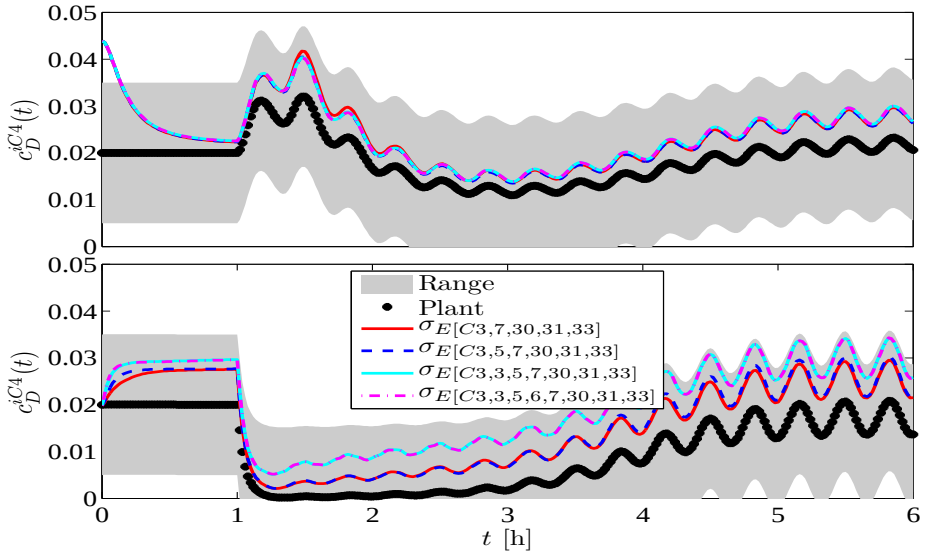

Figure 8.12: EO2, SC2: comparison among the measurement structures $\sigma_{E[C3,5,30,31,33]}$, $\sigma_{E[C3,5,7,30,31,33]}$, $\sigma_{E[C3,3,5,7,30,31,33]}$ and $\sigma_{E[C3,3,5,6,7,30,31,33]}$

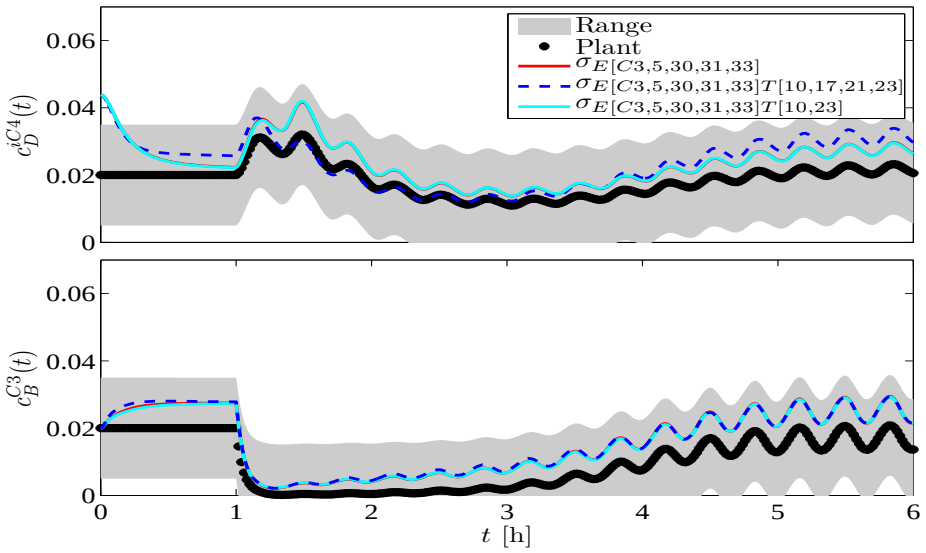

Figure 8.13: EO2, SC2: comparison among the measurement structures $\sigma_{E[C3,5,30,31,33]}$, $\sigma_{E[C3,5,30,31,33]T[10,17,21,23]}$ and $\sigma_{E[C3,5,30,31,33]T[10,23]}$

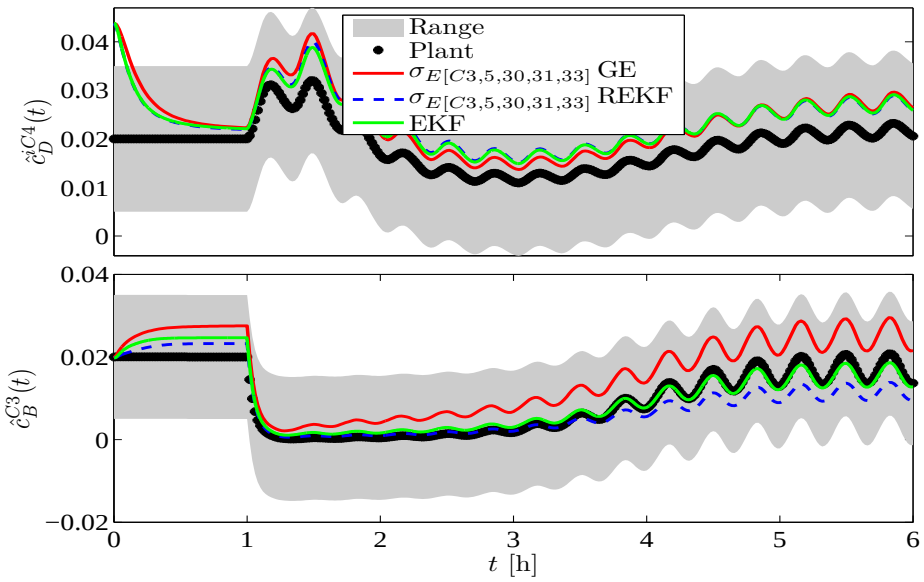

Figure 8.14: EO1, SC2, structure $\sigma_{E[C3,5,30,31,33]}$: comparison among GE, EKF and REKF

.

Comparison between GE and EKF - EO2

A comparison between estimation algorithms is now made when considering the estimation measurement structure with 4 sensors located at 5-th, 30-th, 31-st and 33-rd stage, and C3 as innovated component. Results are reported in Figure 8.14 for Scenario 2, showing that a partial innovation is sufficient in order to achieve the estimation objective, even if better results can be obtained with an EKF with complete innovation: as for SC1 case, this can be deduced form an analysis of the Kalman Gain Matrix in the EKF with complete innovation, which shows that the innovation mainly acts for the C3 in the area where temperature sensors are located.

Overall Considerations

In this Section, it has been shown how a GE based on a reduced model with 3 modeled components in conjunction with 4 temperature sensors is able to infer the composition of both bottom C3 and distillate iC4, according to objective EO2. Differently than the enriching section, only 1 sensor is needed in the stripping one, meaning that a measurement structure with C3 innovated at 1 stripping section stage and 3 enriching section stages allows the achievement of EO2. Moreover,

temperature can be assumed constant in two distinct regions, from 10-th to 17-th stages, and from 21-st to 23-rd stages without altering estimator behavior. Furthermore, the comparison with EKF algorithms shows that EO2 objective can be achieved with partial innovation even if performance is slightly better when using complete innovation.

8.4 Chapter summary

In this Chapter, the estimation structural results are assessed as the best compromise among speed, simplicity and robustness, by testing candidate structures determined in Chapter 6. According to such structures, only C3, iC4 and nC4 are retained in the estimator model.

Best performance for EO1 objective (i.e., estimation of distillate iC4) is obtained by locating 3 sensors at 30-th, 31-st and 33-rd stages and innovating C3. Temperature approximation can be performed by considering it as constant from 1-st to 16-th stage. Furthermore, the comparison with the EKF with complete innovation shows that partial innovation lead to the same performance.

On the other hand, a sensor at 5-th stage with the C3 as innovated component has to be added for achieving EO2 (i.e., joint regulation of bottom C3 and distillate iC4). Temperature approximation can be performed by assuming it as constant from 10-th to 17-th stage and from 21-st to 23-rd stage. Finally, the comparison with the EKF algorithms shows that complete innovation only leads to slightly better results, but partial innovation is sufficient for obtaining good performance.

All estimation results have been obtained without providing any information about the feed composition to the estimator, meaning that such compositions have been set to their nominal value for the whole simulation time.

Chapter 9

Control and estimation structural correlations

In this Chapter, the connection between control and estimation structure selection is analyzed. Such connection is represented by the selection of temperature sensor location, which is a common task in control and estimation structure selection. The sensor selection is performed through a common methodology which consists in the use of the temperature gradient with per-component contribution diagram, in conjunction with a procedure that is slightly different in the two cases. As illustrated in Chapter 5 and Chapter 8, the optimal sensor location can be a bit different, and more sensors can be necessary for effectively solving the estimation problem, compared to the control case. Here, it is shown through dynamic simulations that the sensors selected in order to achieve control objectives can be effectively used for attaining estimation objectives. This is especially useful for industrial purposes, since the expenses due to the purchase of additional sensors for estimation purposes can be avoided if the same sensors employed for control purposes are used.

9.1 Introduction

A common task in the selection of control and estimation structure is the selection of the temperature sensor locations. Such locations are chosen on the basis of a common tool, the temperature gradient with per-component contribution diagram, in conjunction with a systematic procedure that is different in the two cases.

The criteria used for sensor location selection are here summarized:

Sensor location for control purposes. Temperature sensors have to be placed according to the control objective, that is, in the section with the key impurity to regulate. The primary sensor location (for both conventional and cascade-type controllers) has to be placed in an area with large temperature variations, where this gradient is mostly due to key-components. In addition, if a cascade-type controller is used, the secondary sensor can be located either in a stage with large gradient mainly due to key components (as for primary locations), or close to feed stage in order to quickly reject disturbances.

Sensor location for estimation purposes. Temperature sensors have to be placed according to the estimation objective, that is, in the section with the key impurity to estimate. Moreover, such sensors have to be placed in an area with large temperature variations not due to unmodeled components.

The two criteria above stated are slightly different, but in both cases sensors should be placed in a sensitive area (i.e., with large gradients): however, in control case sensor should be located where gradients are mainly due to key-components, whereas in estimation case sensors should be placed where such gradients are not due to unmodeled components. This means that best sensor locations can be different in two cases, but appropriate locations can be used for effectively performing both control and estimation tasks.

Such considerations are very important for industrial purposes, since the expenses due to the purchase of additional sensors for estimation purposes can be avoided if the same sensors are employed for control purposes. The goal in industry is therefore the achievement of both objectives with the minimum number of sensors.

As shown in Chapter 5 and Chapter 8, controller performance is more sensitive to sensor location movement than the estimation one; therefore in the following, sensor location is chosen in order to obtain the best controller performance according to the control objective; thus, such locations are used in order to attain also estimation objective. At first the joint achievement of control objective CO1 (regulation of distillate iC4 around its nominal value) and estimation objective EO1 (estimation of distillate iC4 within a prescribed range) is assessed; then, the same is done for CO2 (joint regulation of bottom C3 and distillate iC4) and EO2 (joint estimation of bottom C3 and distillate iC4).

9.2 Control and estimation objective 1 (CO1,EO1)

In this Section, the control and estimation tasks are jointly carried out with the minimum number of sensors with CO1 and EO1 (joint control and estimation of distillate iC4) as objectives. The problem is assessed with both conventional and CLF controllers, and with the GE as estimation algorithm.

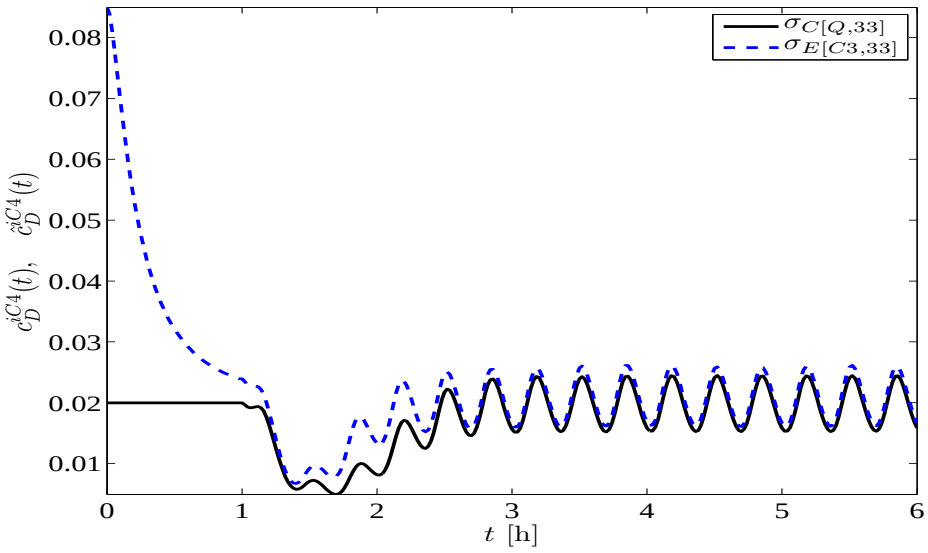

Figure 9.1: CO1, EO1, SC1: controller and estimator performance with only one sensor placed at 33-rd stage

9.2.1 Conventional controller

As illustrated in Chapter 5, the best solution for achieving control objective CO1 with a conventional controller is the location of the temperature sensor at 33-rd stage. However, best estimation sensor location is the 30-th stage. Here the goal is to jointly control and estimate iC4 dynamics with the same sensor: since controller performance is more sensitive to sensor movement than the estimation one, estimator should be implemented with a sensor located at 33-rd stage, in order to use only one sensor. Results are shown in Figure 9.1 when the column is subjected to a disturbance as in Scenario 1 (SC1, see Table 5.2), and show that in this case the entire task can be performed with only one sensor. The same results follow from the analysis of Scenario 2 (SC2, see Table 5.3), as can be seen from Figure 9.2.

9.2.2 CLF controller

When a CLF controller is used, best sensor locations are 33-rd and 34-th for primary and secondary temperature respectively (see Chapter 5). Such locations are in the area with the largest of the enriching section, even if they are not the stages with he largest gradients. Controller and estimator performance are shown in Figure 9.3 (SC1) and Figure 9.4 (SC2), showing that both tasks can be

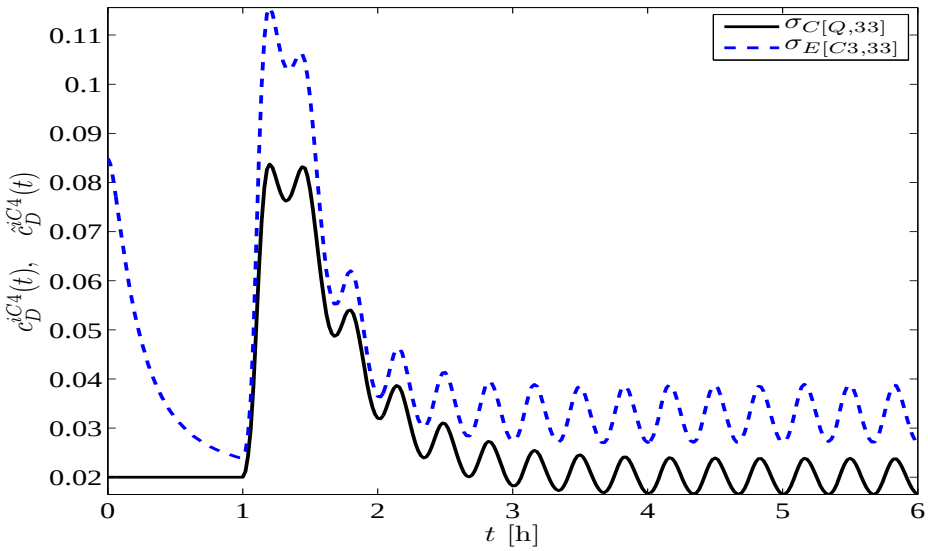

Figure 9.2: CO1, EO1, SC2: controller and estimator performance with only one sensor placed at 33-rd stage, and with a further sensor for estimation purposes at 30-th stage.

effectively achieved with only 2 sensors.

9.3 Control and estimation objective 2 (CO2, EO2)

In this Section, the control and estimation tasks are jointly carried out with the minimum number of sensors with CO2 and EO2 (joint control and estimation of bottom C3 and distillate iC4) as objectives. The problem is assessed with both conventional and CLF controllers, and with the GE as estimation algorithm.

9.3.1 Conventional controller

If the aim is the achievement of control objective CO2 (joint control of bottom C3 and distillate iC4) with a conventional controller, structural results in Chapter 5 have shown that the best locations are the 5-th (stripping section) and the 33-rd stage (enriching section). Estimator performance when sensors are placed at the same locations is shown in Figure 9.5 (SC1) and Figure 9.6 (SC2), where it can be seen that two sensors are sufficient in order to jointly achieve both tasks.

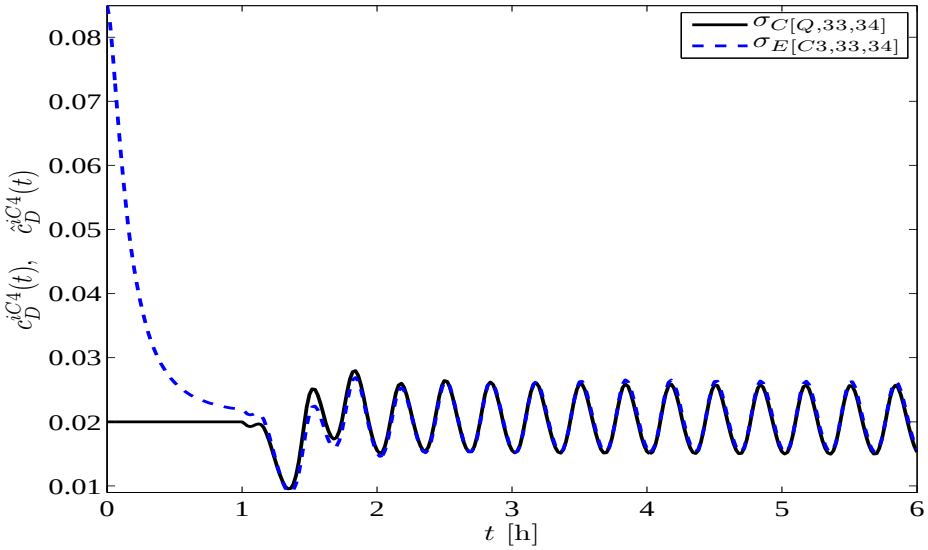

Figure 9.3: CO1, EO1, SC1: controller and estimator performance with only two sensors placed at 33-rd and 34-th stage

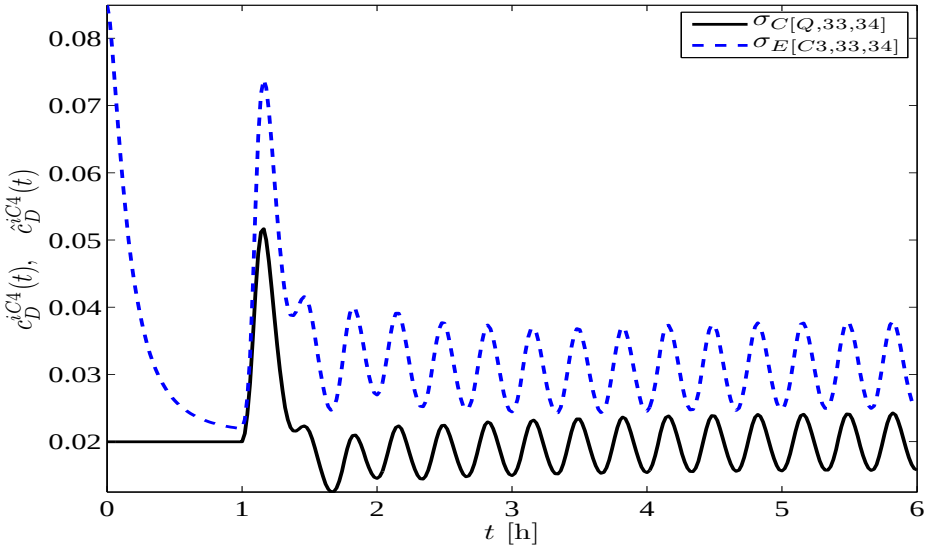

Figure 9.4: CO1, EO1, SC2: controller and estimator performance with only two sensors placed at 33-rd and 34-th stage

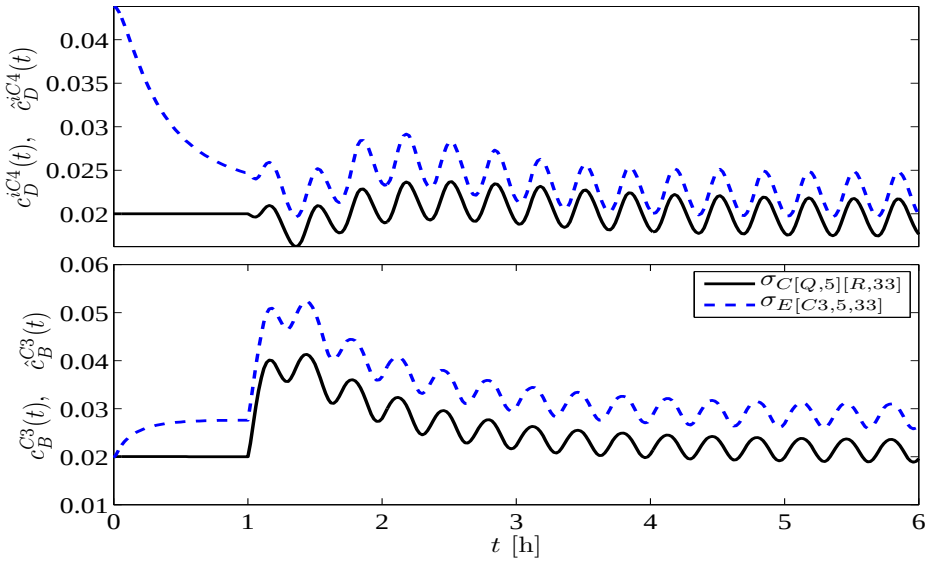

Figure 9.5: CO2, EO2, SC1: controller and estimator performance with two sensors placed at 5-th and 33-rd stage

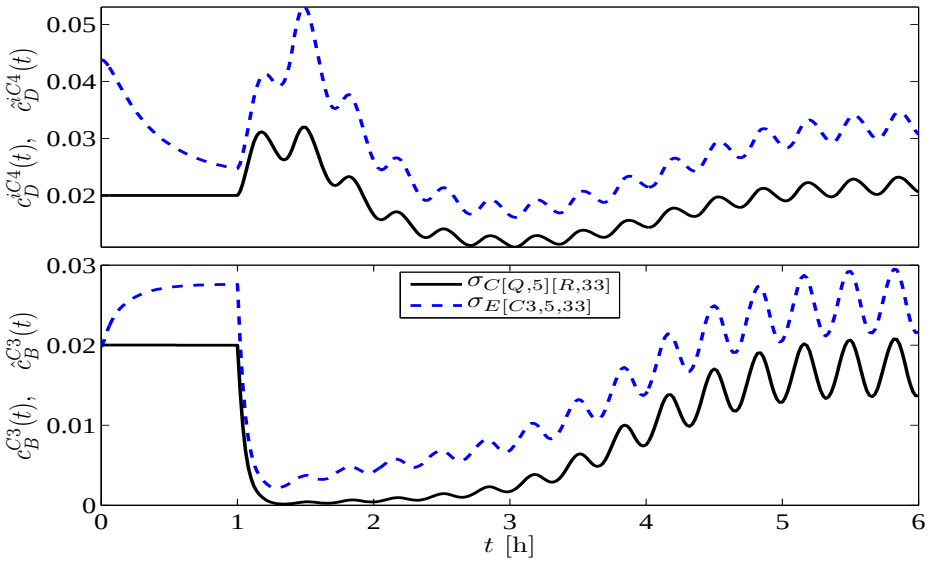

Figure 9.6: CO2, EO2, SC2: controller and estimator performance with two sensors placed at 5-th and 33-rd stage

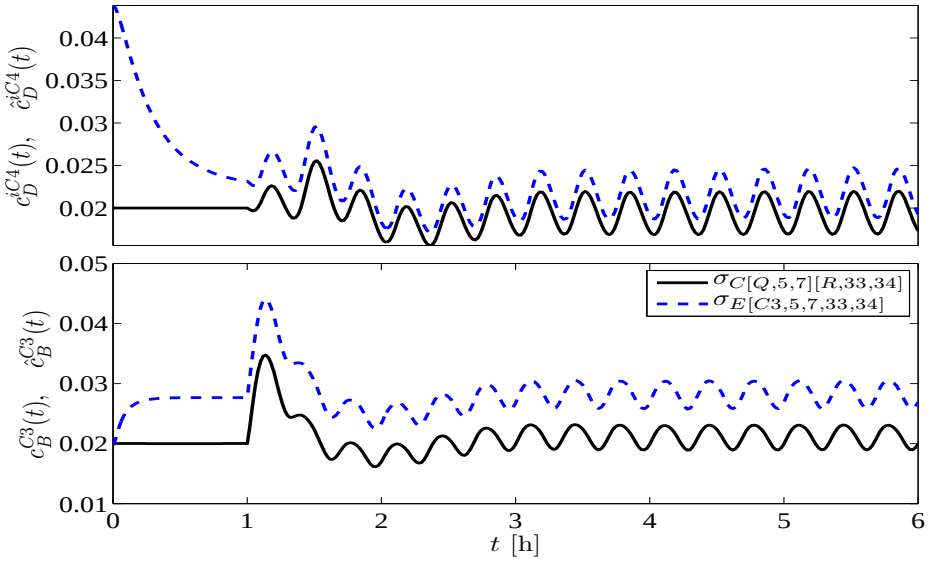

Figure 9.7: CO2, EO2, SC1: controller and estimator performance with four sensors placed at 5-th, 7-th, 33-rd and 34-th stage

9.3.2 CLF controller

When the goal is the achievement of control objective CO2 (joint control of bottom C3 and distillate iC4) with a CLF controller, structural results in Chapter 5 have shown that the best pairs for sensor locations are the 5-th and 7-th stages for stripping section, and the 33-rd and 34-th stages for the enriching section. Estimator performance when sensors are placed at the same locations is shown in Figure 9.7 (SC1) and Figure 9.8 (SC2), where it can be seen that four sensors are sufficient in order to jointly achieve both tasks.

9.4 Chapter summary

In this Section, structural connections between control and estimation have been shown. The temperature gradient with per-component contribution diagram has been used in this Thesis as a common tool for selecting the location of sensors for control (see Chapter 5) and estimation (see Chapter 6) purposes. Criteria for the selection are slightly different in the two cases, and therefore the best location is not the same. However, it has been shown that good joint controller and estimator performance can be obtained using the same sensors for both purposed, and therefore employing the minimum number of sensors. This result is very important from a conceptual point of view, since this shows as the control

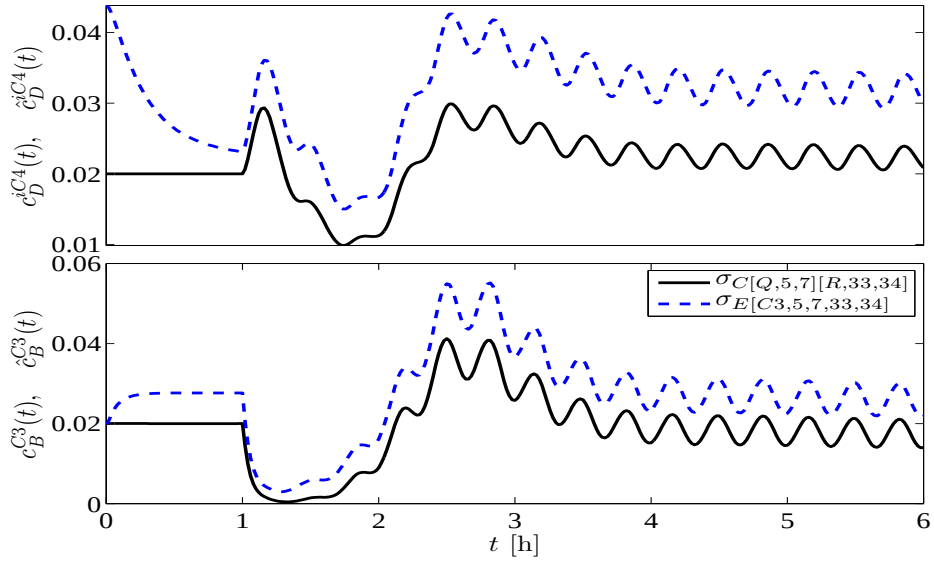

Figure 9.8: CO2, EO2, SC2: controller and estimator performance with four sensors placed at 5-th, 7-th, 33-rd and 34-th stage

and estimation structural problems are strictly connected; moreover, this is also important from the industrial point of view, since the additional costs due to purchase of additional sensors for estimation purposes can be avoided.

Chapter 10

Conclusions and future research

In this Chapter, the most important conclusions of this Thesis are given, together with some recommendations for future research.

10.1 Conclusions

In this Thesis, the problem of controlling and estimating compositions of interest in a multicomponent column with temperature measurements has been addressed. This work has been motivated by the necessity of (i) regulating some of the effluent compositions around the prescribed values for a given separation, in spite of disturbances entering the column as fluctuations in feed flow rate, composition and temperature, and (ii) estimating such compositions in order to monitor the separation.

Temperature measurements have been used because of shortcomings in direct composition analysis, like high costs of purchase and maintenance, reliability issues and measurement delays. Differently from the binary case, in a multicomponent distillation column the compositions in a tray are not uniquely determined by the temperature, and therefore temperature sensors cannot provide composition control and estimation without offset.

In order to solve this problem, a unified methodology that permits the achievement of composition control and estimation objectives within a predetermined tolerance, has been proposed and successfully applied to a six-component C3-C4 splitter through simulation examples. Such methodology consists in the partition of control and estimation problems into a structural and an estimation part,

permits a systematic controller and estimator design, and has been developed by putting together techniques already employed and new ideas.

As regards the control part, the structure has been defined as the joint selection of (i) the temperatures to be regulated and (ii) their pairing with the chosen manipulated variables, while the algorithm is the dynamic data processor that process temperature measurements in order to perform the control task. On the other hand, regarding the estimation part, the structure has been defined as the joint selection of (i) a (possibly reduced) estimation model, (ii) the number and locations of temperature measurements, (iii) the states to be innovated through injection of temperature measurements and (iv) the regions in which the temperature can be approximated as the average one, while the algorithm is the dynamic data processor that processes temperature measurements in order to perform the estimation task.

The temperature gradient with per-component contribution diagram is the main tool of the methodology employed in the present work, and has been proposed and used as the mean for the selection of part of the control structure and of the entire estimation structure. Such diagram consists in plotting temperature gradients at a nominal steady-state together with the contributions due to the components, and is based on the well-known temperature slope criterion, which has extensively been used in control. In this Thesis, it has been shown that the temperature gradient with per-component contribution diagram in conjunction with systematic rules provides a simpler and more intuitive criterion for achieving both control and estimation objectives in a multicomponent column, compared to other well-known methods.

The control algorithm problem has been successfully solved with the use of observed-based controller with anti-windup action, developed on the basis of passivity concepts and nonlinear constructive theory. These controllers are the following: (i) a conventional controller; (ii) a parallel cascade controller; (iii) a cascade-type controller based on Control Lyapunov Functions (CLF). This family of controllers provides a systematic and easy to apply tuning criterion for any admissible control structure.

As regards the control structural problem, the selection of the best temperature sensor location has been solved through the temperature gradient with per-component contribution diagram, on the basis of the following criteria: for all controllers here proposed, primary temperature sensors have to be placed (i) in the section that contains the impurity to be regulated, (ii) in an area where the gradients are large, and (iii) where the gradient is mostly due to key components. In addition, for cascade-type controllers, secondary temperature sensor location should be either a stage selected on the basis of the criterion used for primary location, or a stage close to feed one. On the other hand, manipulated variable and pairing with temperature (for dual-end controllers) have been chosen on the basis of well-known sensitivity criteria.

Excellent control performance has been obtained with all controllers. It has been shown that the best sensor location for achieving CO1 objective (i.e., regulation of distillate iC4 within a prescribed range) is the 33-rd stage (a single-end controller has been used with Q as manipulated variable), while in CO2 case (i.e., joint regulation of bottom C3 and distillate iC4 within prescribed ranges), best sensor locations are the 5-th and the 33-rd stages (a dual-end controller has been used). Cascade controllers is sometimes better than its conventional counterpart for disturbance rejection, and its performance does not considerably depend on secondary sensor location. On the other hand, the CLF controller is by far the controller with the best performance, and best results have been obtained placing a secondary sensor at 34-th (or 23-rd) stage for CO1 case, and at 7-th and 34-th stage for CO2 case. Such performance is due to the better cooperation between primary and secondary control actions.

As well as the control structure case, the whole estimation structural problem has been solved through the temperature gradient with per-component contribution diagram, but in conjunction with a different systematic procedure: (i) the components retained in the estimation model have been the ones that mostly contribute to the overall gradient along the column; (ii) one or more temperature sensors have been placed in the region of interest, in an area with large gradients, where these variations are not due to unmodeled components; (iii) the component to be innovated is the one that mostly contributes to the gradients where temperature sensors are located; (iv) temperature is approximated as the average one in regions with small temperature variations.

On the other hand, the estimation algorithmic problem has been solved with the Geometric Estimator (GE) with partial innovation, and with the EKF with partial or complete innovation. Partial innovation leads to an algorithm with a considerably smaller number of ODEs to be integrated (from 74 to 80) compared to the 2849 ODEs needed if the innovation is complete. Moreover, the GE tuning is systematic and easy to apply for each admissible structure, compared to the trial and error procedure necessary for EKF tuning.

Best estimation results in EO1 case (i.e., estimation of distillate iC4) have been obtained with a 3-component reduced estimation model where (i) only C3, iC4 and nC4 have been modeled, (ii) temperature sensors have been placed at 30-th, 31-st and 33-rd stages, and (iii) C3 has been chosen as innovated component. Moreover, temperature has been approximated as constant in the region from 1-st to 16-th stage, without worsening performance. For EO2 case (i.e., joint estimation of bottom C3 and distillate iC4), a further temperature sensor has been added at 5-th stage. In this case, temperature has been approximated without altering performance from 10-th to 17-th and from 21-st to 23-rd stage. All estimation results have been obtained without providing any information about the feed composition to the estimator, meaning that such compositions have been set to their nominal value for the entire simulation time.

Finally, it has been shown that good performance can be obtained by using the

same temperature sensors for both controller and estimation purposes, leading to a small number of sensors to be located along the column. For CO1 and EO1 case, good results have been obtained by placing one sensor at 33-rd stage when a conventional controller and a GE have been used, and placing two sensors at 33-rd and 34-th stage when a CLF controller and a GE estimator have been used. On the other hand, good performance has been obtained for CO2 and EO2 case by placing 2 sensors at 5-th and 33-rd stage when a conventional controller and a GE have been used, and placing 4 sensors at 5-th, 7-th, 33-rd and 34-th stage when a CLF controller and a GE have been used.

10.2 Future research

A future objective is the further simplification of the estimation model by truncation, that is, by neglecting composition dynamics in some stages of the column.

Another goal is the employment of the estimates produced by the estimators in order to develop direct composition or composition-temperature inferential controllers on the basis of passivity concepts used in this Thesis.

Next, our unified methodology will be extended to multicomponent columns with a much larger number of components, possibly with lots of components in considerable and comparable amounts.

Finally, the future research will deal with the application of both controllers and estimators to industrial columns, in order to assess their functioning in a more challenging case.

Appendix A

Nomenclature

Latin

a	control model slope (conventional, after manipulation)
$\overset{*}{a}$	actual control model slope (conventional)
a_i	primary or secondary control model slope (cascade-type, after manipulation)
A_D	sinusoidal disturbance magnitude
b	control model load disturbance (conventional, after manipulation)
$\overset{*}{b}$	actual control model load disturbance (conventional)
b_i	primary or secondary control model load disturbance (cascade-type, after manipulation)
B_D	step disturbance magnitude
c_i^j	composition of component j at i-th stage
$\mathbf{c}_i$	composition vector at i-th stage
$\mathbf{c}$	composition vector
C	number of actual components
C_M	number of modeled components
$C_{p,i}$	heat capacity at i-th stage
$\mathbf{d}$	modeled disturbance vector
e_2	difference between secondary control input and secondary set-point (cascade-type)
E	efficiency
f_i^j	composition balance function of component j at i-th stage
$\mathbf{f}_c$	composition balance function vector
F	feed flow rate
F_E	jacobian matrix for EKF
$F_{E,i}^j$	jacobian for j-th component at i-th stage for EKF

H_i	holdup at i-th stage
K_c	controller gain (conventional)
$K_{c,i}$	primary or secondary controller gain (cascade-type)
K_E	Kalman gain matrix for EKF
$K_{E,i}^j$	Kalman gain matrix for j-th component at i-th stage for EKF
$K_{I,i}$	integral gain at i-th stage for GE
K_o	observer gain (conventional)
$K_{o,i}$	primary or secondary observer gain (cascade-type)
K_p	proportional gain for PI
$K_{P,i}$	proportional gain at i-th stage for GE
L	liquid flow rate
n	actual model order
n_M	reduced model order
N	number of actual stages
N_F	location of feed stage
p	gain separation factor (cascade-type)
P_i	pressure at i-th stage
P_i^j	partial pressure of component j at i-th stage
$P_{A,k}^j$	approximated partial pressure for component j in the k-th region
P_E	error covariance for EKF
$P_{E,i}^j$	error covariance for j-th component at i-th stage for EKF
q	sensitivity ratio (cascade-type)
Q	reboiler heat duty
Q_E	model error covariance for EKF
$Q_{E,i}^j$	model error covariance for j-th component at i-th stage for EKF
R	reflux flow rate
R_E	measurement error covariance for EKF
$R_{E,i}^j$	measurement error covariance for j-th component at i-th stage for EKF
s_i	location of i-th sensor
T_i	temperature in the i-th stage
T_i^E	temperature measurement error at i-th stage
$T_{A,k}$	approximated temperature in the k-th region
u	controller output (conventional)
u^*	primary controller output (cascade-type)
$\tilde{u}$	secondary controller output (cascade-type)
u_S	saturated control action
u_S^*	saturated primary control action
u^-	saturation lower limit
u^+	saturation upper limit
$\mathbf{u}$	input vector

v_i^j	vapor composition of component j at i-th stage
$v_i^{j,*}$	equilibrium vapor composition of component j at i-th stage
V	vapor flow rate
$\mathcal{V}$	Lyapunov function (CLF controller)
$\mathbf{w}$	disturbance vector
$\mathbf{x}$	modeled composition vector
$\mathbf{x}_I$	innovated state vector
$\mathbf{x}_{II}$	noninnovated state vector
y	controller input (conventional)
y_i	primary or secondary controller input (cascade-type)
y_2^*	secondary controller set-point (cascade-type)
$\mathbf{y}$	output vector
z_i	integral state for i-th stage (GE)

Greek

β_i	bubble-point function at i-th stage
$\beta'_{i,j}$	bubble-point derivative at i-th stage with respect to component j at i-th stage
$\boldsymbol{\beta}$	bubble-point vector
Δ	gradient
λ_i	estimator frequency at i-th stage
$\lambda_{v,i}$	heat of vaporization at i-th stage
μ_k	component innovated at s_k-th stage
ξ_i	damping factor at i-th stage
ρ_i	tag of i-th component
τ_I	integral time (PI)
τ_τ	anti-windup reset time (PI)
ϕ_i	tag of i-th modeled component
χ	control model load disturbance (conventional, after coordinate change)
χi	primary or secondary control model load disturbance (cascade-type, after coordinate change)
ω_i	characteristic frequency at i-th stage
ω_D	disturbance frequency
ω_H	holdup characteristic frequency

Other

Δu_S	difference between real and saturated control action (conventional)
Δu_S^*	difference between real and saturated primary control action (cascade-type)

Subindices

B	bottom
D	distillate
E	enriching section
F	feed
I	innovated
II	noninnovated
N	condenser stage
N_F	feed stage
R	reflux
S	stripping section
T	top tray

Accents

$\tilde{}$	error
$\hat{}$	estimate
$\bar{}$	set-point or nominal value
$\dot{}$	time derivative

Acronyms

CLF	control Lyapunov function
CO	control objective
EKF	Extended Kalman Filter
EO	estimation objective
GE	Geometric Estimator
REKF	Extended Kalman Filter with partial innovation
SC	scenario
SS	steady-state

Components

C2	ethane
C3	propane
iC4	iso-butane
nC4	n-butane
iC5	iso-pentane
nC5	n-pentane

Structures

$\sigma_{C[j,i]}$	single-end control structure where the manipulated variable j is used for controlling the temperature at i-th stage (conventional)
$\sigma_{C[j,i]k}$	single-end control structure where the manipulated variable j is used for controlling the temperature at i-th stage, with the quantity k kept fixed (conventional)
$\sigma_{C[j_1,i_1][j_2,i_2]}$	dual-end control structure where the manipulated variable j_k is used for controlling the temperature at i_k-th stage, with $k = 1, 2$ (conventional)
$\sigma_{C[j,i_p,i_s]}$	single-end control structure where the manipulated variable j is used for controlling primary temperature at i_p-th stage with the assistance of secondary temperature at i_s-th stage (cascade-type)
$\sigma_{C[j_1,i_{p_1},i_{s_1}][j_2,i_{p_2},i_{s_2}]}$	dual-end control structure where the manipulated variable j_k is used for controlling primary temperature at i_{p_k}-th stage with the assistance of secondary temperature at i_{s_k}-th stage, with $k = 1, 2$ (cascade-type)
$\sigma_{E[\mu,s_1,\ldots,s_k]}$	measurement structure where the component μ is innovated in stages $s_1, \ldots, s_m$
$\sigma_{E[\mu,s_1,\ldots,s_k]T[I_1,F_1,\ldots,I_q,F_q]}$	estimation structure where the component μ is innovated in stages $s_1, \ldots, s_m$, and the temperature is approximated from I_k-th to F_k-th stage, for $k = 1, \ldots, q$

Bibliography

Álvarez, J. (2000). Nonlinear state estimation with robust convergence. *J. Process Contr.* **10**, 59–71.

Álvarez, J. and C. Fernandéz (2009). Geometric estimation of nonlinear process systems. *J. Process Contr.* **19**, 247–260.

Álvarez, J. and T. López (1999). Robust dynamic state estimation of nonlinear plants. *AIChE J.* **45**(1), 107–123.

Balasubramhanya, L. S. and F. J. Doyle III (1997). Nonlinear control of a high-purity distillation column using a traveling-wave model. *AIChE J.* **43**(3), 703.

Baratti, R., A. Bertucco, A. Da Rold and M. Morbidelli (1995). Development of a composition estimator for binary distillation colums. application to a pilot plant. *Chem. Eng. Sci.* **50**(10), 1541–1550.

Baratti, R., A. Bertucco, A. Da Rold and M. Morbidelli (1998). A composition estimator for multicomponent distillation column - development and experimental test on ternarymixtures. *Chem. Eng. Sci.* **53**(20), 3601–3612.

Benallou, A., D. E. Seborg and D. A. Mellichamp (1986). Dynamic compartmental models for separation processes. *AIChE J.* **32**, 1067–1078.

Castellanos-Sahagún, E., J. Álvarez, A. Frau and R. Baratti (2010). Two-point lyapunov control of binary distillation columns with four temperature measurements. In: *IFAC-DYCOPS 2010*. Leuven, Belgium. pp. 55–60.

Castellanos-Sahagún, E., J. Álvarez-Ramírez and J. Álvarez (2005). Two-point temperature control structure and algorithm design for binary distillation columns. *Ind. Eng. Chem. Res.* **44**, 142–152.

Castellanos-Sahagún, E. and J. Álvarez (2006). Synthesis of two-point linear controllers for binary distillation columns. *Chem. Eng. Comm.* **193**, 206–232.

Castellanos-Sahagún, E., J. Álvarez-Ramírez and J. Álvarez (2006). Two-point composition-temperature control of binary distillation columns. *Ind. Eng. Chem. Res.* **45**, 9010–9023.

Dalaouti, N. and P. Seferlis (2006). A unified modeling framework for the optimal design and dynamic simulation of staged reactive separation processes. *Comput. Chem. Eng.* **30**, 1264–1277.

Fagervik, K. C., K. V. Waller and L. G. Hammarstrom (1983). Two-way or one-way decoupling in distillation. *Chem. Eng. Comm.* **21**, 235–249.

Fernandéz, C. (2007). Diseño de la estructura de estimación de composiciones para columnas de destilación binaria: un enfoque geométrico. PhD thesis. Universidad Autonóma Metropolitana, Unidad Itzapalapa. In spanish.

Fernandéz, C. and J. Álvarez (2007). Constructive estimation design for binary distillation columns. In: *International Symposium on Advanced Control of Chemical processes*. Cancún, México. pp. 75–80.

Gani, R., C. A. Ruiz and I. T. Cameron (1986). A generalized model for distillation columns - I. *Computers and Chemical Engineering* **10**(3), 181–198.

Gmehling, J., J. Menke, K. Krafczyk and K. Fischer (1994). *Azeotropic Data, Part I and Part II*. VCH Publishers.

Hankins, N. P. (2007). A non-linear wave model with variable molar flows for dynamic behavior and disturbance propagation in distillation columns. *Chem. Eng. Res. & Des.* **85**(A1), 65–73.

Hermann, R. and A. J. Krener (1977). Nonlinear controllability and observability. *IEEE Transactions on Automatic Control* **AC-22**(5), 728–740.

Hori, E. S. and S. Skogestad (2007). Selection of control structure and temperature location for two-product distillation columns. *Transactions of institution of chemical engineers, Part A* **85**(3), 293–306.

Humphrey, J. L. and A. F. Seibert (1992). New horizons in distillation. *Chem. Eng.* **99**(12), 86–98.

Huss, R. S. and A. W. Westerberg (1996). Collocation methods for distillation design. 1. model description and testing. *Ind. Eng. Chem. Res.* **35**(5), 1603–1610.

Jazwinsky, A. H. (1970). *Stochastic processes and Filtering Theory*. Academic Press. New York.

Joseph, B. and C. B. Brosilow (1978). Inferential control of processes. *AIChE J.* **24**(3), 485–492.

Kano, M., K. Miyazaki, S. Hasebe and I. Hashimoto (2000). Inferential control system of distillation compositions using dynamic partial least squares regression. *J. Process Contr.* **10**, 157–166.

Kothare, M. V., P. J. Campo, M. Morari and C. N. Nett (1994). A unified framework for the study of anti-windup desings. *Automatica* **30**(12), 1869–1883.

Levine, J. and P. Rouchon (1991). Quality control of binary distillation columns via nonlinear aggregated models. *Automatica* **27**(3), 463–480.

Levy, R. E., A. S. Foss and E. A. Grens II (1969). Response modes of a binary distillation column. *Industrial and Engineering Chemistry Fundamentals* **8**(4), 765–776.

Linhart, A. and S. Skogestad (2009). Computational performance of aggregated distillation models. *Chem. Eng. Sci.* **33**, 296–308.

Linhart, A. and S. Skogestad (2010). Reduced distillation models via stage aggregation. *Chem. Eng. Sci.* **65**, 3439–3456.

Lucia, A. (2007). The long and the short of energy consumption in distillation. AIChE Annual Meeting, Salt Lake City, Utah.

Luyben, W. L. (1973). Parallel cascade control. *Industrial and Engineering Chemistry Fundamentals* **12**(4), 463–467.

Luyben, W. L. (1989). *Process modeling, simulation and control for chemical engineers*. 2nd ed.. McGraw-Hill.

Luyben, W. L. (2006). Evaluation of criteria for selecting temperature control trays in distillation columns. *J. Process Contr.* **16**, 115–134.

Mejdell, T. and S. Skogestad (1993). Output estimation using multiple secondary measurements: High-purity distillation. *AIChE J.* **39**(10), 1641–1653.

Moore, C. F. (1992). *Practical Distillation Control*. Chap. Selection of controlled and manipulated variables. Van Nostrand Reinold.

Oisiovici, R. M. and S. L. Cruz (2000). State estimation of batch distillation columns using an extended kalman filter. *Chem. Eng. Sci.* **55**, 4667–4680.

Oisiovici, R. M. and S. L. Cruz (2001). Inferential control of high-purity multicomponent batch distillation columns using an extended kalman filter. *Ind. Eng. Chem. Res.* **40**(12), 2628–2639.

Pulis, A. (2007). Soft sensor design for distillation columns. PhD thesis. Università degli Studi di Cagliari.

Quintero-Marmol, E., W. L. Luyben and C. Georgakis (1991). Application of an extended luenberger observer to the control of multicomponent batch distillation. *Ind. Eng. Chem. Res.* **30**(8), 1870–1880.

Rademaker, O., J. E. Rijnsdorp and A. Maarleveld (1975). *Dynamics and control of continuous distillation units*. Elsevier.

Reid, R. C., J. M. Prausnitz and B. E. Poling (1998). *The properties of gases and liquids*. fourth ed.. McGraw-Hill. Singapore.

Sepulchre, R., M. Jankovic and P. V. Kokotovic (1997). *Constructive Nonlinear Control*. Springer.

Shin, J., H. Seo, M. Han and S. Park (2000). A nonlinear profile observer using tray temperatures for high-purity binary distillation column control. *Chem. Eng. Sci.* **55**, 807–816.

Skogestad, S. (1997). Dynamics and control of distillation columns: a tutorial introduction. *Trans IChemE, Part A* **75**, 539–559.

Skogestad, S. and M. Morari (1988). Understanding the dynamic behavior of distillation columns. *Ind. Eng. Chem. Res.* **27**(10), 1848–1862.

Tolliver, T. L. and L. C. McCune (1980). Finding the optimum temperature control trays for distillation columns. *InTech* **27**(9), 75.

Tronci, S., F. Bezzo, M. Barolo and R. Baratti (2005). Geometric observer for a distillation column: development and experimental testing. *Ind. Eng. Chem. Res.* **44**, 9884–9893.

Tyreus, B. D., W. L. Luyben and W. E. Schiesser (1975). Stiffness in distillation models and the use of an implicit integration method to reduce computation times. *Ind. Eng. Chem. Proc. Des. Dev.* **14**(4), 427–433.

Venkateswarlu, C. and B. J. Kumar (2006). Composition estimation of multicomponent reactive batch distillation with optimal sensor configuration. *Chem. Eng. Sci.* **61**, 5560–5574.

Venkateswarlu, C. and S. Avantika (2001). Optimal state estimation of multicomponent batch distillation. *Chem. Eng. S* **56**, 5771–5786.

Willems, J. C. (1972). Dissipative dynamical systems - part i: General theory. *Arch. Ration. Mech. Anal.* **45**, 321–351.

Yang, D. R. and K. S. Lee (1997). Monitoring of a distillation column using modified extended kalman filter and a reduced order model. *Comput. Chem. Eng.* **21**, 565–570.

Yu, C-C. and W. L. Luyben (1984). Use of multiple temperatures for the control of multicomponent distillation columns. *Ind. Eng. Chem. Proc. Des. Dev.* **23**(3), 590–597.

Yu, C-C. and W. L. Luyben (1987). Control of multicomponent distillation columns using rigorous composition estimators. *IChemE Symposium Series* **104**(A), 29–69.

Zamprogna, E., M. Barolo and D. E. Seborg (2005). Optimal selection of soft sensor inputs for batch distillation columns using principal component analysis. *J. Process Contr.* **15**, 39–52.

Acknowledgements

First of all, I would like to thank my tutor, Prof. Roberto Baratti, for the possibility of undertaking this PhD, and for his support and advice during these three years at the Department of Chemical Engineering and Materials (DICM).

I would also like to thank my Mexican tutor, Prof. Jesús Álvarez, for his help during my stay in Mexico City at UAM, and for his support. I especially remember with pleasure the long meetings at night at his home, and the discussions while having lunch, a coffee or a beer!

I wish to thank all my colleagues at DICM: especially Mariarosa, for being a good friend, for his advice and for the many fruitful discussions about everything, Massimiliano, for his support, and Anuta, with whom I shared the worries when ending our PhD thesis, even if she says that I wasn't as worried as her!

I want to thank all my Mexican colleagues: first of all Miguel, with whom I spent my time in the office at UAM, but also Alexander, Fausto, Salvador, José, Oscar, Gamaliel, Pablo, Sandra, Jorge and Eduardo, since all of them gave me the opportunity of knowing Mexican culture. Moreover, I also wish to thank Kathia, Rodrigo, the Coyote Flaco staff and guests, and my Polish flatmate Jurek, with whom I remember the fantastic trips in Yucatan, Guatemala and Belize, and especially the 24-hour long travel from Guatemala to Mexico, with the river crossing and the tax gatherer on the bus.

Moreover, I want to thank my friends, especially Checco, Fabio, Giuvans, Mauro, Giovanni but also all the other ones, for the nice moments spent during the free time in these years, that have allowed me to carry out this PhD with more serenity.

Thanks also to the beer, with whom I shared many moments during these years, and to LaTeX, which has allowed me to write this Thesis without Microsoft Word, therefore without getting crazy.

Last but not least, I am greatful to my family, who has permitted me to be what I am, and therefore to reach this important goal.